NEAR SHORE INFLUENCE OF A NATURAL TIDAL INLET

A THESIS

Presented to

Virginia Institute of Marine Science

The College of William and Mary in Virginia

In Partial Fulfillment

Of the Requirements for a Degree of

Master of Arts in Marine Science

---

by

Jerome Peter Sovich

1974

APPROVAL SHEET

This thesis is submitted in partial fulfillment of
the requirement for the degree of
Master of Arts in Marine Science

Jerome Peter Sovich

Approved, June 1974

R. J. Byrne, Ph.D.

J. M. Zeigler, Ph.D.

B. J. Neilson, Ph.D.

P. A. Haefner, Jr., Ph.D.

C. L. Smith, Ph.D.

TABLE OF CONTENTS

ACKNOWLEDGMENTS

The work described herein was supported by the Office of Naval Research Geography Programs, Contract N00014-71-C-0334, Task No. NR388-103, with the Virginia Institute of Marine Science, which was directed by Dr. R. J. Byrne.

The author gratefully acknowledges the assistance of Mr. Joseph DeAlteris, Mr. Dave Tyler, and Mr. Michael Carron who participated in the field program. Thanks and appreciation are also given to Dr. J. Zeigler, Dr. B. Neilson, and Mr. Carl Hobbs for their critical reading of the manuscript and to Mr. Joseph Gilley and Mr. Kenneth Thornberry for their contribution to the art work.

Special thanks are extended to Dr. R. J. Byrne for the guidance and advice offered throughout the study.

LIST OF TABLES

LIST OF FIGURES

LIST OF FIGURES (cont'd)

ABSTRACT

Tidal inlets during flood tide conditions act as a sink into which currents flow carrying sediment supplied by littoral drift. The ebb currents issue as a confined jet scouring the channel and maintaining it against the choking forces of littoral drift. The coastal current zone adjacent to tidal inlets are directly affected by the currents issuing from and converging to the inlet.

Wachapreague Inlet, a stable natural inlet located on the lower Delmarva Peninsula of Virginia's Eastern Shore was studied to determine the zone of influence of the inlet's hydraulic currents and their role in sediment transport. The Wachapreague Inlet complex is made up of Parramore Island, which is offset seaward, and forms the inlet's southern boundary, and Cedar Island which forms the inlet's northern boundary. A crescent shaped ebb tidal delta lies at the eastern extreme of the main channel. Ephemeral shoals flank the main channel and are especially well developed in front of Cedar Island. The inlet has a maximum depth of 22 meters and is 450 meters wide at its throat.

Current drogue studies in front of Cedar Island indicate that currents flow toward the inlet and parallel to the coast during flood and away from the inlet and parallel to the coast during ebb. Flood currents are stronger than ebb currents and their strength rapidly increases as the inlet is approached. This zone of significant flood tidal influence extends 1500 meters north of the inlet and is absent during ebb.

During flood, tracer sediment studies show that advection of sediment toward the inlet increases with decreasing distance from the inlet. During ebb, sediment transport rates are less than during flood and sediment moves away from the inlet and parallel to Cedar Island.

Wave activity in front of Cedar Island adjacent to the inlet is restricted to waves approaching from the east through northeast. The ebb tidal delta and flanking shoals cause waves approaching from the south or southeast to be refracted orienting their approach

to the east to northeast. Wave activity will increase sediment movement toward the inlet and may mask the effect of the weak ebb tidal currents.

The offset character of the inlet with ephemeral shoals on the north flank of the channel results in variable lateral inflow. Observations indicate a strong flood convergence on the north side controlled by the configuration of the ebb delta bar. The ebb currents are weak in this zone, thus the zonal influence of the flood currents enhance the tendency for net sediment advection into the inlet.

NEAR SHORE INFLUENCE OF A

NATURAL TIDAL INLET

I.

INTRODUCTION AND DESCRIPTION OF AREA

Coastal areas in the vicinity of tidal inlets are subject to the forces of winds, waves, and tidal currents which continually operate on beach fronts remote from the inlet. Near an inlet differences in water surface elevation between the ocean and the bay generate swift currents which in turn affect local nearshore processes.

Of practical interest concerning engineering problems of navigable channel maintenance and stability is the area adjacent to and seaward of the inlet. Past studies (Brown 1928, Per Brunn 1966, O'Brien 1966, 1969) have emphasized the influence of littoral drift, tidal currents and sediment characteristics on tidal inlets. These studies have shown that local littoral drift, along with flood tidal currents often act to close the inlet; whereas the ebb tidal jet tends to scour the channel and flush the inlet of sediment supplied by littoral drift. The coastal current zone located seaward of the breakers and adjacent to the inlet merits special attention; since, within this zone, the hydraulic currents of the inlet strongly influence the local current field and sediment transport and since it is in the coastal current zone where jetties, breakwaters, or other protective engineering structures are likely to be placed.

Recent study (DeAlteris 1973, Byrne 1973) has added much insight and knowledge into the behavior and characteristics of Wachapreague Inlet located on the lower Delmarva Peninsula of Virginia's Eastern Shore (Figure 1). This study seeks to investigate the effect of Wachapreague Inlet on nearshore currents and related sediment transport.

The Eastern Shore of Virginia lies between the Chesapeake Bay on the west and the Atlantic Ocean on the east. A series of barrier islands, marshes, tidal flats, bays and channels fronts the coastal zone facing the sea. The islands lying on the northern Delmarva Peninsula tend to be linear and continuous and at times impinge upon the mainland. South of the recurved spit of Fishing Point on Assateague Island the system is indented, frequently broken by inlets, and the marsh complex behind the barrier is shallower and not as broad as these features to the north. The barrier island system is composed of a thin veneer of sand and shell which lies upon Holocene marsh deposits. During periods of high energy the sand often is eroded exposing patches of the marsh.

Wachapreague inlet is an example of a natural "offset coastal inlet" as described by Hayes et.al. (1971). Parramore Island, forming the inlet's southern boundary, protrudes approximately 1000 meters farther into the Atlantic Ocean than Cedar Island which forms the

Figure 1. Wachapreague Inlet, located on the lower Delmarva Peninsula of Virginia's eastern shore.

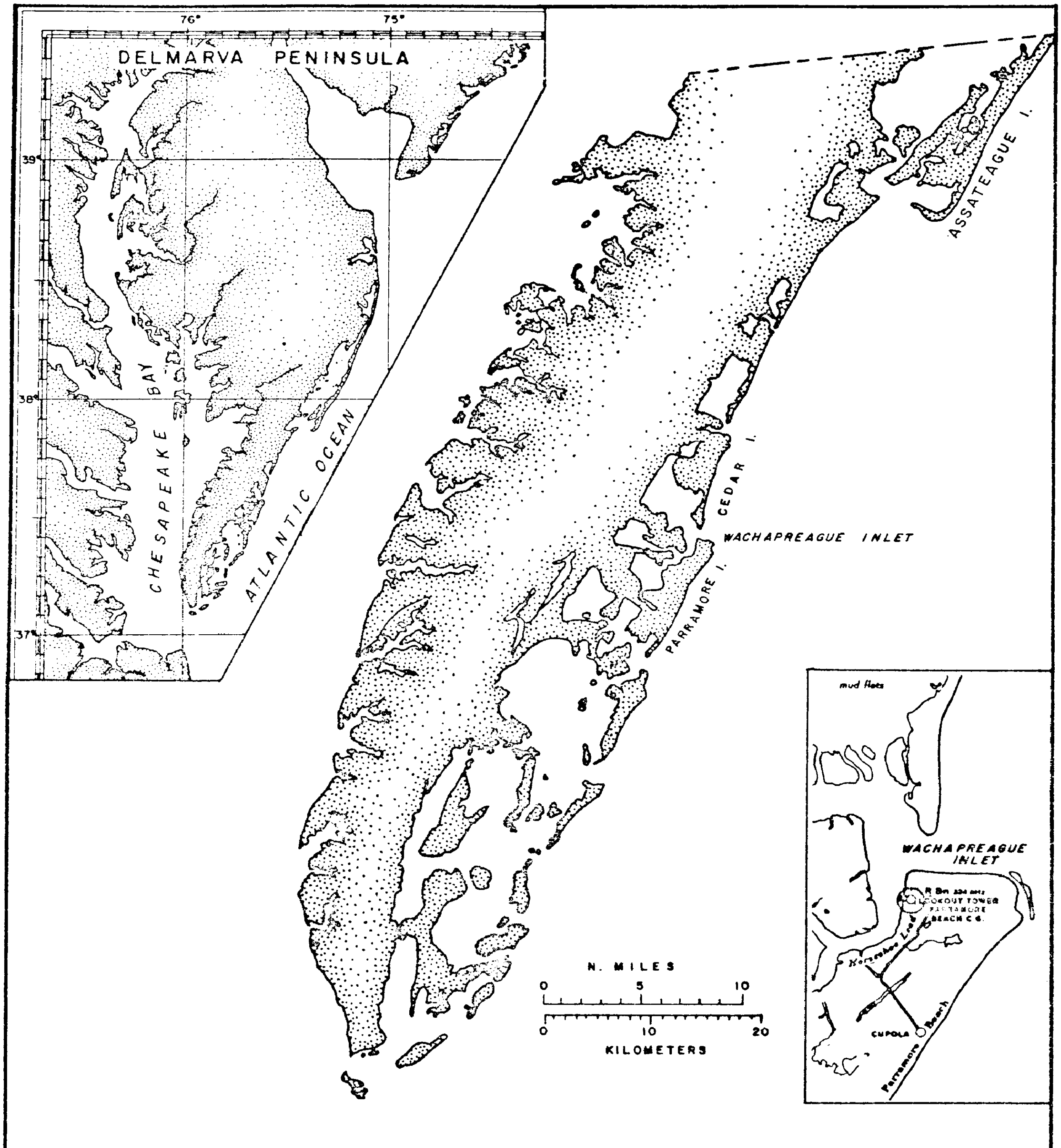

SOUTHERN DELMARVA PENINSULA

inlet's northern boundary. The 1500 meter long main channel is steeply banked (average 30°) on the south and consists of consolidated lagoonal mud deposits. The northern bank of the channel slopes gently (inclination averaging 3.5°) to a maximum depth of 22 meters opposite the spit shaped tip of Cedar Island. A well developed, crescent-shaped, ebb tidal delta lies at the eastern extreme of the main channel. Ephemeral shoals, often exposed at low tide, flank the main channel and are especially well developed in front of Cedar Island (Figure 2). The marsh and tidal complex behind the barrier islands extends 12 km. to the west until reaching the town of Wachapreague on the mainland.

The regional semi-diurnal tide has a mean range of 1.16 meters with a spring maximum range of 1.5 meters. There is a difference in the duration between the rising and falling tide. The rising tide lasts about 0.4 hours longer than the falling tide. This difference in duration is apparently due to the storage characteristics of the marsh channel system behind the inlet. Maximum ebb velocities exceed those of flood and occur earlier in the tidal cycle than do the maximum flood velocities which occur near the middle of the flood's cycle. Figure 3 illustrates this asymmetry under conditions of mean tidal range occurring during times of mean low and mean high water levels.

Figure 2. Wachapreague Inlet, August, 1973.

Figure 3. Tidal velocities in inlet throat under conditions of mean tidal range and mean low and mean high tide levels.

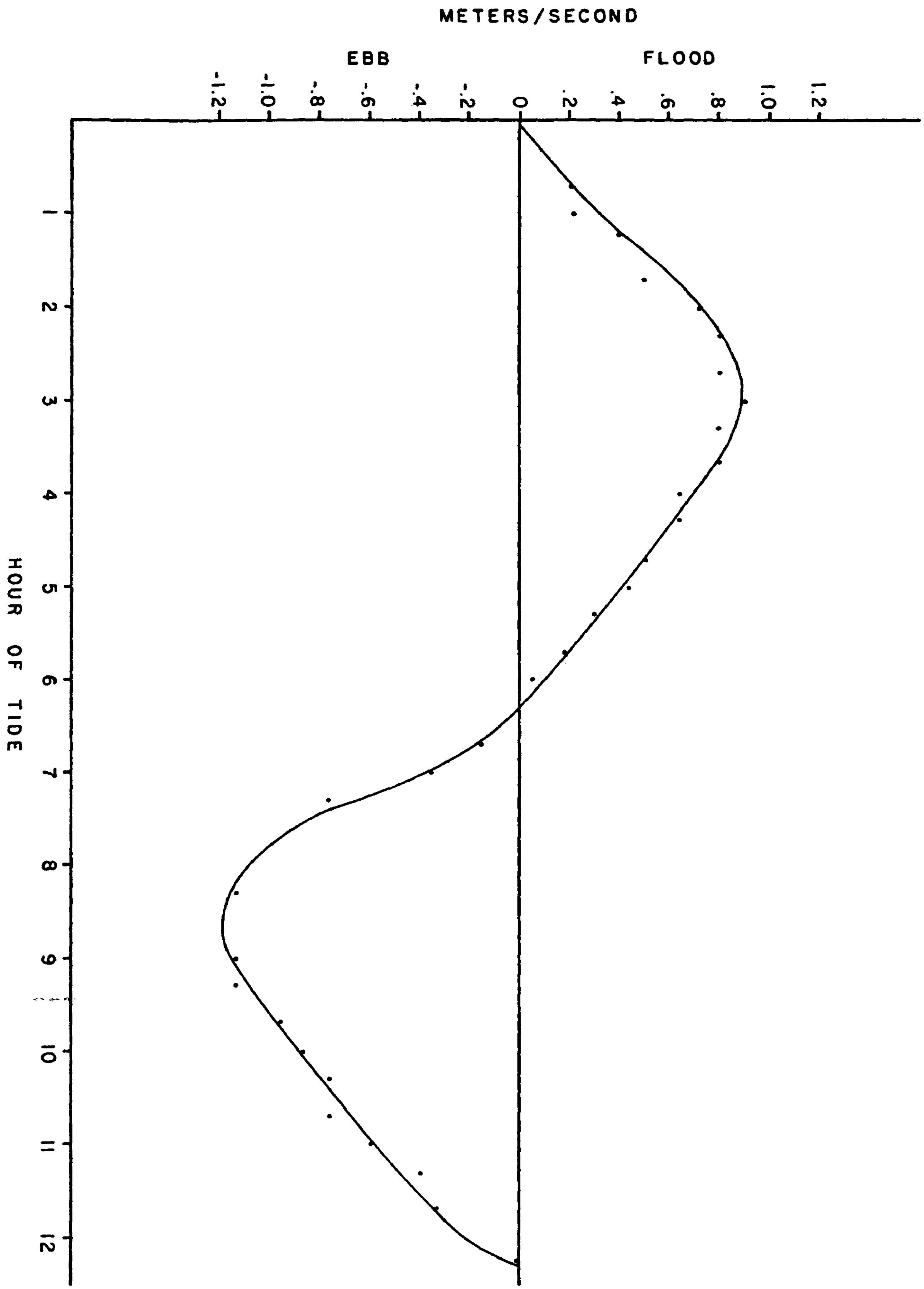
METERS/SECOND
EBB
FLOOD
-1.2
-1.0
-.8
-.6
-.4
-.2
0
.2
.4
.6
.8
1.0
1.2
1
2
3
4
5
6
7
8
9
10
11
12
HOUR OF TIDE

Flow gaging investigations in the inlet channel (Byrne 1973) revealed that 35% of the flood water entering the inlet passed over the north flank of the channel compared with 15% flowing out during ebb. This gaging was conducted while the north flanking shoals were small leading to probable maximum lateral inflow conditions. This behavior fits the generalized conception of an inlet acting as a sink with radial inflow during flood while the ebb issues as a confined plane jet.

Short term changes of 10-15% in the cross sectional area in response to storm climate conditions and periods of large tidal prisms have been documented (Byrne 1973). It is suspected that there is an interchange of sediment on and off the ebb tidal delta and flanking shoals during these periods since sediment budget calculations and estimated longshore drift cannot account for the volume of sand passing through the system.

During flooding conditions, flow gaging has shown more water entering the inlet laterally whereas the ebb water exits as a confined jet. This phenomenon leads to more intense hydraulic currents adjacent to the inlet during flood than during ebb.

The bathymetry and local sea conditions adjacent to and seaward of the inlet interact with the hydraulic currents influencing the mode and manner of water and sediment movement. To what extent and in what areas the hydraulic currents operate and how the local bathymetry may effect their behavior is the subject of this study.

II.

LITERATURE REVIEW

Brown (1928) recognized that littoral drift tends to choke and close inlets and that strong ebb tidal currents tend to scour and maintain the channel. He predicted that a critical velocity of flow is necessary in the channel to maintain the inlet in equilibrium with the closing stream of littoral drift supplied sand. Brown also found an intimate association between the size of the inlet and the size of the interior bays.

O'Brien (1931, 1966, 1969), using data collected from a number of inlets on sandy coasts, found cross sectional areas of inlets in equilibrium to be uniquely a function of their tidal prisms. He discounted the effects of jetties, tractive forces, and size of bed material in controlling equilibrium flow areas but did recognize the importance of littoral drift in reducing the tidal prism and closing inlets.

Littoral drift in the vicinity of tidal inlets is influenced by tidal currents converging toward and issuing from the inlet. Figure 4 is a reproduction of O'Brien's interpretation of the configuration of tidal current behavior on flood and ebb flow for an inlet without an offset. O'Brien displayed the flood currents converging to the inlet entrance from all directions.

Figure 4. O'Brien's interpretation of the configuration of tidal current behavior on flood and ebb flow.

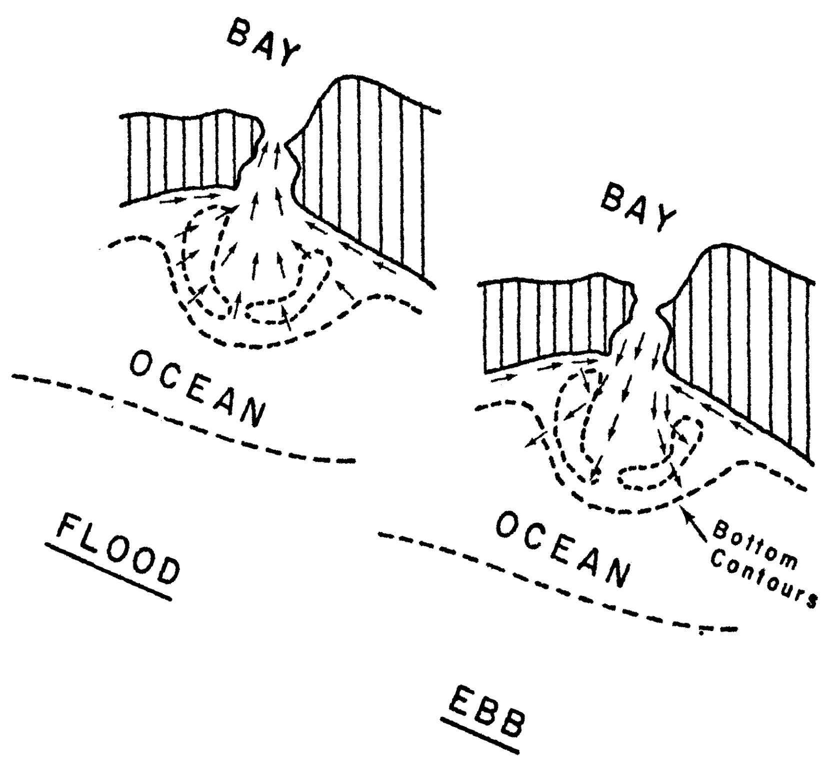
BAY
OCEAN
FLOOD
BAY
OCEAN
Bottom Contours
EBB

The ebb currents, driven by their momentum, issue seaward as a jet with entrainment inducing eddies to either side with resultant nearshore currents flowing toward the inlet. To the best of this writer's knowledge the above described ebb current pattern has not been documented for offset inlets nor has the extent or manner of attenuation of the hydraulic currents in the coastal current zone been established.

Per Brunn (1966) discussed the relationship between inlet flushing ability and littoral drift. He found that a stable channel will adjust its cross-sectional area to those dimensions which produce the necessary high velocities and bottom shear stress to flush itself of surplus material. The actual value of the "stability shear stress" is dependent on the inlet's geometry, sediment size, channel roughness, and magnitude of littoral drift.

Price (1963) discussed the importance of flow channeling in tidal inlets. He identified the ebb flow as a plane hydraulic jet flaring typically at an angle of 20° from its orifice; the flood occupies lateral channels converging toward the inlet's entrance. Both flows are confined and distorted by local tidal deltas, shoals, and near shore currents.

Oertel (1971) dealt with the near shore area and entrance shoals of the Doboy Sound Estuary, Georgia. He used fluorescent tracers to show seaward sediment transport during ebb tidal flow up to the area of refracted waves on the shoals. At this point the sediment flow turned landward. During ebb, in the near shore zone adjacent to the estuary Oertel found two distinct directions of sediment transport. Shoreward of the breaker zone sediment was found to move toward the inlet under the influence of breaking waves. Seaward of the breakers sediment moved parallel to the coast away from the estuary in response to the ebb tidal currents.

Sediment transport theories and studies attempt to relate the strength of water flow to the initiation of sediment movement and rate of transport. The bulk of these studies have been made in controlled laboratory flumes and wave tanks far removed from the complicated natural environment of interacting waves, tidal currents, and meteorologically induced flow, all acting over a rough deformable bed. Sediment motion is initiated when fluid forces exceed the forces acting to restrain the sediment particle. At present, no formula or theory has been field verified to describe sediment motion for a given set of interacting wave and current conditions.

Early work by Hjulstrom (1939) resulted in a now commonly used relationship between grain size and the velocity of unidirectional flow measured one meter above the bottom, necessary to initiate motion. Komar (1973) developed a similar relationship for sediment transport under oscillatory wave conditions. Previously, Hjulstrom's or the similar work of Shields (1936) had been used to deal with both modes of flow.

Most formulas for bed load transport involve the concept of shear stress, some using a semirational, semidimensionless argument, while other formulae are purely empirical. The DuBoys (1879) formula for bed load transport is based on empirical values for the critical shear stress and is one of the simplest models still in use. DuBoy divided the bed into a series of layers, the velocity of each layer varying linearly by equal increments from zero to a maximum. A critical shear stress is achieved when the top layer just resists motion. Einstein (1942), using the concepts of boundary layer theory and turbulence, derived a formula based on the probability of a particle being discharged from the bed and transported through time and space. Einstein's relationship is in agreement with the earlier work of Shields and agrees well with empirical data based on low sediment discharge and uniform grain size material. For higher discharge rates and for sediment transport over beds of graded sediment the agreement with empirical data diminishes. Bagnold (1966) approached the problem of bed load motion from rational considerations of energy balance and mechanical equilibrium as deduced from the principles of physics. His treatment is independent of empirical data and makes no pretense of being complete.

The agreement of the relationship with the available facts over a wide range of conditions suggests that the theory's foundations are sound.

Ripple marks appear shortly after the inception of bed load movement. Their height, wavelength, and form are related to the sediment size and strength of flow. These features are instrumental in initiating flow separation at the ripple crest and the resulting series of eddies and flow expansions and contractions. Inman and Bowen (1963) and Inman and Tunstall (1972) found that asymmetrical sand ripples could cause net sand transport to be opposite that of the drift current. This phenomenon was first observed in flume experiments with current flowing in the direction of wave travel. Later, field experiments were conducted by changing the orientation of prefabricated asymmetrical bed.forms placed on the bottom under near shore wave conditions. Depending on the orientation of the asymmetrically rippled bed, sediment transport could be directed either shoreward or seaward. This interaction, associated with the phase dependent mechanism of vortex formation in the lee of the ripple crest, further complicates the question of transport rate and direction.

III.

EXPERIMENTAL DESIGN

Drogue Study

The investigation of the effect of the hydraulics of the inlet on the coastal current zone in front of Cedar Island was made in two separate parts. The first phase of the investigation was concerned with the hydraulic currents and with defining the zone of influence of the inlet through the use of current drogues. The effect of these currents on the local sediment transport during periods of varying wave activity was then investigated using fluorescent tracer sands.

Drogue design and technology date back to the voyage of the Challenger (1885) where drogues were used, then as now, in the study of currents at the selected drogue depth. More recently, thought has been given to errors inherent in the commonly used drogue float system. Terhune (1968) pointed out the importance of maximizing the area of the drogue with respect to the float in order to minimize the drag effect the float has on the drogue. The surface effect of the float becomes a greater problem as the shear stress between the surface float and the drogue increases. This can happen when high winds cause the depth of the effected surface layer to increase.

Terhune applied the equation of fluid drag $F = \frac{1}{2}C_d A p V^2$ (where F is the drag force, C_d the drag coefficient, A the cross sectional area, p mass density of fluid, and V the velocity) to compute the worst possible effect of the float on the drogue. This technique could be utilized to estimate the magnitude of the probable error if the shear stress in the system were known.

Monahan, et.al. (1973) proceeded one step further by actually subtracting the error caused by the shear of the float from the drogue. Assuming steady state conditions, this treatment corrects for the effect of the float and gives a more accurate picture of the current velocities along the original drogue track.

Like Terhune, Monahan's treatment begins with the equation of fluid drag; the actual drag forces on Monahan's drogue float system were measured during tow tank experiments so computation of the drag force was not necessary. The drag coefficient became apparent once the drag force was measured experimentally and the velocity noted. A log-log plot of the drag force and velocity measurements for the drogue float is shown in Figure 5. Using this relationship the error in the current measurement could be calculated provided one knew the magnitude of the surface current and, ultimately a value determined for the current velocity at the depth of the drogue. Monahan's original handling of this

Figure 5. Log-log plot of drag force vs. relative velocity for drogue (F_d) and float (F_f).

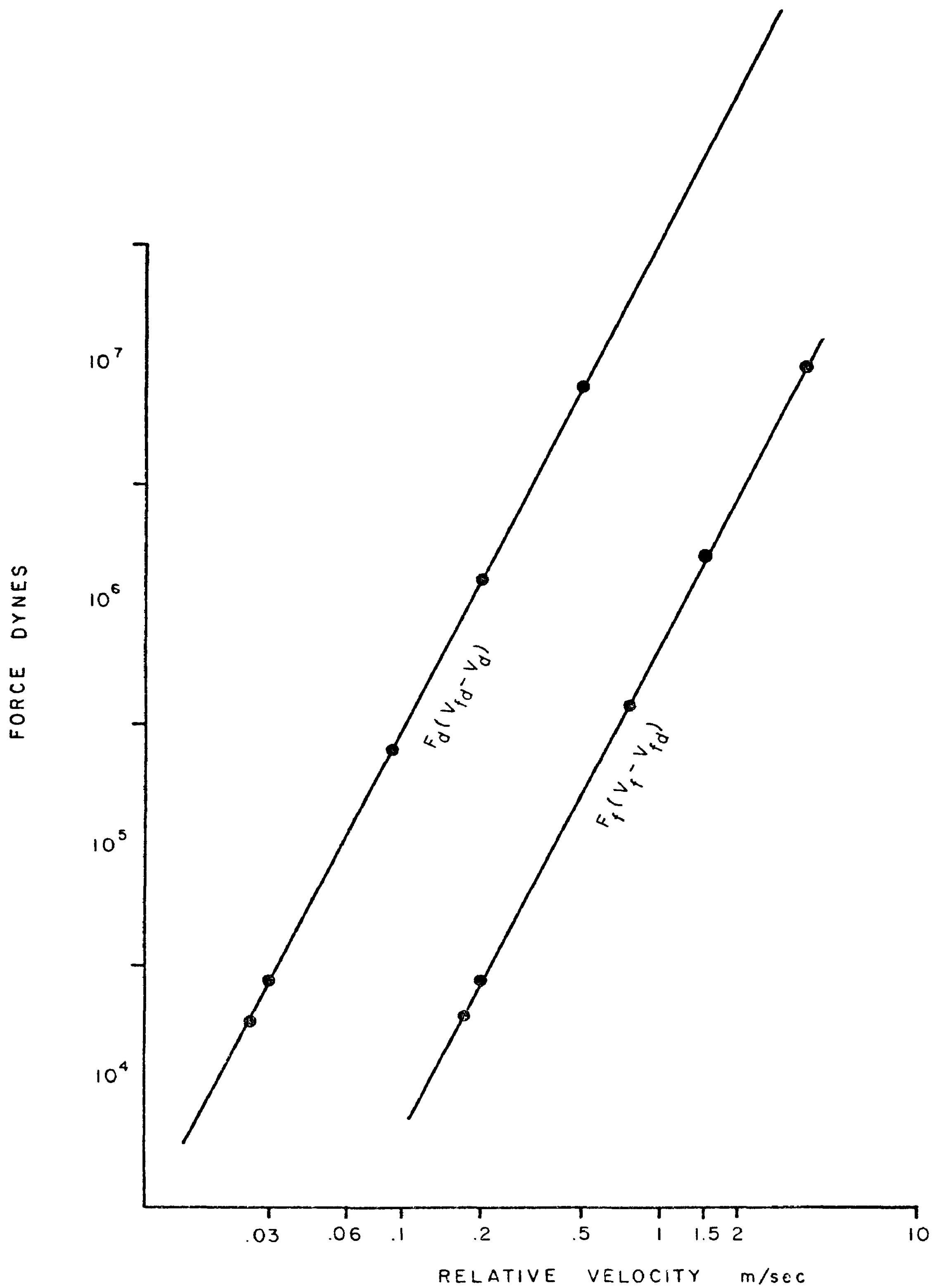

FORCE DYNES
10^7
10^6
10^5
10^4
$F_d(V_{fd}-V_d)$
$F_f(V_f-V_{fd})$
.03
.06
.1
.2
.5
1
1.5
2
10
RELATIVE VELOCITY m/sec

correction method was restricted to the colinear case of both drogue and surface float moving in the same direction but at different velocities. Vector addition and subtraction were utilized to adapt this technique to the two dimensional case encountered in the field.

The fundamental argument for this system lies in the fact that the forces on the surface float and on the drogue are the same. Thus each point on the float curve (F_f) corresponds to a point on the drogue curve (F_d) along the same horizontal line. This procedure consists of vector subtraction of the velocity of the drogue float system (obtained by monitoring such a system) from the velocity of the surface current (V_f) (obtained by monitoring a surface float with no drogue attached). This gives a relative velocity for the surface current with respect to the drogue float system. The value of the drag force on the float can be obtained by going to the graph at this particular relative velocity and finding the force on the float corresponding to that velocity $F_f(V_f-V_{fd})$. Moving horizontally along the graph (the force on the float and the force on the drogue are equal) to the curve for the drogue $F_d(V_{fd}-V_d)$ and then down vertically to the velocity scale one can obtain the velocity of the drogue through the water at its depth of deployment. The final step consists of vectorially subtracting this velocity (speed of drogue through the water) from the velocity of the drogue float system and arriving at the corrected current velocity at the respective drogue depth. A sample of the above calculation is presented in the appendix.

This method of correction, with some modifications, was utilized during the study. As tow tank facilities were not available; graphs were plotted assuming a constant drag ratio (a valid assumption for flat plates at high Reynolds numbers, such as those encountered during the study). Arbitrary velocities which might occur during a drogue run were selected and the projected area of the drogue and float calculated. This led to the computation of the drag forces on the float and the drogue as plotted in Figure 5.

Sediment Study

The sediment transport experiment was designed to determine what effect the ambient current field had on the regional sediment movement. Methods described by Inman (1957, 1962) and Yasso (1962, 1966) were slightly modified and were used to dye local sands. Samples were taken using greased cards (Inman and Bowen 1963, Ingle 1962), and the analysis was made by exposing the sample to radiation in the ultraviolet range of the spectrum.

IV.

PREPARATION AND FIELD STRATEGY

Drogue Study

Drogues were tracked by following the deployed drogues from a boat. At periodic intervals the boat was positioned next to the drogue and sextant angles were taken to reference markers on the beach. Positions were later plotted with a three arm protractor on a reference chart.

Initially eight positions were marked in the sand dunes of Cedar Island at 600 meter intervals using a steel tape. Later, NASA Wallops Island radar based in the town of Wachapreague was used to locate accurately these and other points of interest. Targets were attached to twelve-foot long two-by-fours which were placed at the reference positions for ease of identifications from offshore. To facilitate handling of the data and to delineate the zones of tidal inlet influence, the coastal current zone was divided into eight zones as illustrated in Figure 6. Drogue experiments were conducted when the lateral flanking shoals in front of Cedar Island were small. This condition leads to probable maximum lateral inflow and outflow relative to conditions when the shoals are more developed and extend closer to Cedar Island.

Figure 6. Region under investigation showing individual areas.

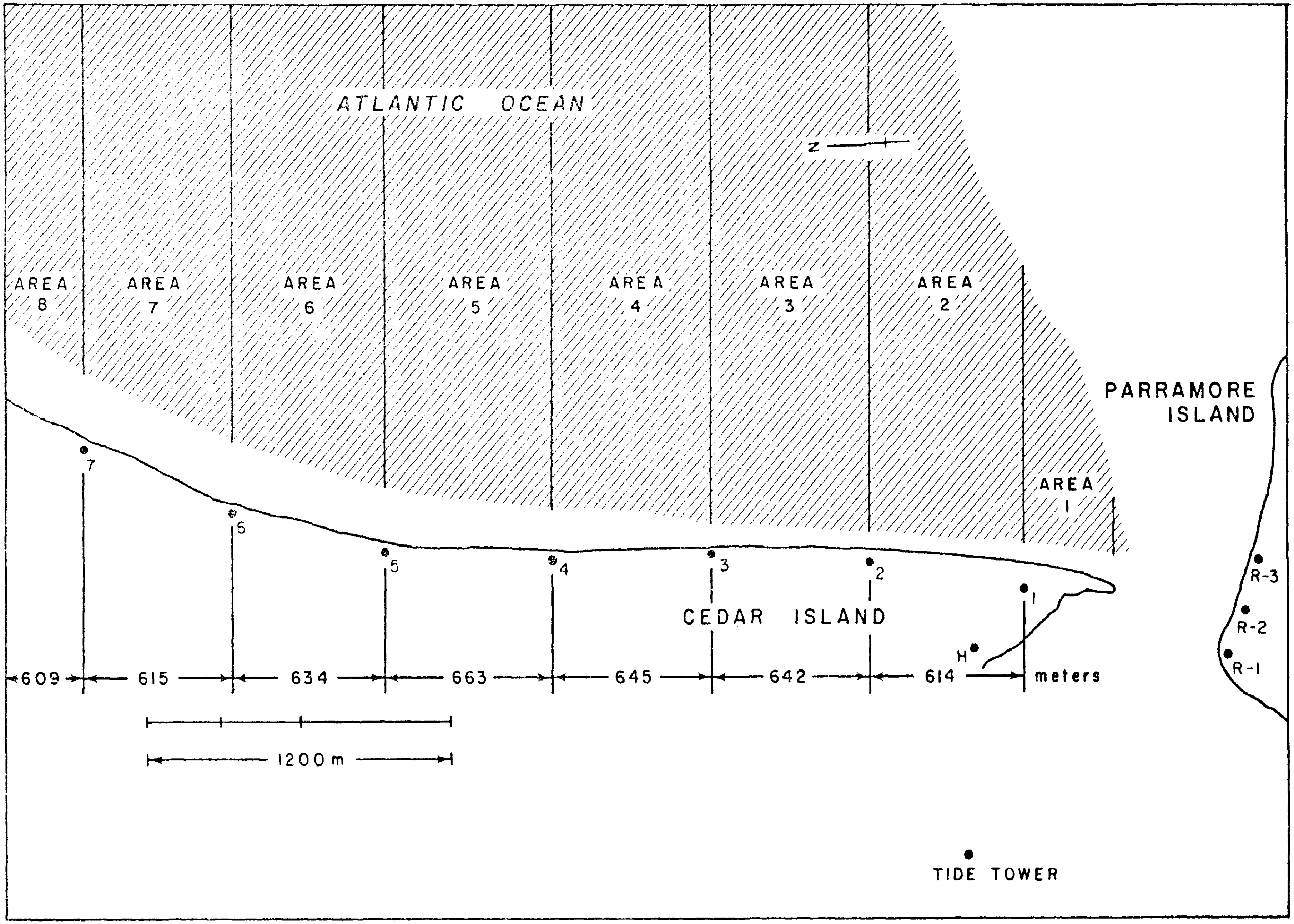

ATLANTIC OCEAN
N
AREA 8
AREA 7
AREA 6
AREA 5
AREA 4
AREA 3
AREA 2
AREA 1
PARRAMORE ISLAND
R-3
R-2
R-1
7
6
5
4
3
2
1
H
CEDAR ISLAND
609
615
634
663
645
642
614
meters
1200 m
TIDE TOWER

Simple current cross drogues were constructed from canvas and iron pipe (Figure 7). Their dimensions were large yet their design permitted the folding and breakdown of the crosses to facilitate handling and storing in small boats. Floats consisted of styrofoam sandwiched between wooden plates with a bamboo staff and flag attached to aid tracking. A simple lanyard the length of which could be varied connected the float to the drogue.

Drogue runs were made on days when wind, wave, and sea conditions were unlikely to have major influence on the float drogue system. Most runs were made with wind velocities less than 4.5 m/sec. (10 miles per hour) and under calm sea conditions. Wind velocity and wave height data were collected during each drogue run. Drogues were deployed from a small boat at the beginning of a tidal cycle and their positions determined at half hour intervals. Usually three drogues and a surface float were deployed. Drogues or floats were recovered and recycled when they strayed out of the study area, entered the inlet, went aground, or drifted so far from shore that the fixed markers on Cedar Island could no longer be seen. It was hoped to obtain complete coverage of the area under investigation during different stages of the tide, and at different positions in the study area. A total of 59 separate drogue tracks were run on

Figure 7. Drogue and float as used to define current field.

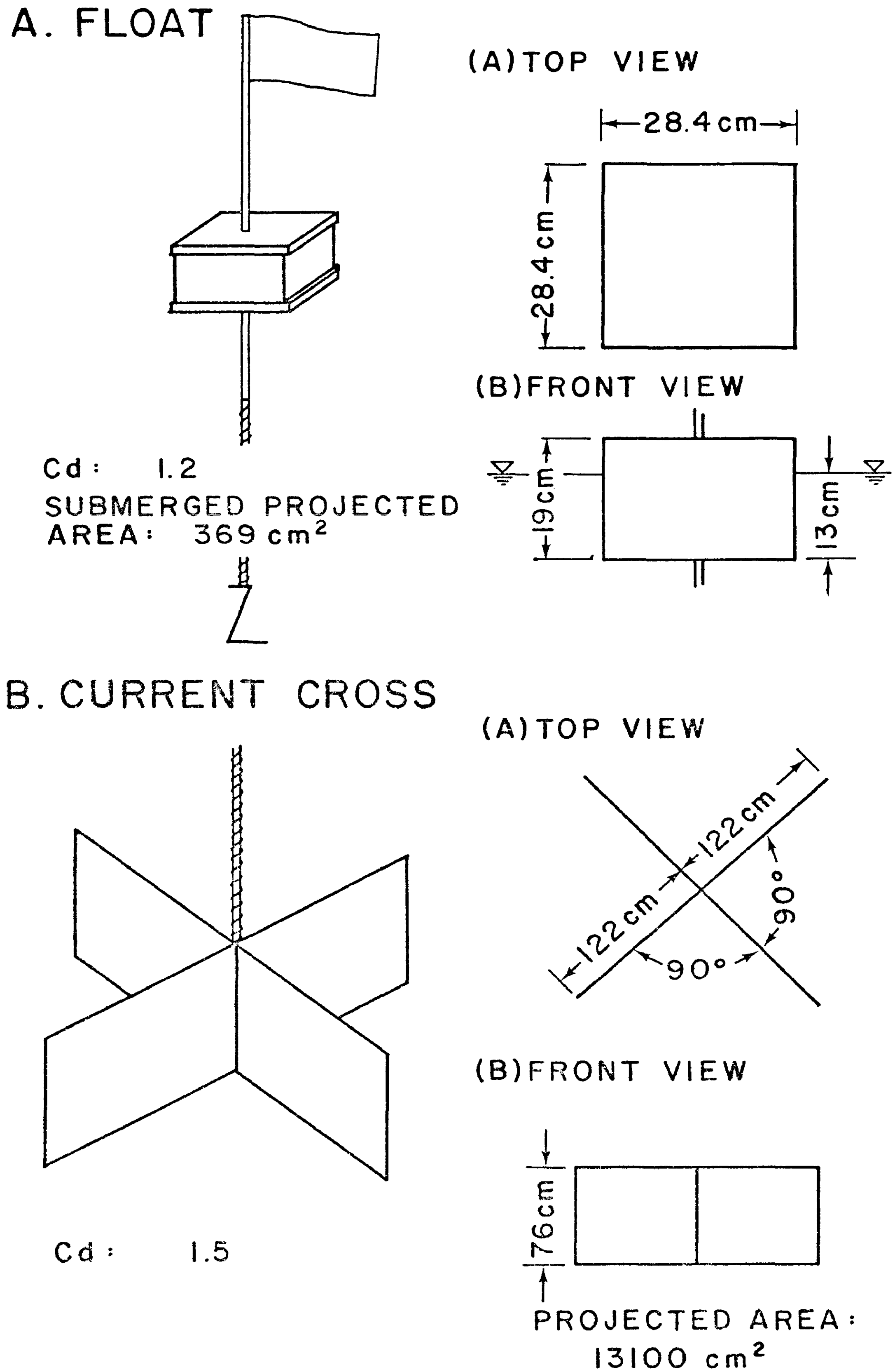
A. FLOAT
(A) TOP VIEW
28.4 cm
28.4 cm
(B) FRONT VIEW
19 cm
13 cm
Cd: 1.2
SUBMERGED PROJECTED AREA: 369 cm²
B. CURRENT CROSS
(A) TOP VIEW
122 cm
122 cm
90°
90°
(B) FRONT VIEW
76 cm
Cd: 1.5
PROJECTED AREA: 13100 cm²

eleven different days (six floods, five ebbs). A recording Savonius rotor current meter was maintained in the inlet throat to obtain base data on the inlet current velocities so that the near shore currents could be compared with flow speeds in the inlet. The drogues were deployed at a depth below mid-water and above the bottom. This usually was two or three meters below the water surface.

There came occasion to test and compare the Lagrangian data gathered by the drogues with the Eulerian data being gathered by the current meter stationed at a depth of thirty feet in the inlet. On June 21, 1973, three drogue tracks came within 50 meters of the current meter; their corrected speeds were .74, .77, and .59 meters/second. Speeds recorded in the inlet by the current meter were .74, .75, and .48 meters/second respectively, all within 11% of the drogue speeds and the first two agreeing within 2%. It is assumed that since neither drogues nor current meter is near any boundary their speeds should be the same.

Sediment Study

Sediment to be dyed was obtained from the ebb drop site area (Figure 8) as this was the most appropriate source (Ingle 1966) to insure introduction of a dyed sediment of the same natural size and hydraulic properties. The sand was washed to remove the silt and clay fractions

Figure 8. Position of sampling grid used during tracer sediment experiments.

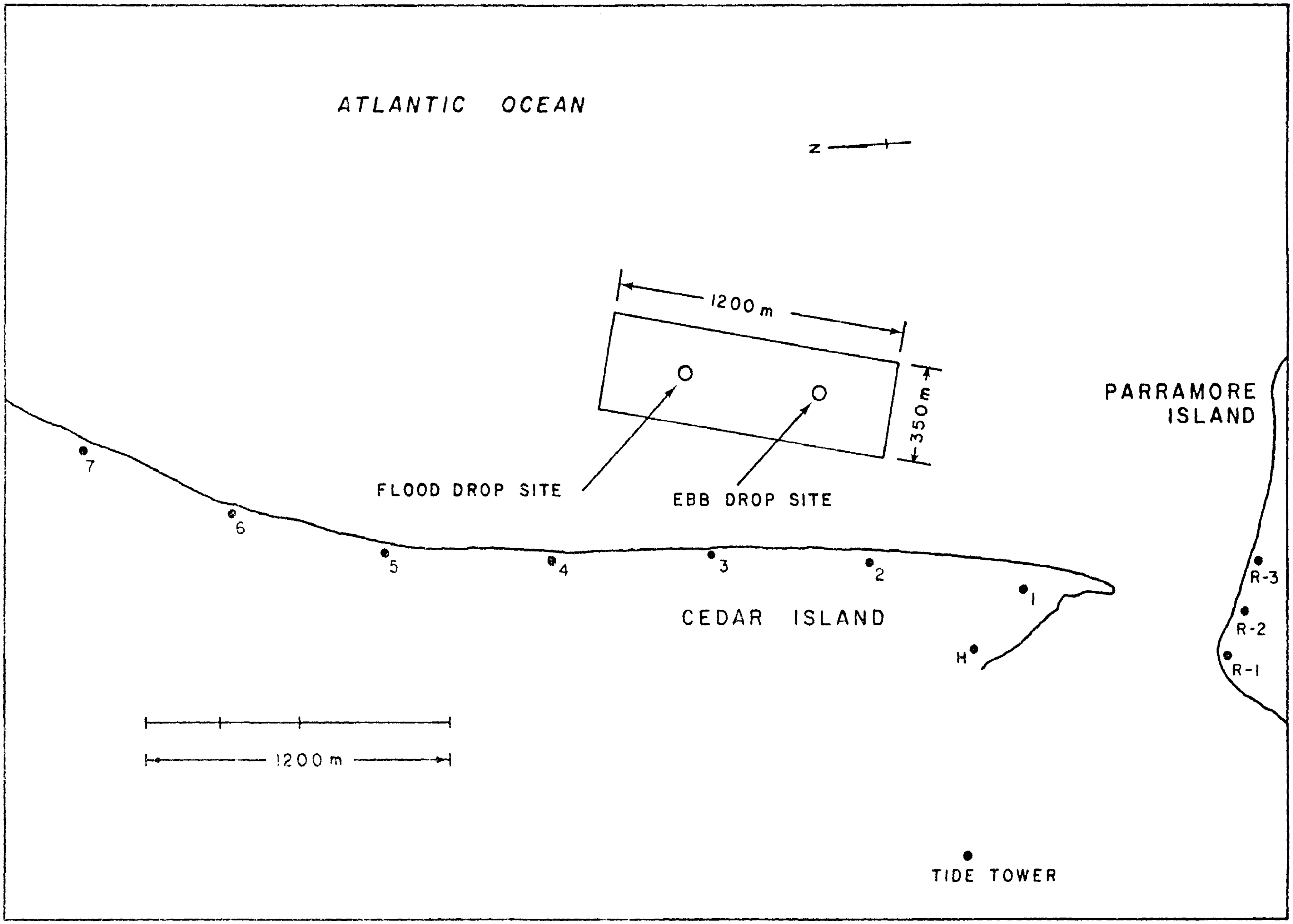
ATLANTIC OCEAN
N
1200 m
350 m
FLOOD DROP SITE
EBB DROP SITE
PARRAMORE ISLAND
7
6
5
4
3
2
1
H
CEDAR ISLAND
R-3
R-2
R-1
1200 m
TIDE TOWER

which would not be dyed effectively and to remove salts which might interfere with the drying process. The sediment then was spread on canvas to dry. When dry, the sediment was saturated with a three to one mixture of toluene and "Day Glo" fluorescent lacquer and again spread to dry in the sun. During the drying process large clumps of sediment were broken apart and after drying the entire sample was sieved through a 1 mm sieve to assure the absence of small clumps which do not occur in the natural environment (all of the sand collected was less than 0.5 mm).

One day prior to a sediment drop a sampling grid was set up situated with its long axis parallel to the beach and in the direction of the general tidal currents. Approximately 50 grid markers consisting of numbered plastic floats attached with rope to 30 cm (12 in.) cinder block anchors were placed in the study area (Figure 8). The positions of the markers were fixed by horizontal sextant angles the day of the experiment.

Just prior to introduction of the dyed tracer sand, samples of the bottom at the release point were taken, ripple mark wave length and height were measured and the bed form was noted. Ninety to one hundred ten pounds of tracer, previously wetted with detergent to reduce surface tension, were released onto the bottom from plastic garbage bags. A current drogue was continually cycled from the drop point to monitor currents.

Several times during the experiment, wave periods and directions were measured and wave height and length estimated (later these estimates were compared to curves of wave period vs. length for specific water depth (King 1973)).

Two rubber boats were employed to gather the samples after the dyed sand was released. At each numbered sampling marker, a 23 x 23 mm card greased with petroleum jelly was removed from a slotted box. The time and station number were recorded on the card. The card was then fixed to a weighted board with rubber bands and lowered to the bottom. After the initial impact the card was raised a short distance and allowed to contact the bottom again. This was repeated a third time to obtain sufficient coverage since numerous closely spaced ripples tended to bias the sample toward ripple crests. The card was retrieved, placed back in the slotted box and the boat moved to another collection site. A total of 180 samples were taken during each of the four experiments; two during ebb and two during flood.

The cards were read by exposing them to UV light in an enclosed box containing a window through which tracer grains could be counted. This method is reputed to be able to distinguish one grain in 10^5 (Ingle 1966). Cards having tracer sediments were placed under a transparent grid where the area of the sand on the card was determined. Thus, it was possible to estimate the concentration of tracer sand per square meter.

V.

DATA REDUCTION AND RESULTS

Drogue Study

The drogue positions were plotted on a large grid (1mm = 5 meters) of the target area prepared from the radar mapping of the Cedar Island stations and adjacent areas. Lines were drawn connecting the points, distances measured, and time interval between successive positions noted. Velocity was computed from this data. The angle was measured with a protractor using a base line drawn between Cedar Island stations number two and number four.

After this base data was obtained a computer program was written to calculate the surface effect of the float on the drogue and determine the corrected current speed and direction. Incorporated in this program was the tidal current velocity in the inlet occurring at the specific time of the drogue track. This was used to generate a dimensionless number (corrected current speed/ speed of current in inlet throat) to compensate for the differences in tidal range and level encountered on the different study days and lead to a more rational comparison of the data.

Plotted drogue tracks for ebb and flood conditions are shown in Figures 9-31. The dotted lines represent the corrected current velocities. An inspection of the drogue and corrected current velocity plots for the ebb phase of the tide shows the tidal currents moving away from the inlet and generally parallel to the coast, except close to area one and two where the currents tend to move seaward. The corrected plots are similar to the actual tracks but represent the prevailing water movement rather than the movement of the float drogue system.

During ebb no direct spatial or temporal response in the coastal current zone in front of Cedar Island due to changing current conditions in the inlet could be seen. Figure 32 shows the mean velocity current ratio (corrected current speed/speed in tidal inlet) diminishing slowly away from the inlet for each consecutive hour of the tide and showing no well defined zone of influence but a near constant current away from the inlet regardless of inlet tidal conditions.

Drogue tracks during flood (Figures 9-22) ran parallel to the island and approached the inlet. Response to changing tidal velocities in the inlet throat were found in the coastal current zone through area number three. Past area number three this response quickly attenuates and velocities remain nearly constant. Further documentation of this trend can be seen in the

Figure 9. Drogue tracks, May 10, 1973 flood. Solid line actual drogue float velocity. Dotted line corrected current speed.

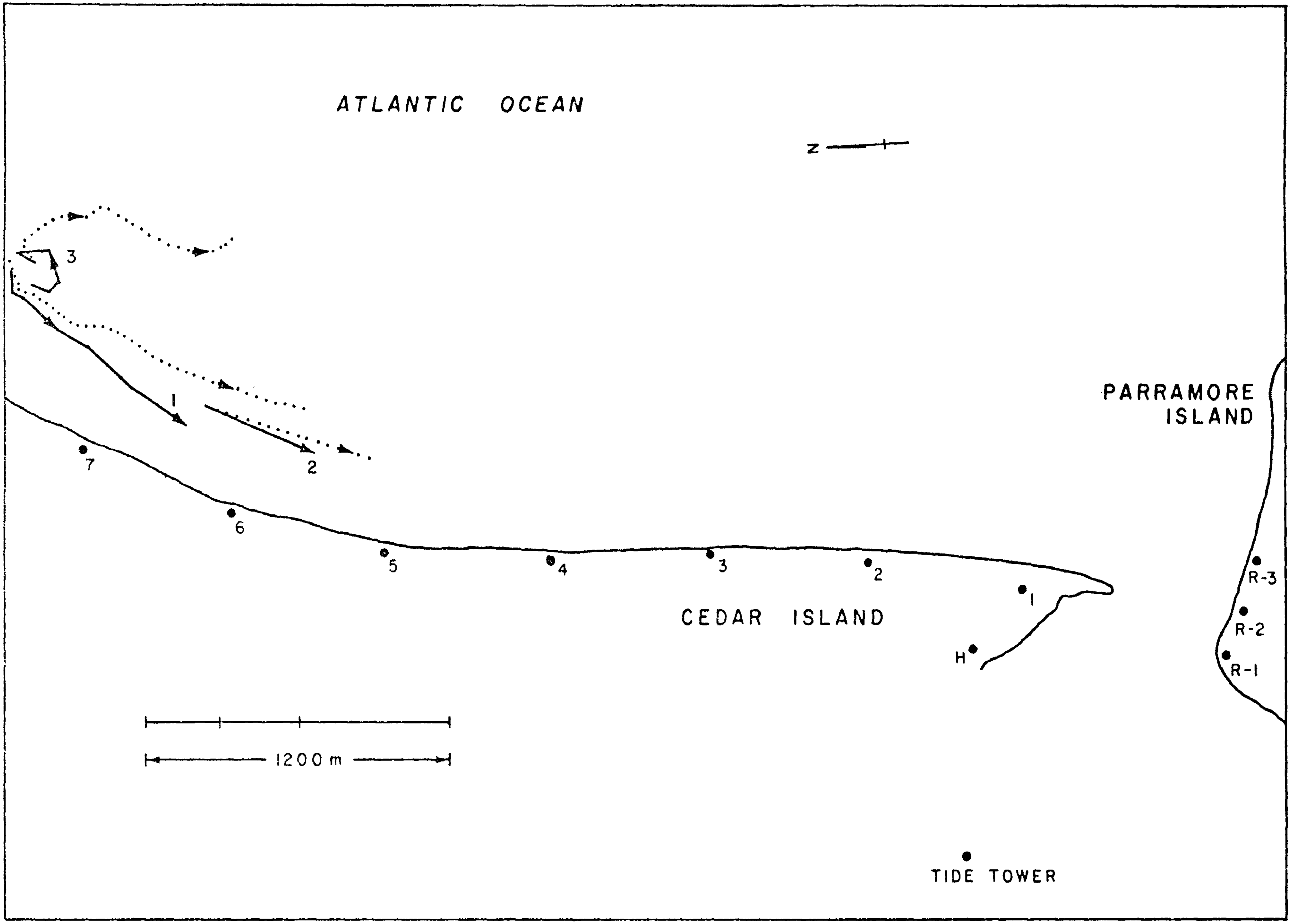
ATLANTIC OCEAN
N
3
1
2
7
6
5
4
3
2
1
H
CEDAR ISLAND
PARRAMORE ISLAND
R-3
R-2
R-1
1200 m
TIDE TOWER

MAY 10

Figure 10. Drogue tracks, May 11, 1973 flood. Solid line actual drogue float velocity. Dotted line corrected current speed.

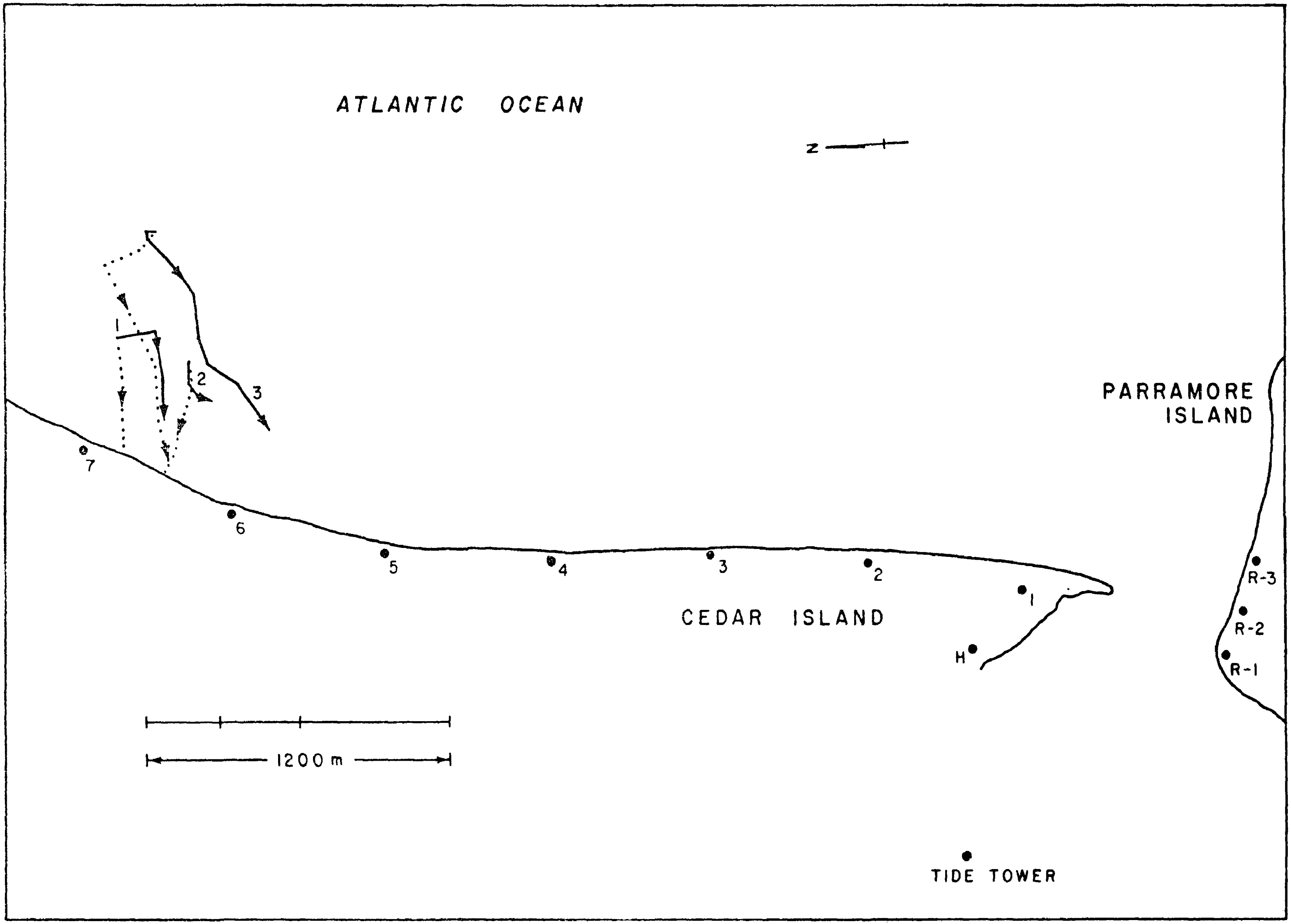
ATLANTIC OCEAN
N
PARRAMORE ISLAND
CEDAR ISLAND
TIDE TOWER
1200 m
R-3
R-2
R-1
H
1
2
3
4
5
6
7

MAY 11

Figure 11. Drogue tracks, May 22, 1973 flood. Solid line actual drogue float velocity. Dotted line corrected current speed.

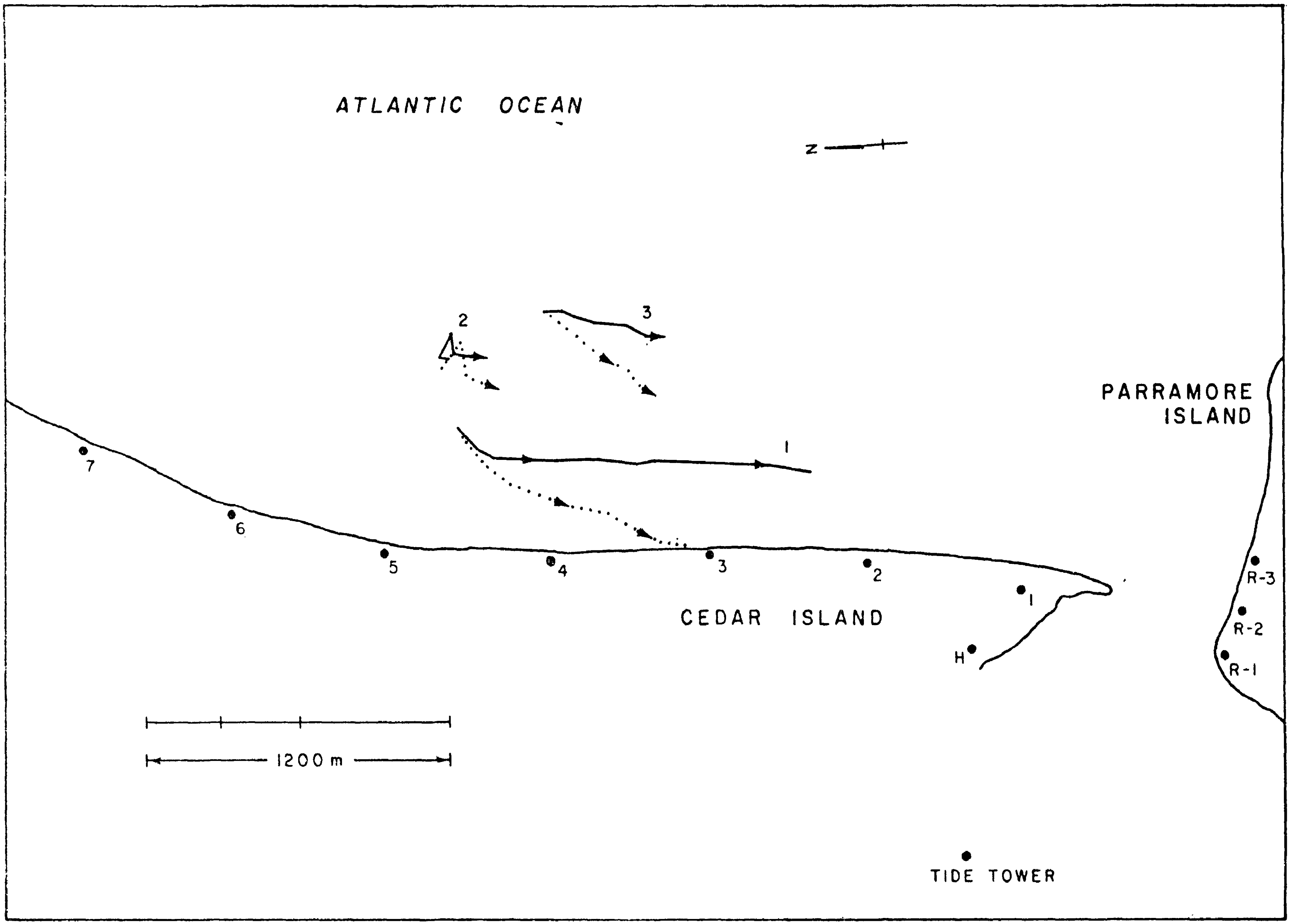
ATLANTIC OCEAN
N
PARRAMORE ISLAND
CEDAR ISLAND
TIDE TOWER
1200 m
1
2
3
4
5
6
7
H
R-1
R-2
R-3

MAY 22

Figure 12. Drogue tracks, June 5, 1973 flood. Solid line actual drogue float velocity. Dotted line corrected current speed.

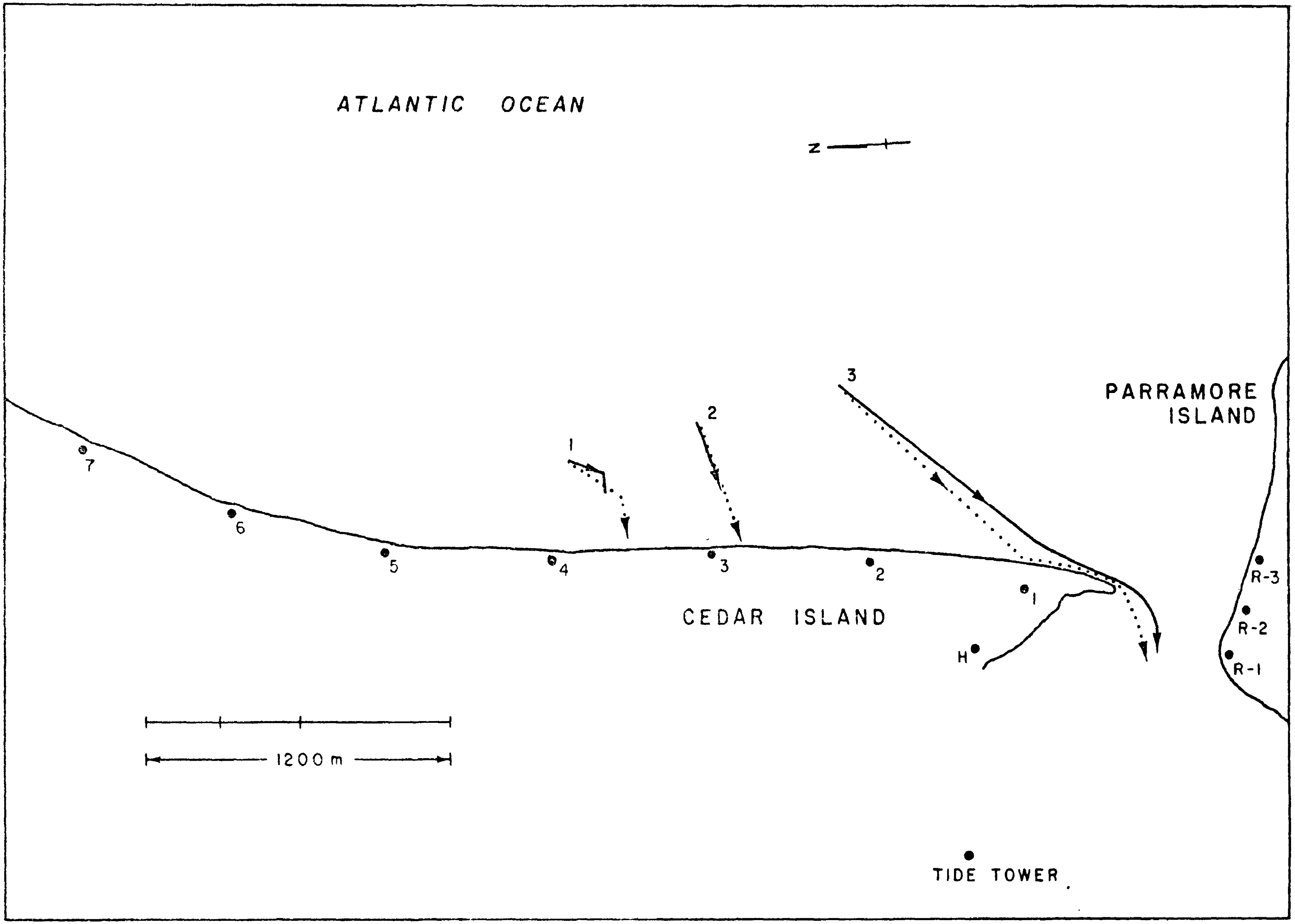
ATLANTIC OCEAN
N
PARRAMORE ISLAND
R-3
R-2
R-1
CEDAR ISLAND
1
2
3
4
5
6
7
H
TIDE TOWER
1200 m

JUNE 5

Figure 13. Drogued tracks, June 5, 1973 flood.
Solid line actual drogue float velocity.
Dotted line corrected current speed.

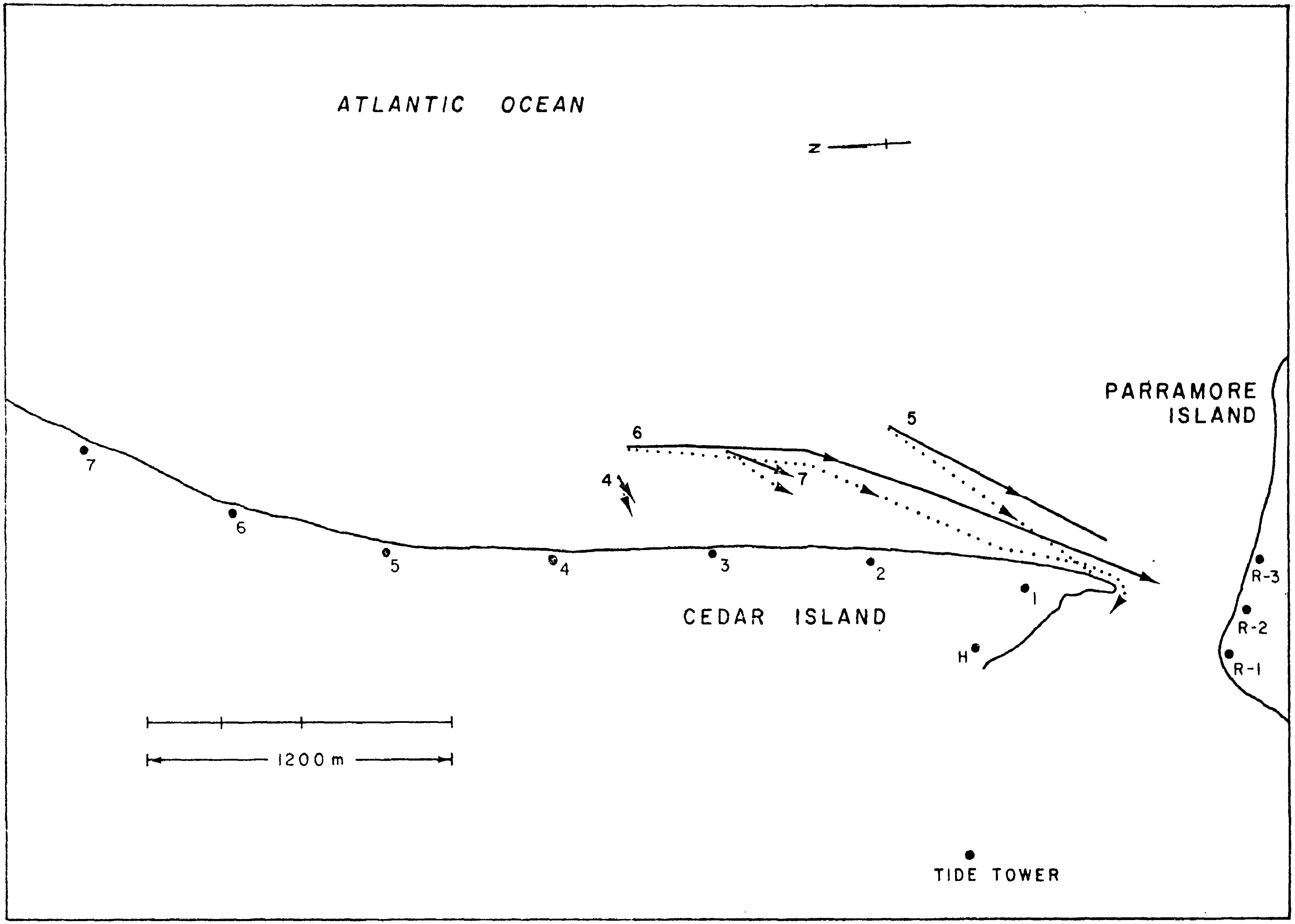
ATLANTIC OCEAN
N
PARRAMORE ISLAND
CEDAR ISLAND
TIDE TOWER
1200 m
R-1
R-2
R-3
H
1
2
3
4
5
6
7

JUNE 5

Figure 14. Drogue tracks June 5, 1973 flood.
Solid line actual drogue float velocity.
Dotted line corrected current speed.

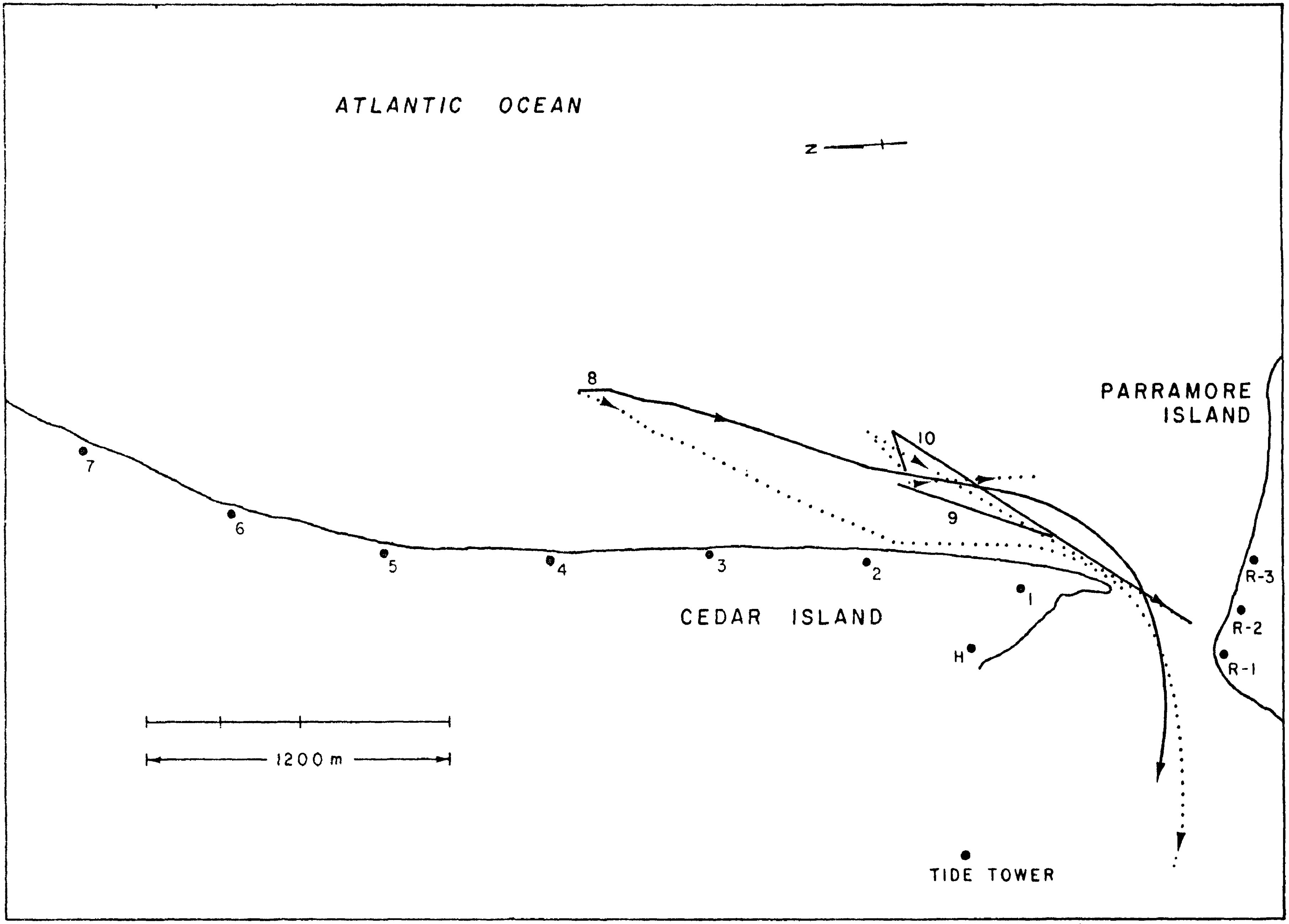
ATLANTIC OCEAN
N
PARRAMORE ISLAND
8
10
9
7
6
5
4
3
2
1
R-3
R-2
R-1
CEDAR ISLAND
H
1200 m
TIDE TOWER

JUNE 5

Figure 15. Drogue tracks, June 7, 1973 flood.
Solid line actual drogue float velocity.
Dotted line corrected current speed.

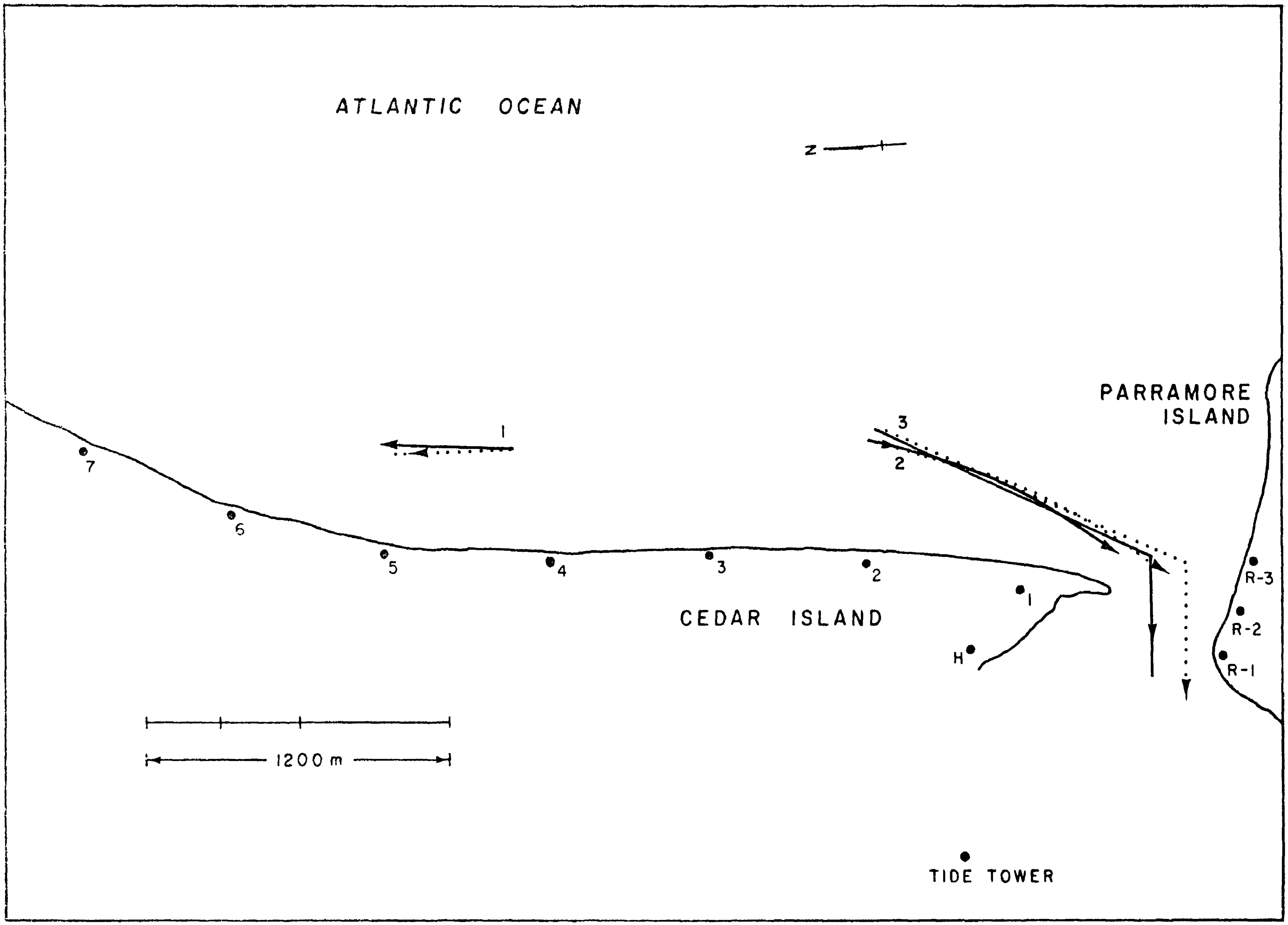

ATLANTIC OCEAN
N
1
3
2
PARRAMORE ISLAND
7
6
5
4
3
2
1
H
R-3
R-2
R-1
CEDAR ISLAND
1200 m
TIDE TOWER

JUNE 7

Figure 16. Drogue tracks, June 7, 1973 flood.
Solid line actual drogue float velocity.
Dotted line corrected current speed.

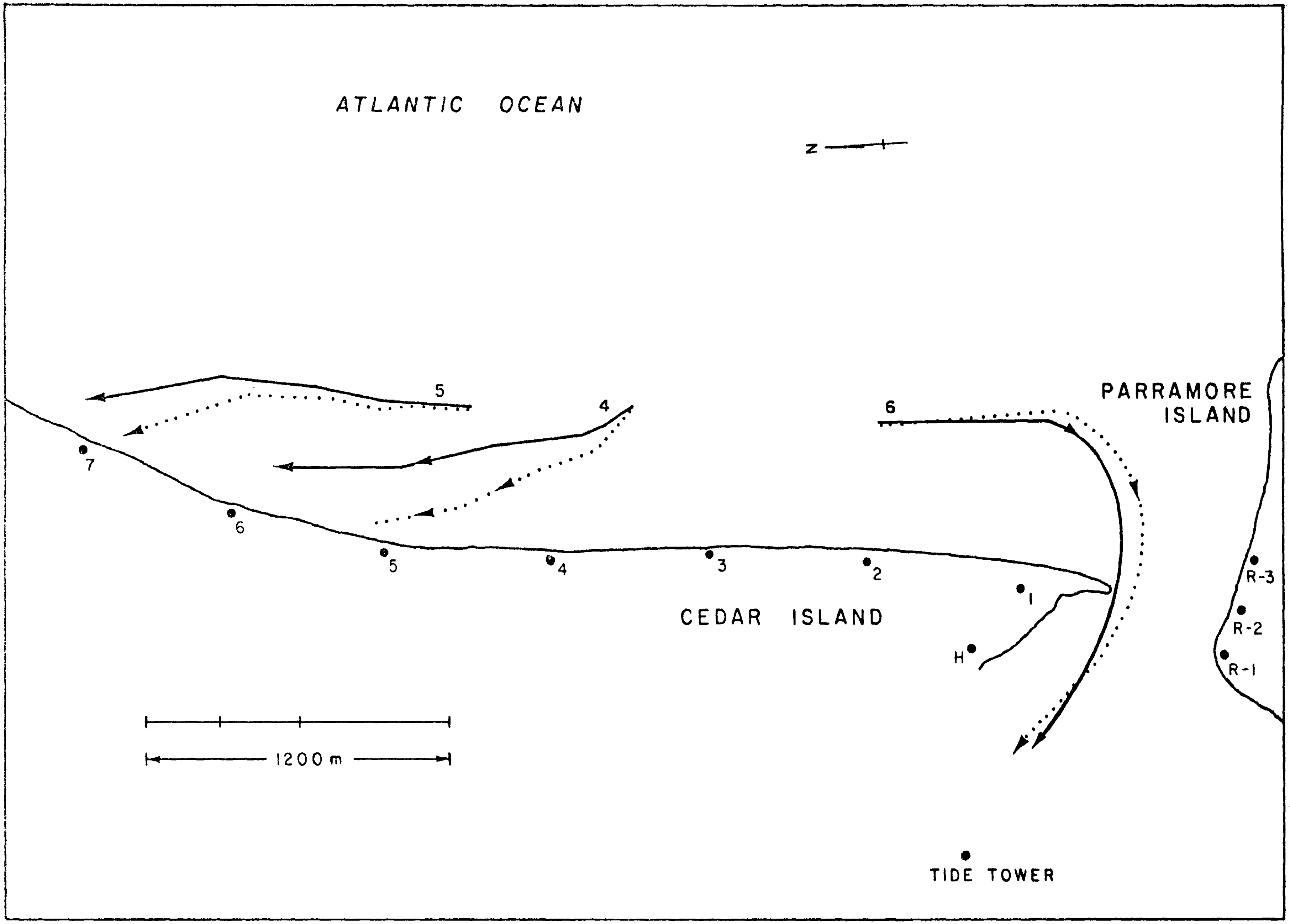
ATLANTIC OCEAN
N
PARRAMORE ISLAND
CEDAR ISLAND
TIDE TOWER
1200 m
R-3
R-2
R-1
H
1
2
3
4
5
6
7
4
5
6

JUNE 7

Figure 17. Drogue tracks June 7, 1973 flood.
Solid line actual drogue float velocity.
Dotted line corrected current speed.

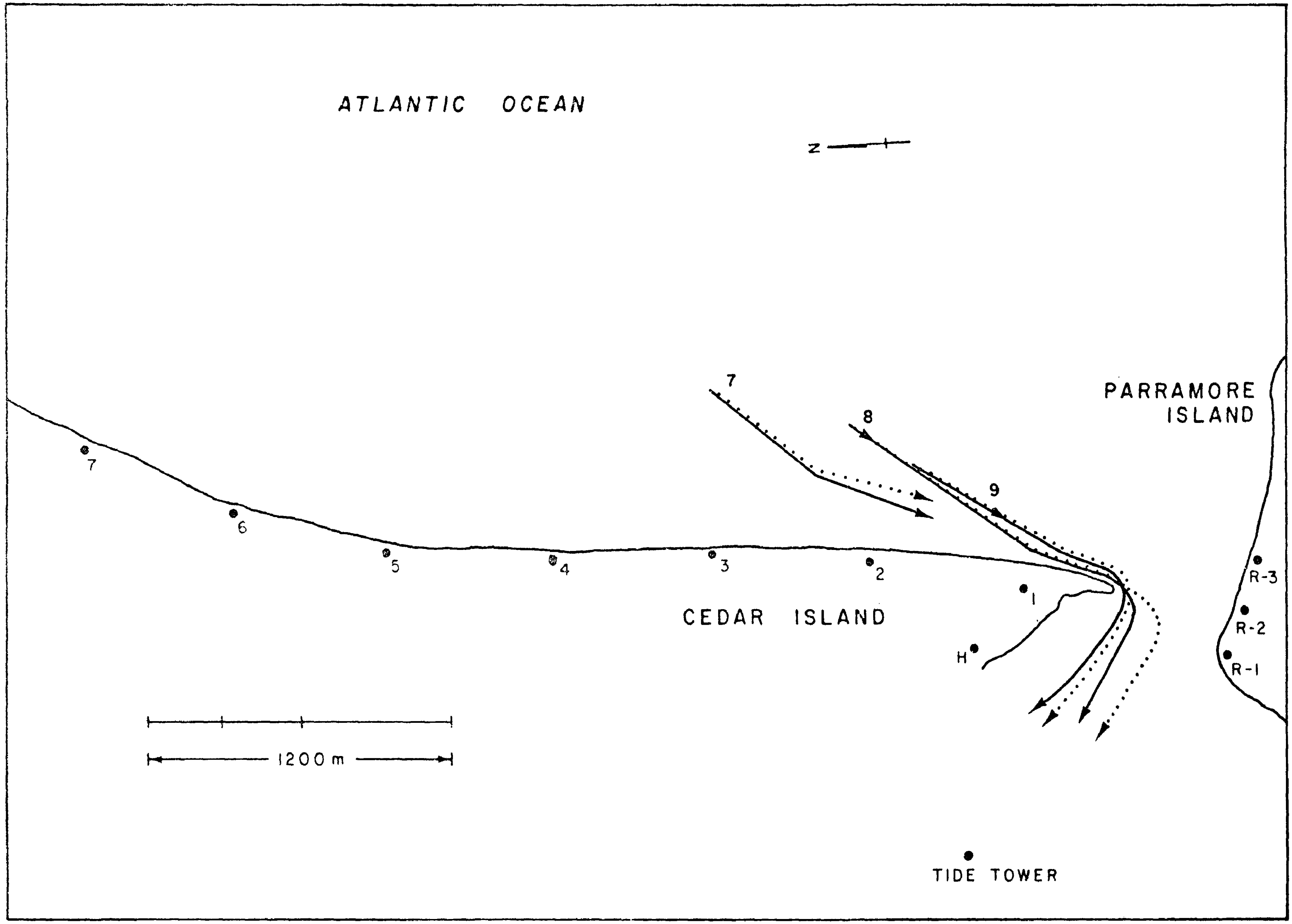
ATLANTIC OCEAN
N
PARRAMORE ISLAND
R-3
R-2
R-1
7
8
9
7
6
5
4
3
2
1
H
CEDAR ISLAND
1200 m
TIDE TOWER

JUNE 7

Figure 18. Drogue tracks, June 21, 1973 flood.
Solid line actual drogue float velocity.
Dotted line corrected current speed.

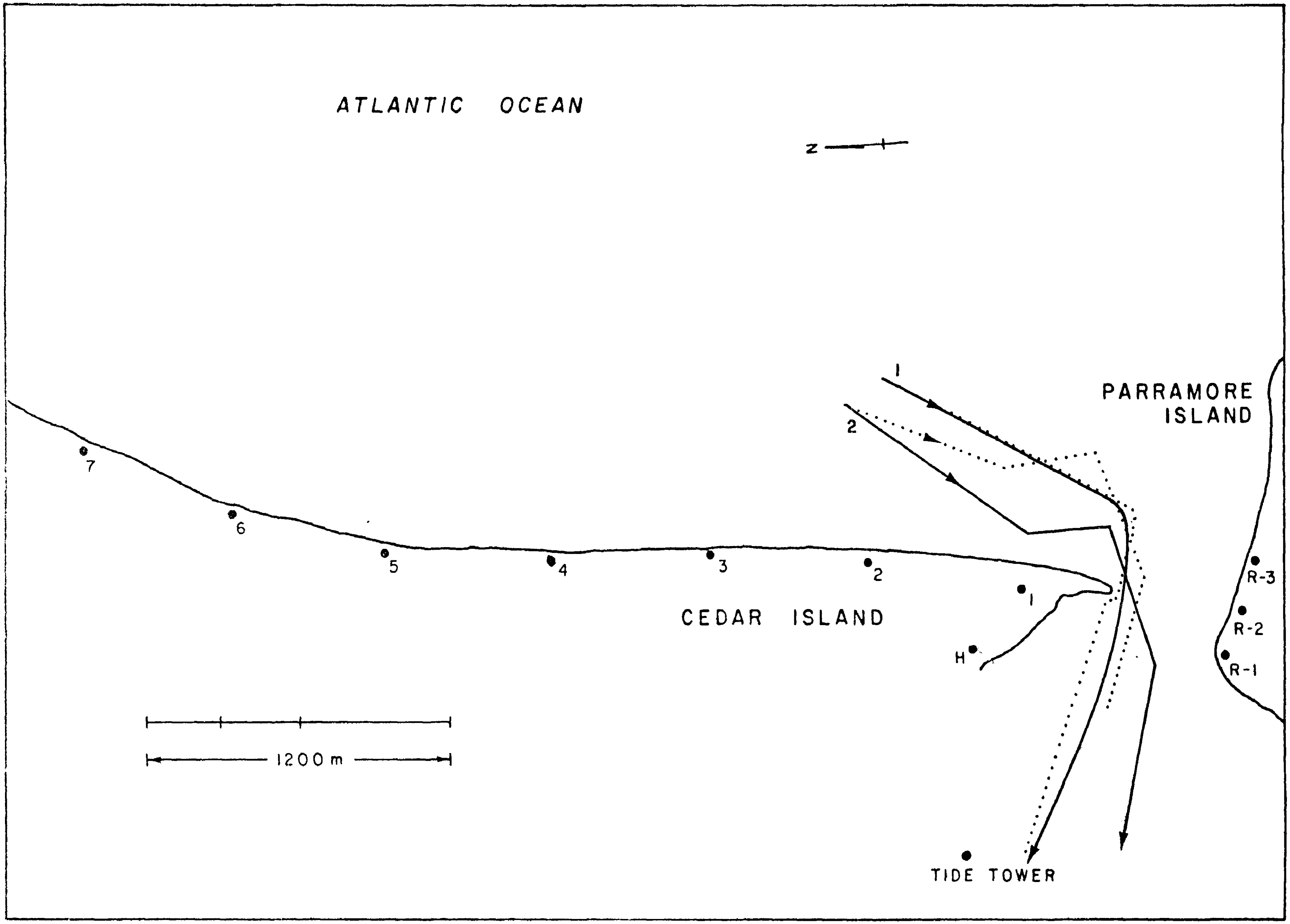
ATLANTIC OCEAN
N
PARRAMORE ISLAND
R-3
R-2
R-1
1
2
CEDAR ISLAND
7
6
5
4
3
2
1
H
1200 m
TIDE TOWER

JUNE 21

Figure 19. Drogue tracks, June 21, 1973 flood.
Solid line actual drogue float velocity.
Dotted line corrected current speed.

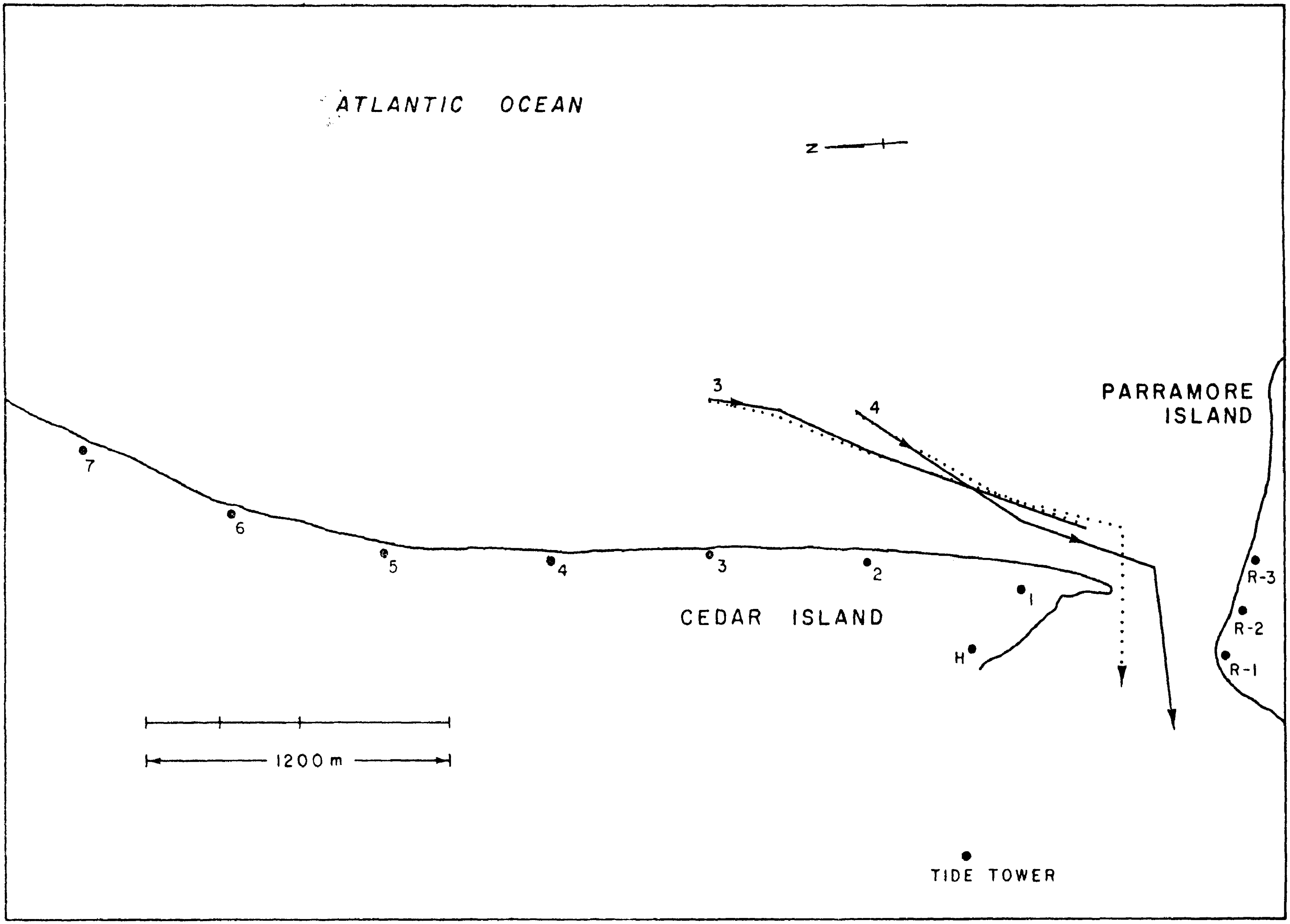
ATLANTIC OCEAN
N
PARRAMORE
ISLAND
3
4
7
6
5
4
3
2
1
H
CEDAR ISLAND
R-3
R-2
R-1
1200 m
TIDE TOWER

JUNE 21

Figure 20. Drogue tracks, June 21, 1973 flood.
Solid line actual drogue float velocity.
Dotted line corrected current speed.

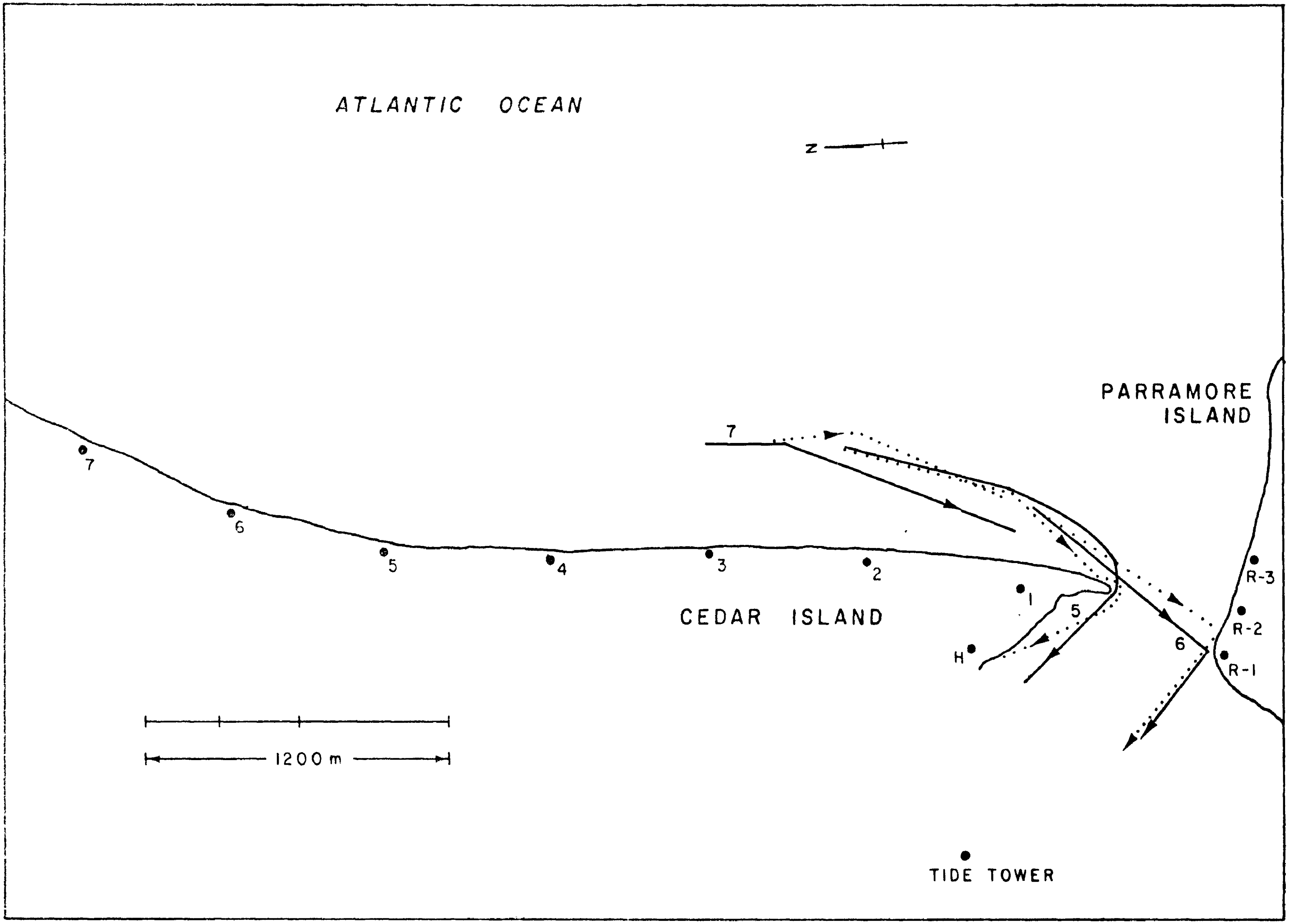
ATLANTIC OCEAN
N
PARRAMORE ISLAND
CEDAR ISLAND
TIDE TOWER
1200 m
7
6
5
4
3
2
1
H
R-1
R-2
R-3

JUNE 21

Figure 21. Drogue tracks, June 21, 1973 flood.
Solid line actual drogue float velocity.
Dotted line corrected current velocity.

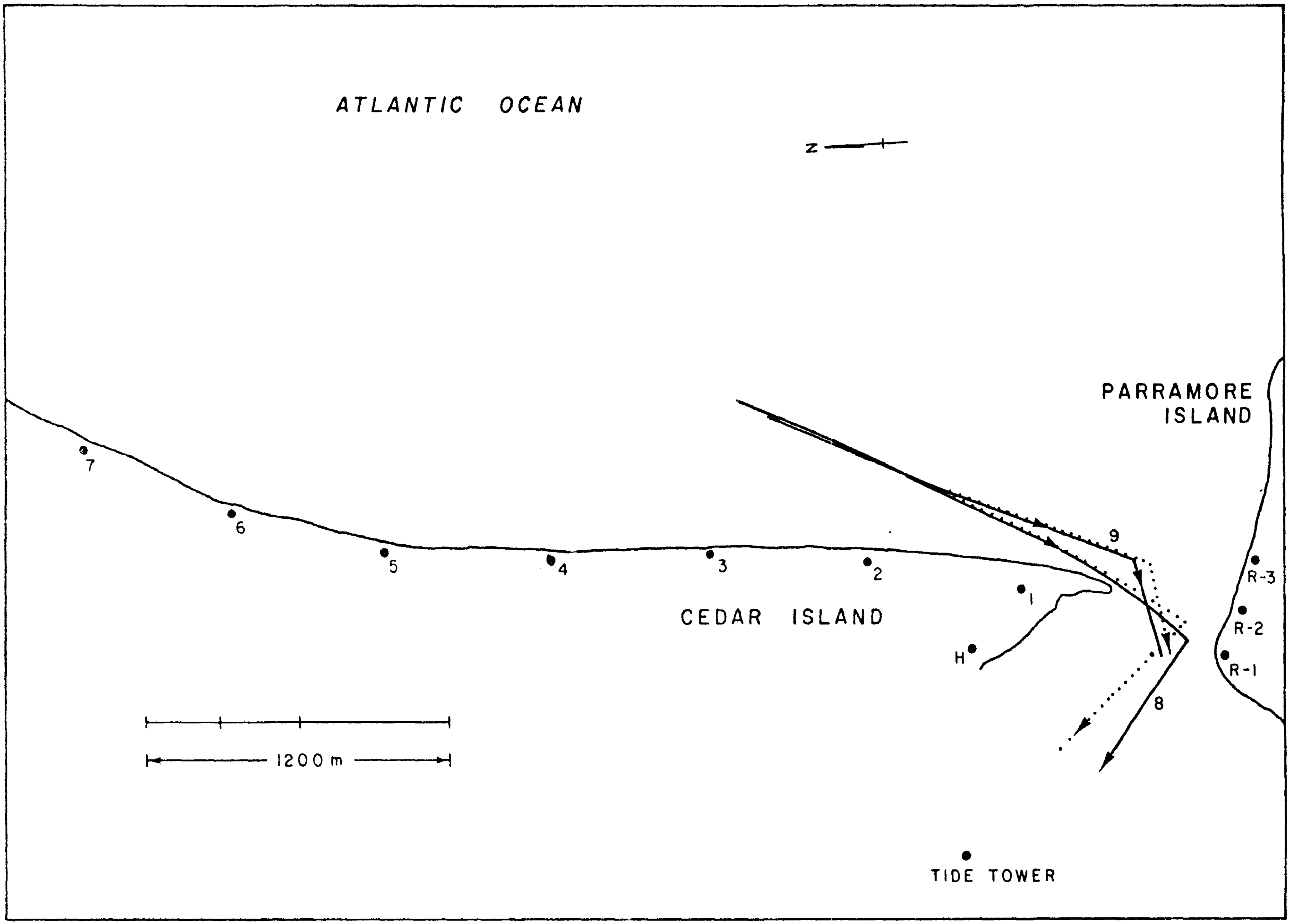
ATLANTIC OCEAN
N
PARRAMORE ISLAND
R-3
R-2
R-1
9
8
7
6
5
4
3
2
1
H
CEDAR ISLAND
1200 m
TIDE TOWER

JUNE 21

Figure 22. Drogue tracks, June 21, 1973 flood.
Solid line actual drogue float velocity.
Dotted line corrected current velocity.

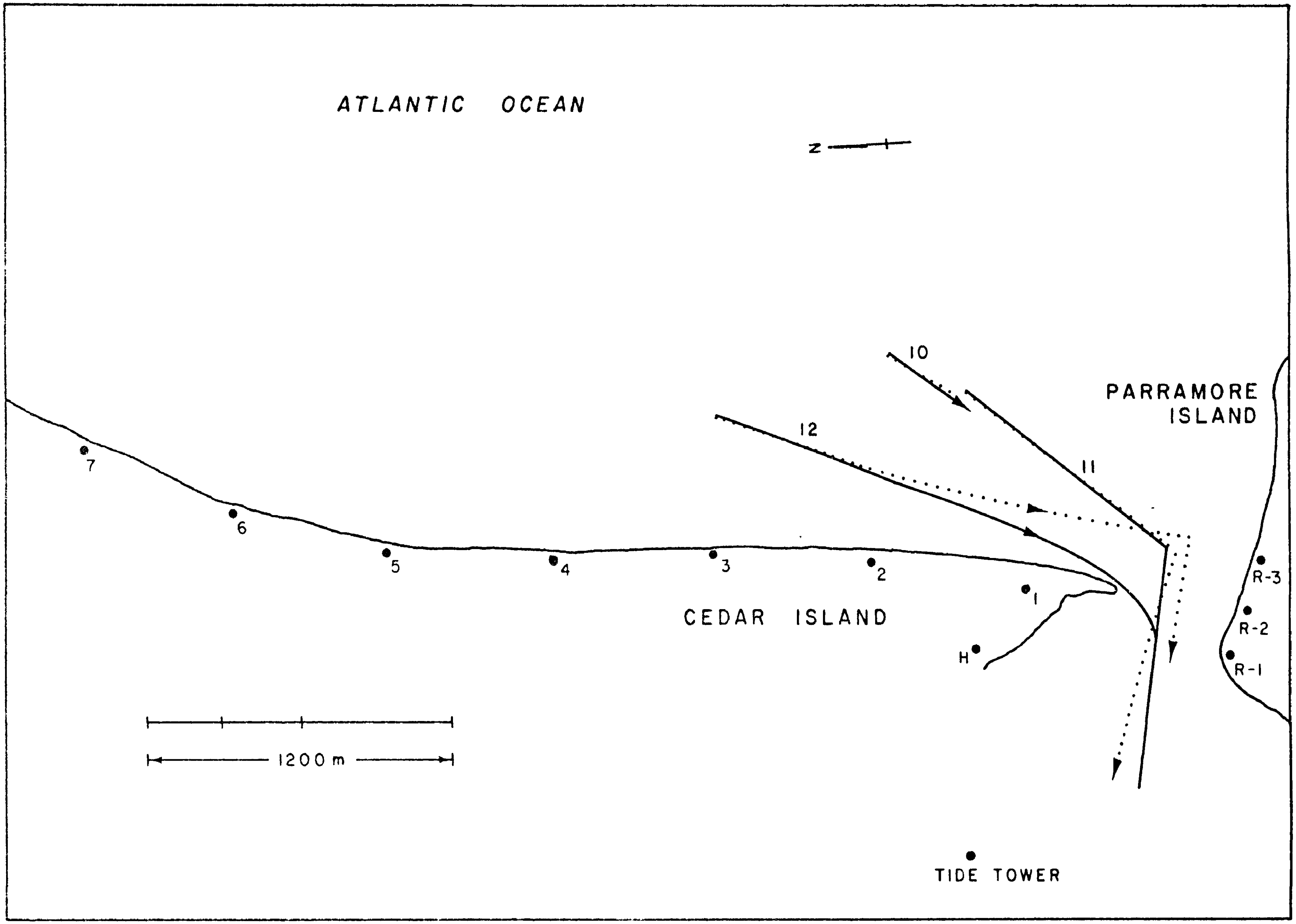
ATLANTIC OCEAN
N
10
12
11
PARRAMORE
ISLAND
7
6
5
4
3
2
1
H
CEDAR ISLAND
R-3
R-2
R-1
1200 m
TIDE TOWER

JUNE 21

Figure 23. Drogue tracks, May 4, 1973 ebb.
Solid line actual drogue float velocity.
Dotted line corrected current velocity.

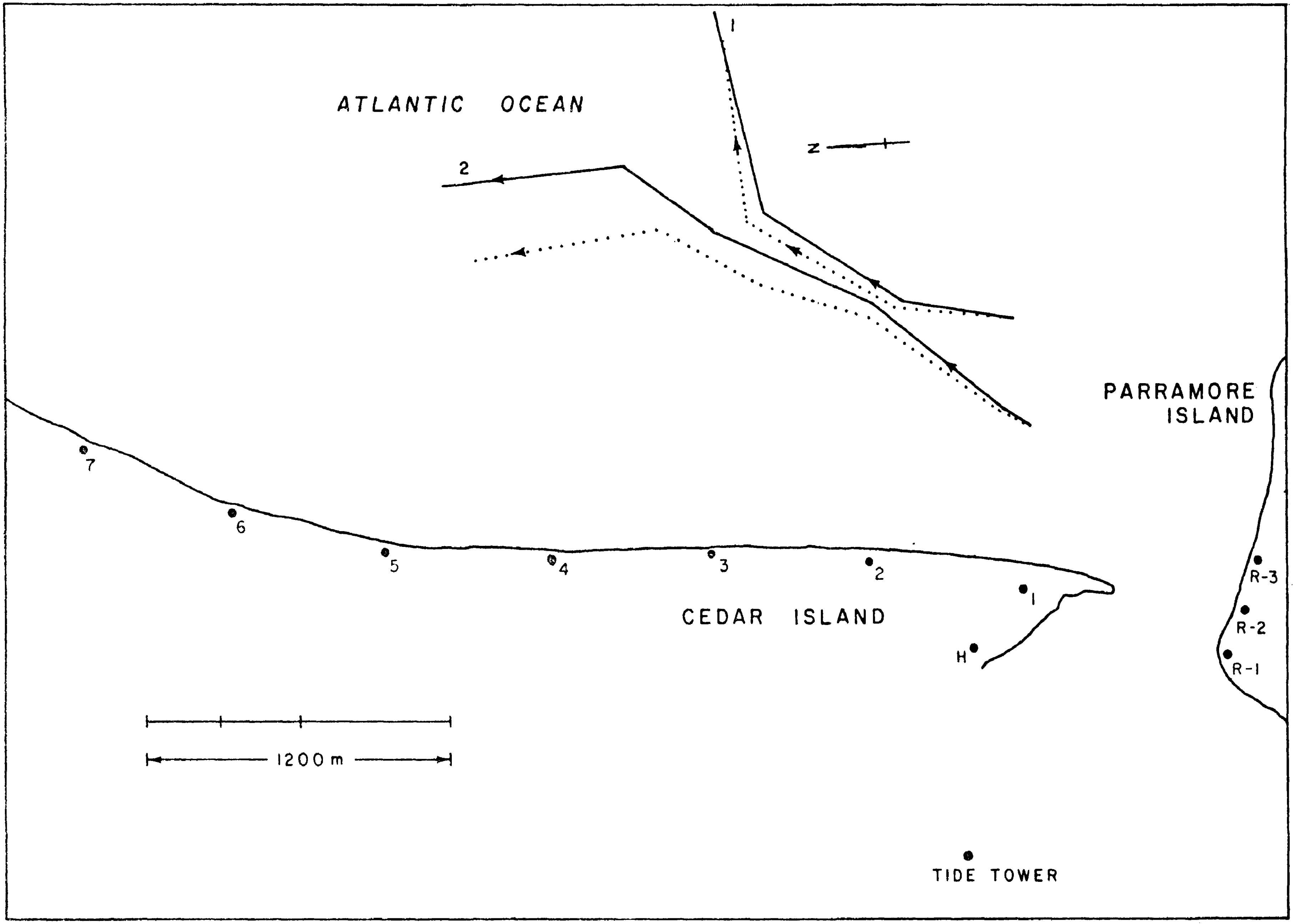
ATLANTIC OCEAN
1
2
N
PARRAMORE ISLAND
CEDAR ISLAND
7
6
5
4
3
2
1
H
R-3
R-2
R-1
1200 m
TIDE TOWER

MAY 4

Figure 24. Drogue tracks, May 4, 1973 ebb.
Solid line actual drogue float velocity.
Dotted line corrected current velocity.

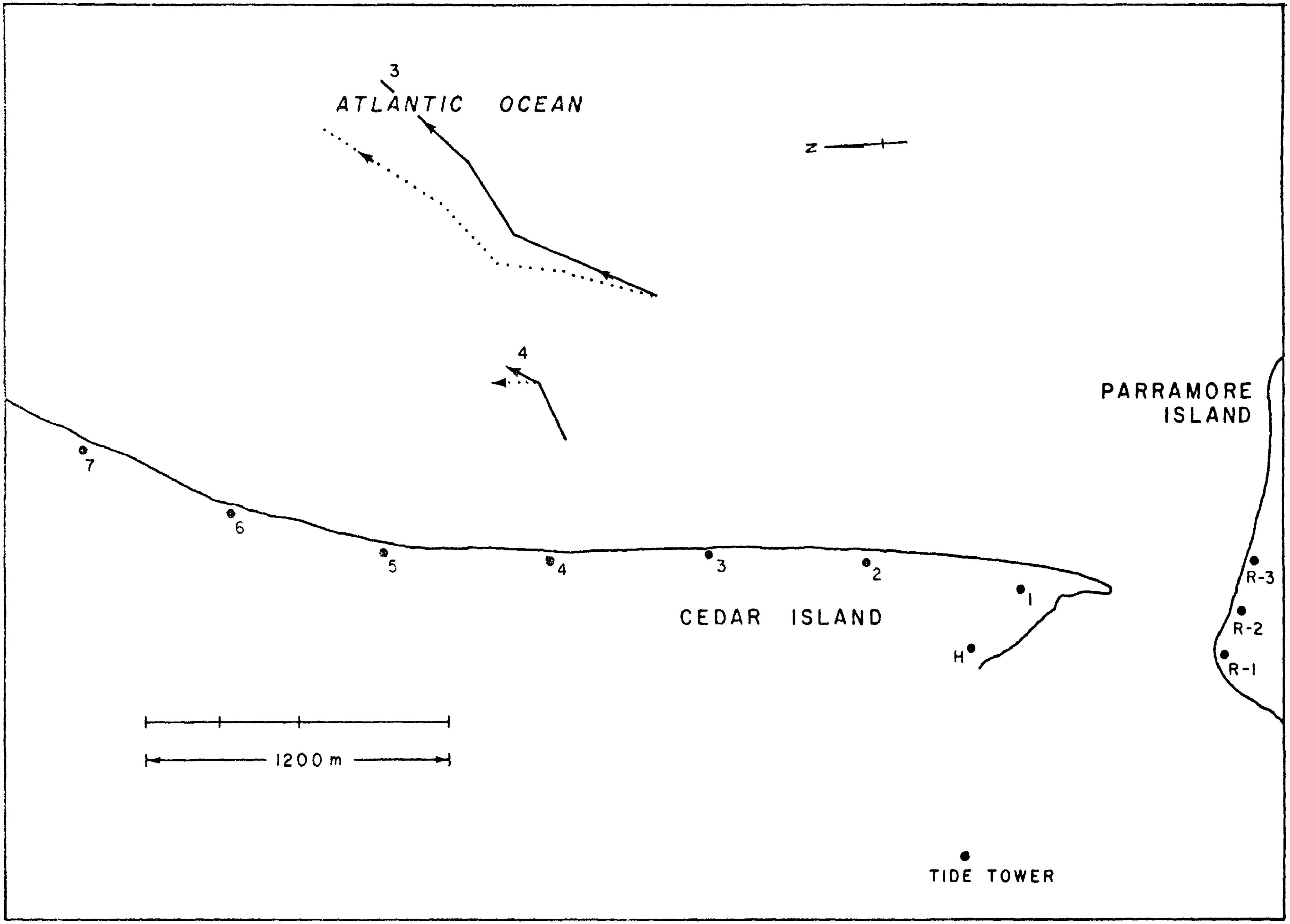
3
ATLANTIC OCEAN
N
4
PARRAMORE ISLAND
7
6
5
4
3
2
1
CEDAR ISLAND
H
R-3
R-2
R-1
1200 m
TIDE TOWER

MAY 4

Figure 25. Drogue tracks, May 21, 1973 ebb.
Solid line actual drogue float velocity.
Dotted line corrected current velocity.

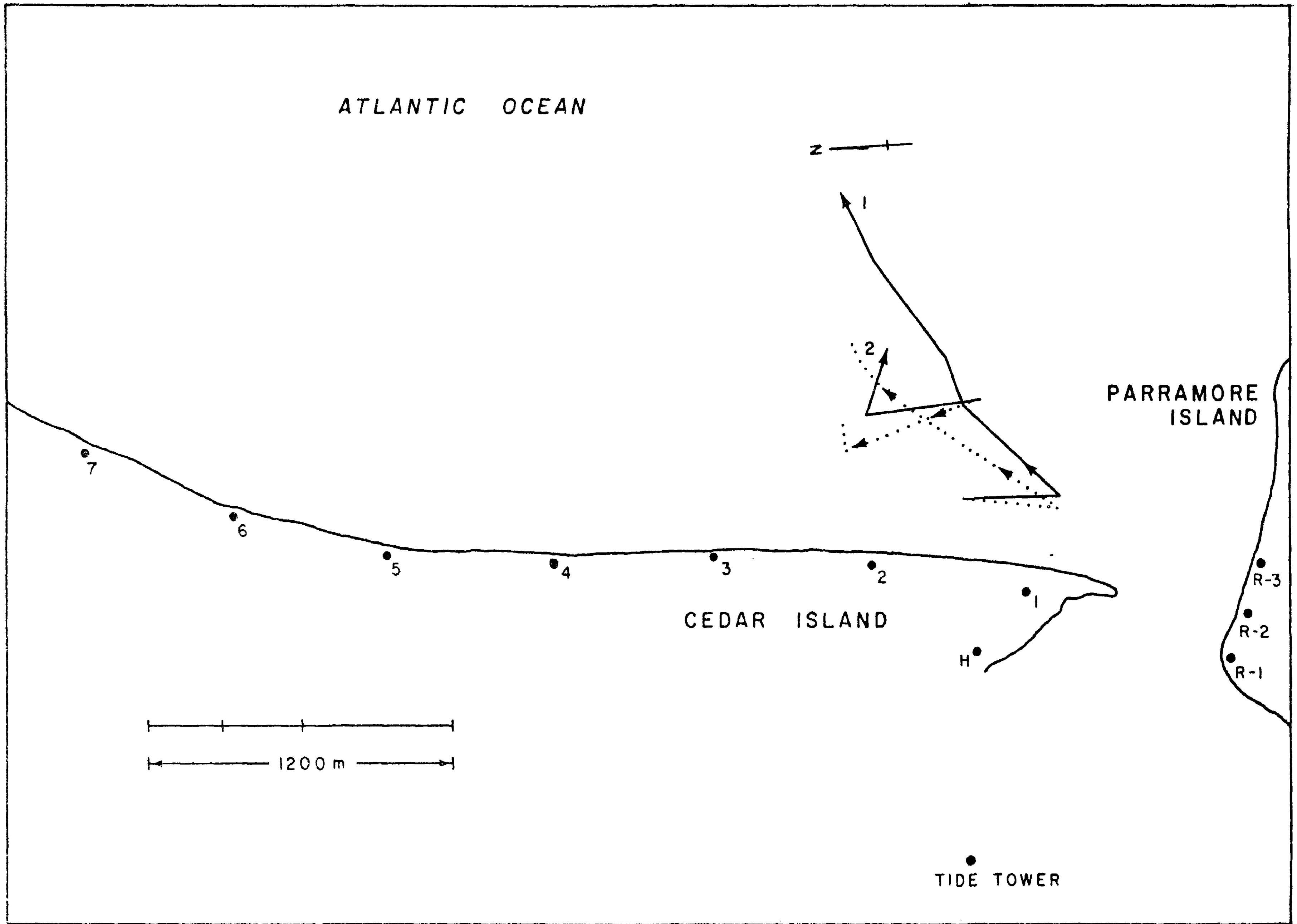
ATLANTIC OCEAN
N
1
2
PARRAMORE ISLAND
7
6
5
4
3
2
1
CEDAR ISLAND
H
R-3
R-2
R-1
1200 m
TIDE TOWER

MAY 21

Figure 26. Drogue tracks, May 21, 1973 ebb.
Solid line actual drogue float velocity.
Dotted line corrected current velocity.

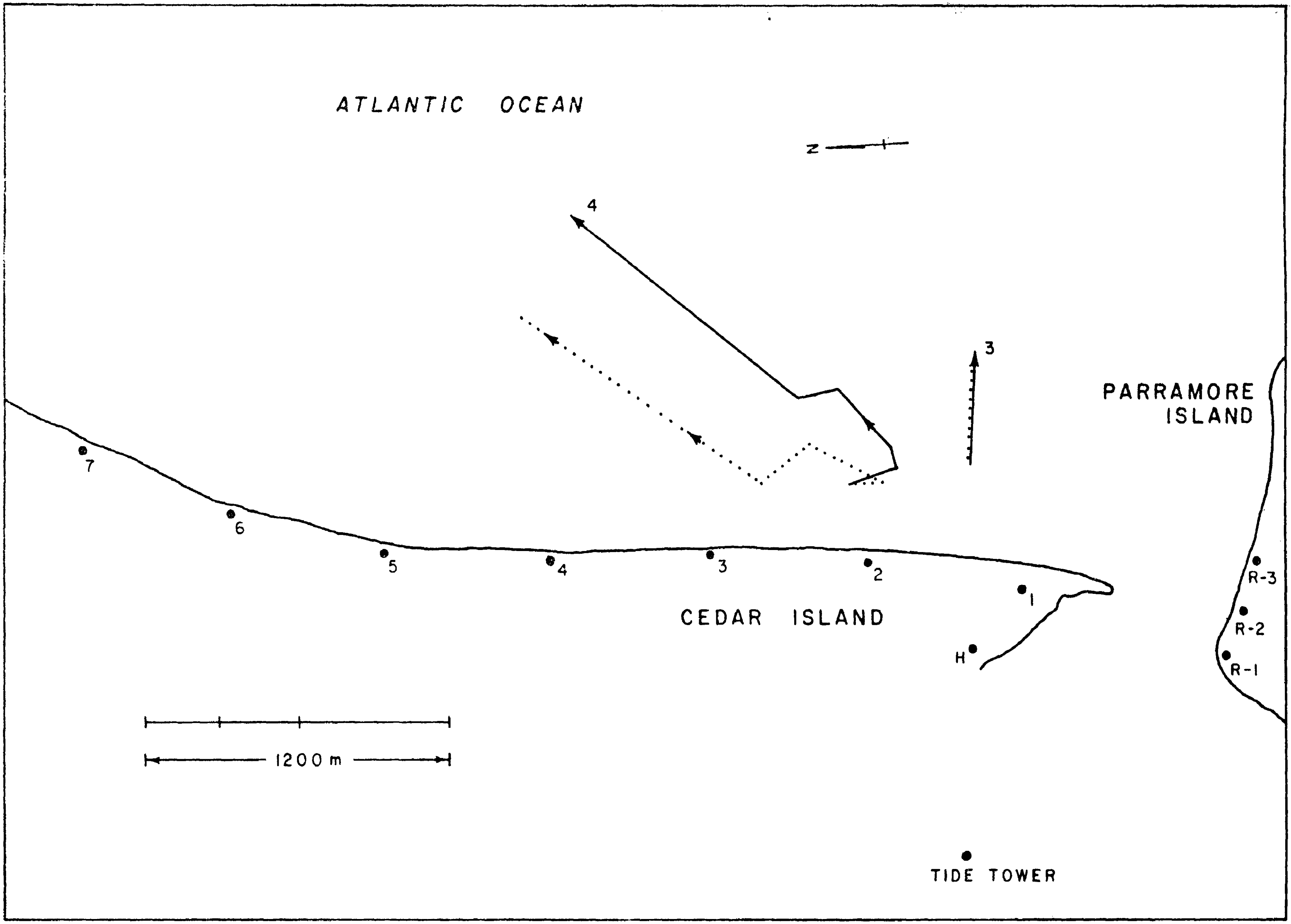
ATLANTIC OCEAN
N
4
3
PARRAMORE ISLAND
7
6
5
4
3
2
1
CEDAR ISLAND
H
R-3
R-2
R-1
1200 m
TIDE TOWER

MAY 21

Figure 27. Drogue tracks, June 4, 1973 ebb.
Solid line actual drogue float velocity.
Dotted line corrected current velocity.

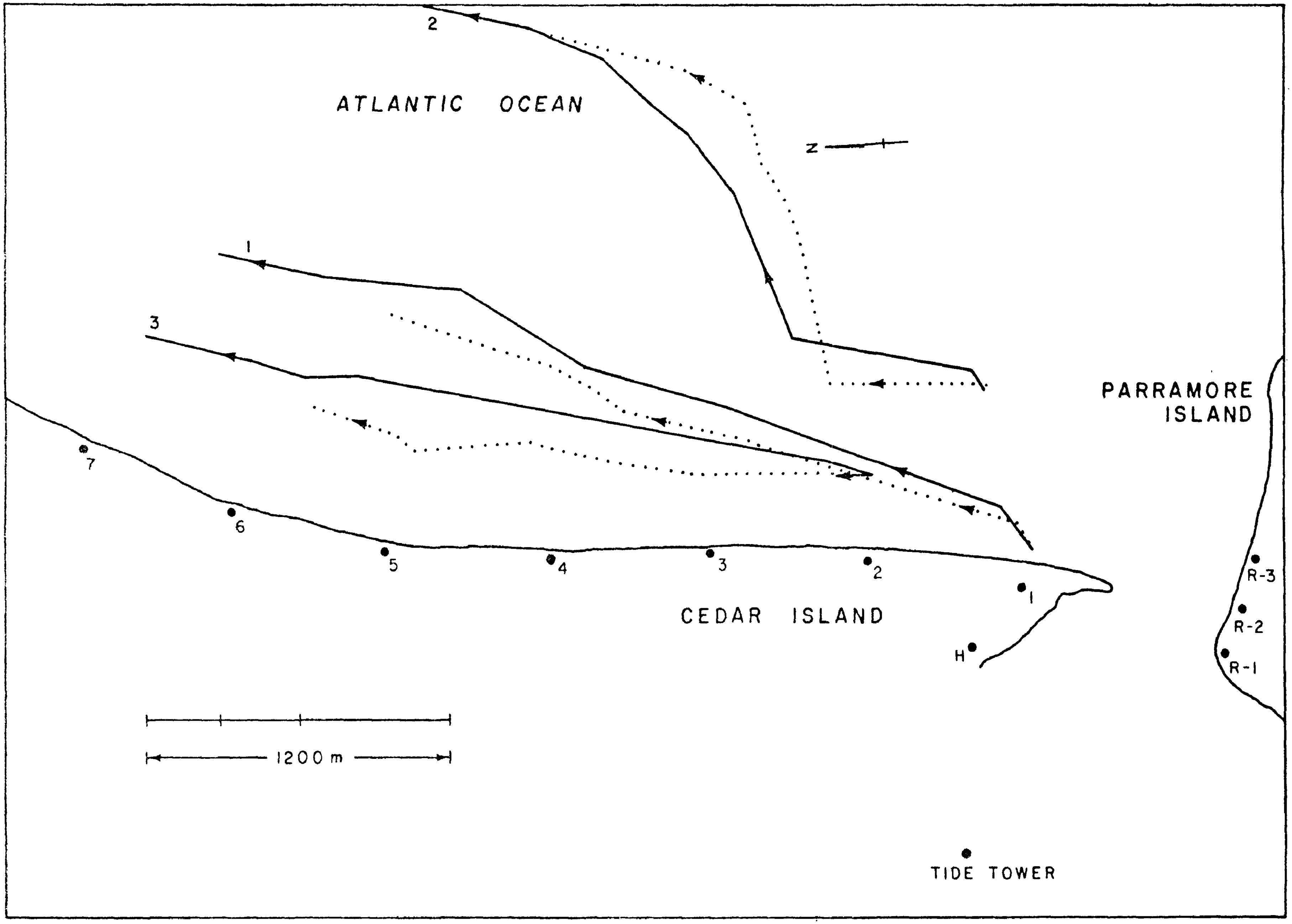
ATLANTIC OCEAN
PARRAMORE ISLAND
CEDAR ISLAND
TIDE TOWER
N
1
2
3
4
5
6
7
H
R-1
R-2
R-3
1200 m

JUNE 4

Figure 28. Drogue tracks, June 13, 1973 ebb.
Solid line actual drogue float velocity.
Dotted line corrected current velocity.

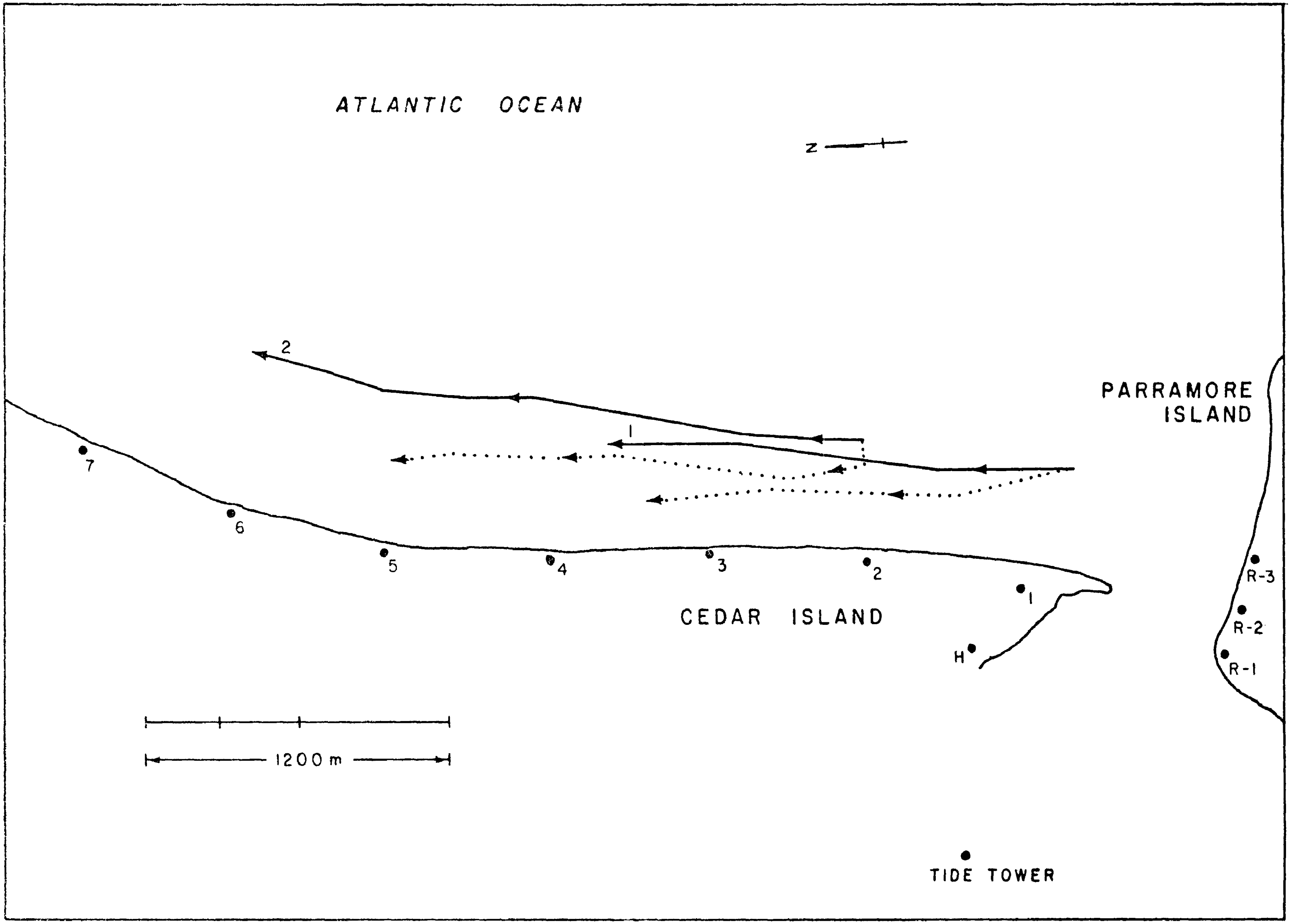
ATLANTIC OCEAN
N
2
1
PARRAMORE ISLAND
7
6
5
4
3
2
1
CEDAR ISLAND
H
R-3
R-2
R-1
1200 m
TIDE TOWER

JUNE 13

Figure 29. Drogue tracks, June 13, 1973 ebb.
Solid line actual drogue float velocity.
Dotted line corrected current velocity.

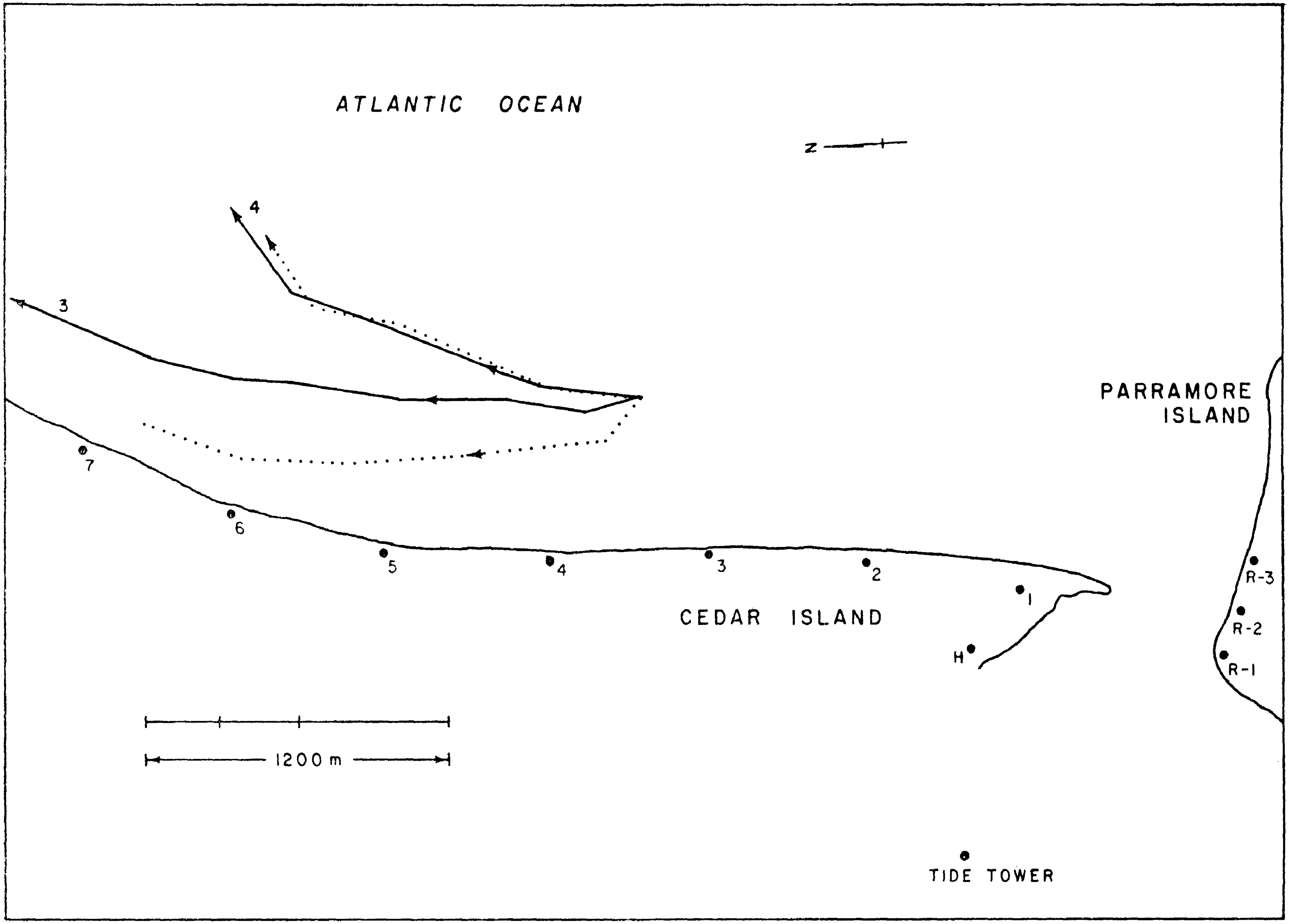
ATLANTIC OCEAN
N
4
3
PARRAMORE
ISLAND
7
6
5
4
3
2
1
H
R-3
R-2
R-1
CEDAR ISLAND
1200 m
TIDE TOWER

JUNE 13

Figure 30. Drogue tracks, June 14, 1973 ebb.
Solid line actual drogue float velocity.
Dotted line corrected current velocity.

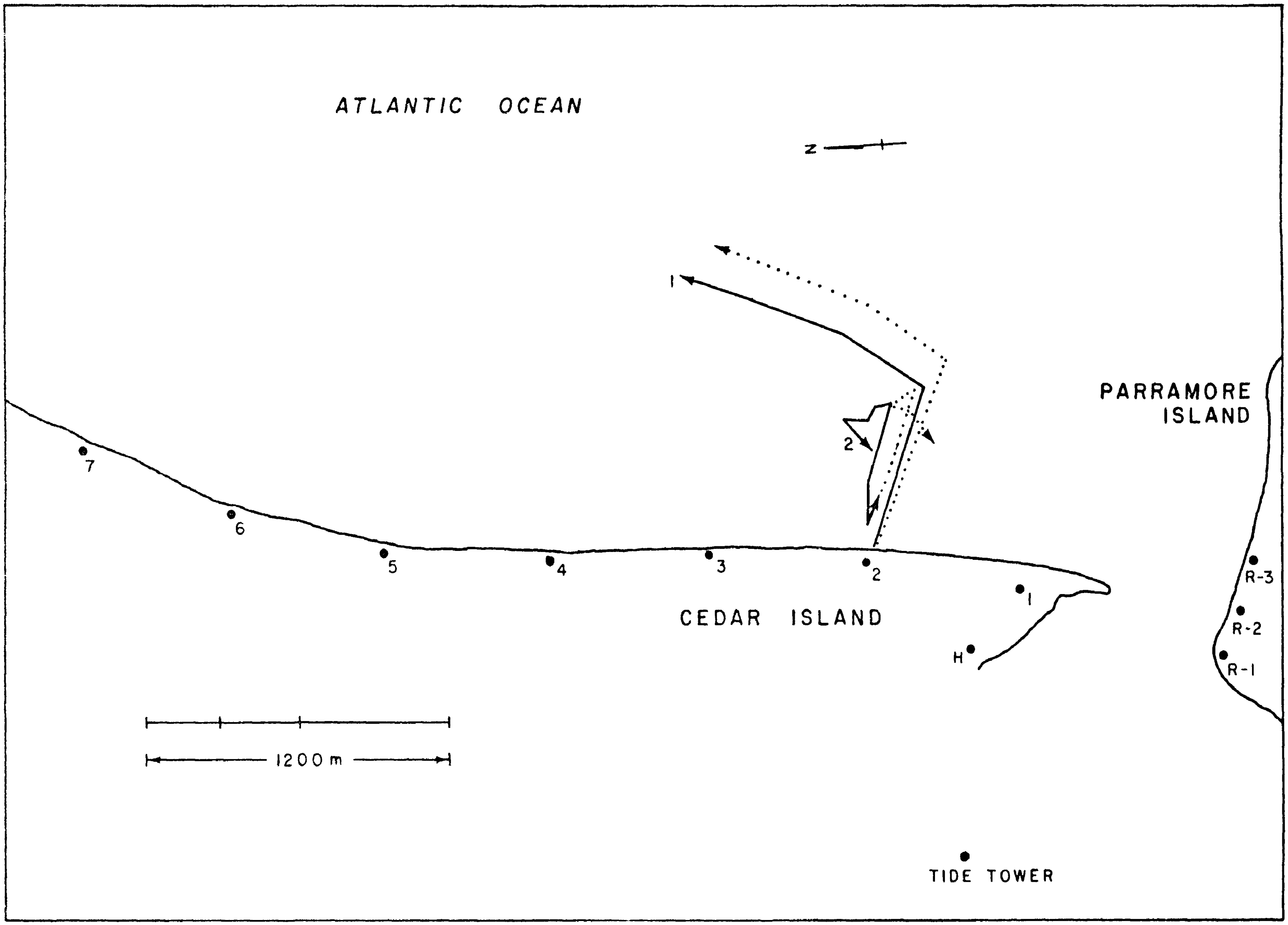
ATLANTIC OCEAN
N
1
2
PARRAMORE ISLAND
7
6
5
4
3
2
1
H
CEDAR ISLAND
R-3
R-2
R-1
1200 m
TIDE TOWER

JUNE 14

Figure 31. Drogue tracks, June 14, 1973 ebb.
Solid line actual drogue float velocity.
Dotted line corrected current velocity.

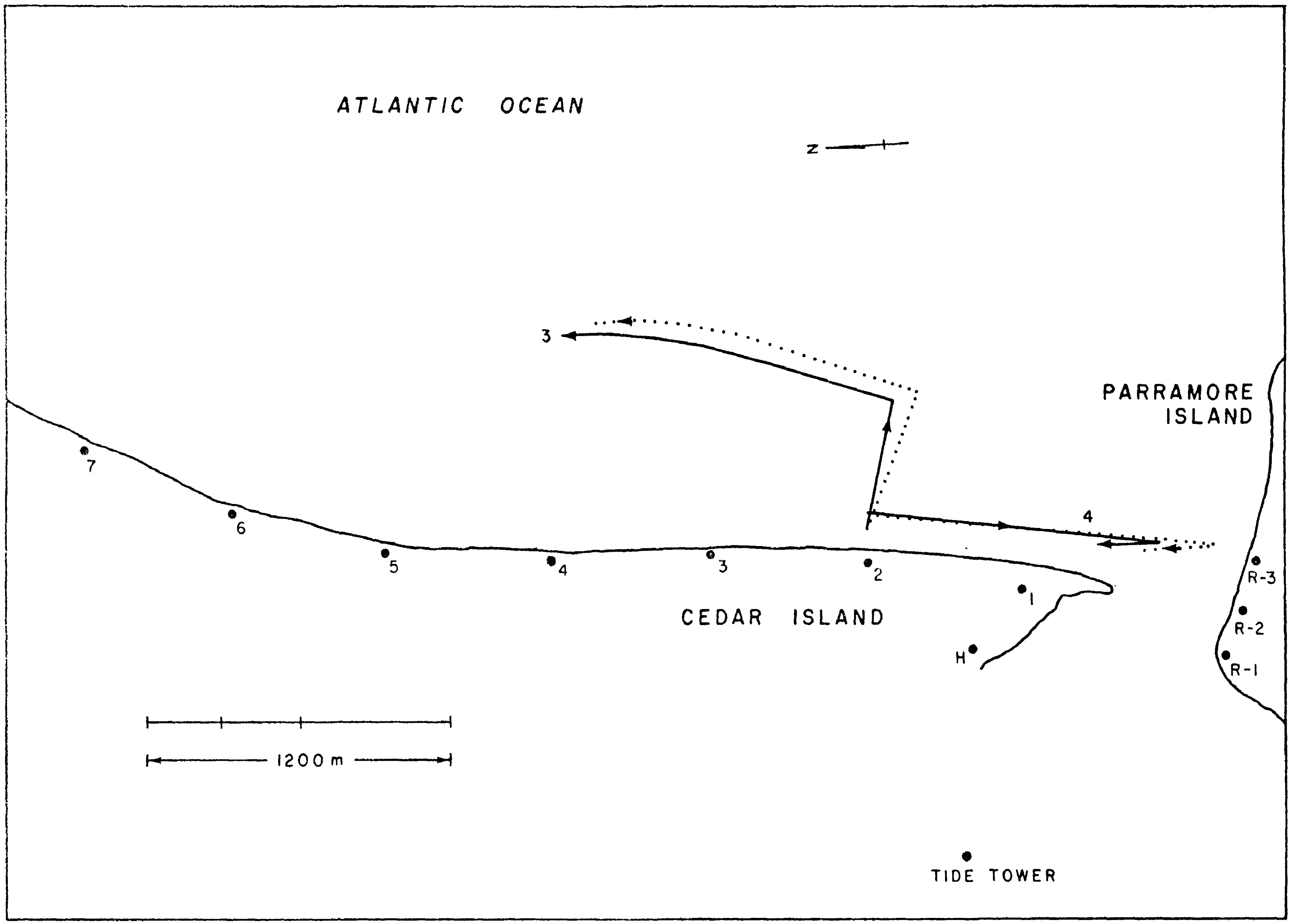
ATLANTIC OCEAN
N
3
PARRAMORE ISLAND
4
7
6
5
4
3
2
1
H
R-3
R-2
R-1
CEDAR ISLAND
1200 m
TIDE TOWER

JUNE 14

Figure 32. Mean velocity current ratio (corrected current velocity/velocity in inlet) vs. distance up Cedar Island (numbers refer to the mid-points between stations on Cedar Island approximately 630 meters apart), shown for six (I-VI) consecutive hours during ebb tide. Average velocity represented by • , standard deviation by ▲.

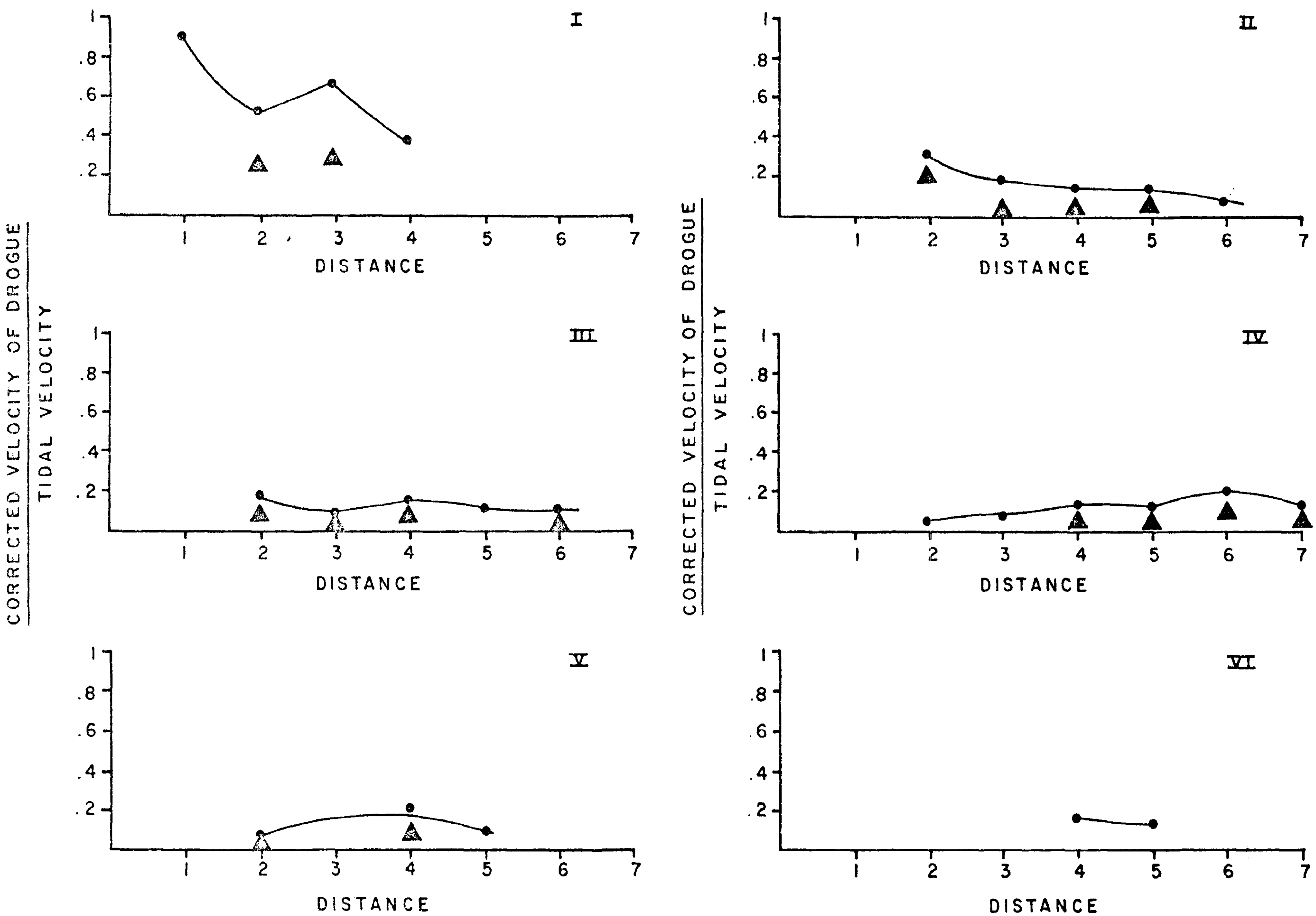

CORRECTED VELOCITY OF DROGUE
TIDAL VELOCITY
I
II
III
IV
V
VI
DISTANCE
1
.8
.6
.4
.2
1 2 3 4 5 6 7

Figure 33. Mean velocity current ratio (corrected current velocity/velocity in inlet) vs. distance up Cedar Island (numbers refer to the mid-points between stations on Cedar Island approximately 630 meters apart), shown for six (I-VI) consecutive hours during ebb tide. Average velocity represented by • , standard deviation by ▲.

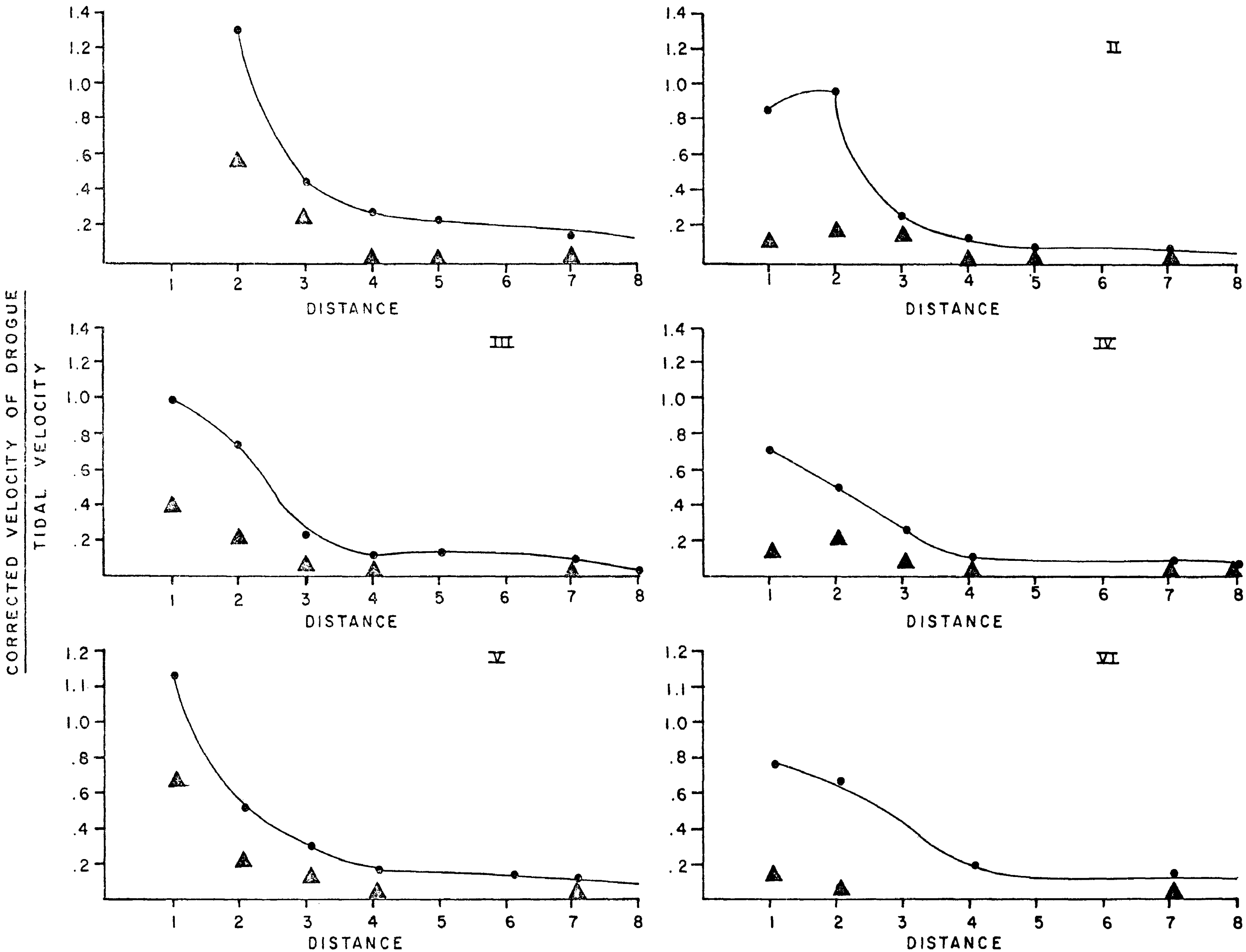
CORRECTED VELOCITY OF DROGUE
TIDAL VELOCITY
DISTANCE
II
III
IV
V
VI
1.4
1.2
1.1
1.0
.8
.6
.4
.2
1 2 3 4 5 6 7 8

velocity ratio vs. distance plots for consecutive hours of the tide (Figure 33) which show a dramatic decrease in the velocity ratio past area number three; this effect is consistent through time. These findings demonstrate that there exists a reasonably well defined zone of significant flood tidal influence extending some 1500 meters north of the inlet.

Sediment Study

Prior to flood, the water in the collection zone was very turbid due to abundant fine silts and clays flushed from the marsh and held in suspension by wave and ebb tidal current action.

Before and during the first hour of ebb, water in the drop zone was clear with visibility of 2½ meters. Immediately above the bottom was a turbid layer ½ meter thick in which a diver would disappear from observers on the surface. Visibility in this layer was 25 centimeters and sediment movement could clearly be seen prior to the transport of the turbid water from the marsh into the area of study.

Sieve analysis of the sediments gathered before each tracer sediment release is presented in the cumulative frequency diagram (Figure 34). It should be noted that sediment farther away from the inlet (Aug. 24 and Sept. 7 drops) contained finer sand (mean .010 cm.) with a higher percentage of silt and clay (9%)

than the samples gathered at the ebb drop site (Aug. 29 and Aug. 30) nearer the inlet (mean .016 cm. silts and clays .3%). Fine grained sediment near the inlet is probably sorted out by the strong tidal currents.

The dyed sediment, also represented by a cumulative frequency curve (Figure 34) shows a striking resemblance to sediment in the ebb drop site: the area from which it was taken. This similarity does not exist in the sediment gathered at the beginning of the flood cycle. The introduction of a slightly coarser sand into the flood drop site should not effect the interpretation of the results since the local sediment size increases as the inlet is approached, and all the sand considered is in the fine to very fine range.

Bedforms were present at both drop sites, showing evidence of sufficient energies present to initiate sediment movement as bed load. Bedform wave length and height increased toward the inlet, and the type varied from linear ripples away from the inlet (flood drop site) to lunate linguoid ripples near the inlet. Boothroyd (1969) interprets this trend as a manifestation of sequential increases in current velocities in the lower flow regime. A similar increase in flow as the inlet is approached has already been documented by the drogue studies.

Figure 34. Cumulative frequency curves.

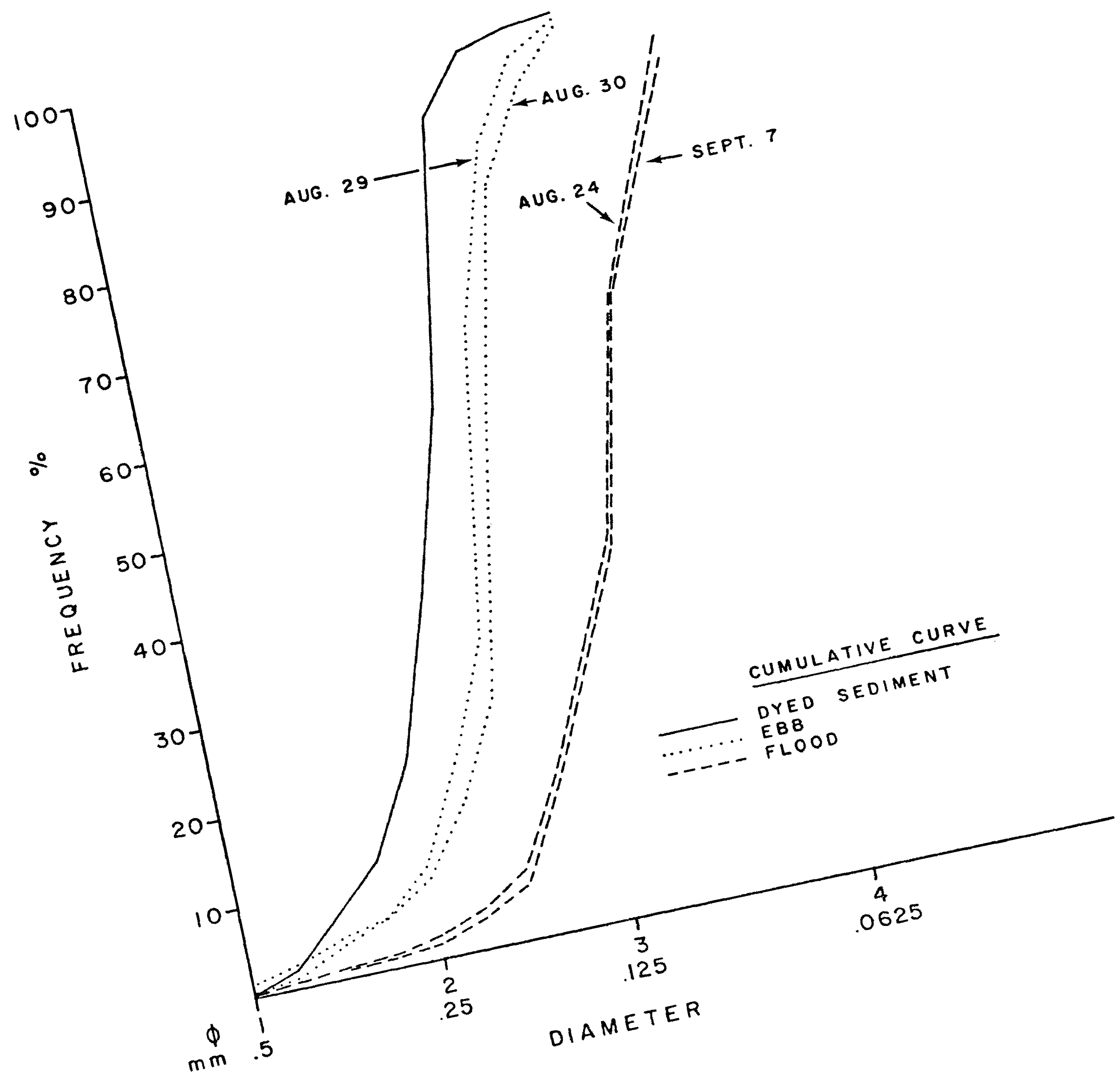
100
90
80
70
60
50
40
30
20
10
FREQUENCY %
AUG. 29
AUG. 30
AUG. 24
SEPT. 7
CUMULATIVE CURVE
DYED SEDIMENT
EBB
FLOOD
ϕ
mm
1
.5
2
.25
3
.125
4
.0625
DIAMETER

Results of the four sediment drops are displayed on Figures 35-46 which show the patterns of sediment concentration through three successive time intervals. To clarify and to aid in interpreting the movement of the sediment, the sampling grid was divided into ten equal sectors perpendicular to the direction of the tidal currents. The average tracer concentrations for all the samples taken in any sector were plotted longitudinally for the three equal time intervals, as shown in Figures 47 & 48.

The dyed sediment releases during flood were made in area number four which, according to the results of the drogue experiment, lies beyond significant flood tidal current influence. Within this zone the dimensionless velocity ratio is nearly constant and tidal currents are consistently near 10 cm/sec. According to Hjulstrom's curve, this velocity is sufficient to transport sediment but not to initiate movement.

The August 24th flood experiment was conducted when the incident wave height was about one meter and the wave period and length were eight seconds and forty meters respectively. These wave conditions yield a maximum bottom orbital velocity ($U_m = \frac{1}{2}(H/d)C$, where H is wave height, d water depth, and C the celerity of the wave,(Shepard,1963))of 81 cm/sec., more than sufficient to transport sediment according to Komar's

Figure 35. Dyed sediment concentration contours. First time period, August 24, 1973 flood, time of drop 10:46 am EST. Arrow indicates velocity of deployed drogue, circled numbers show extremes of sampling grid, 36 represents drop site, number below scale is station on Cedar Island.

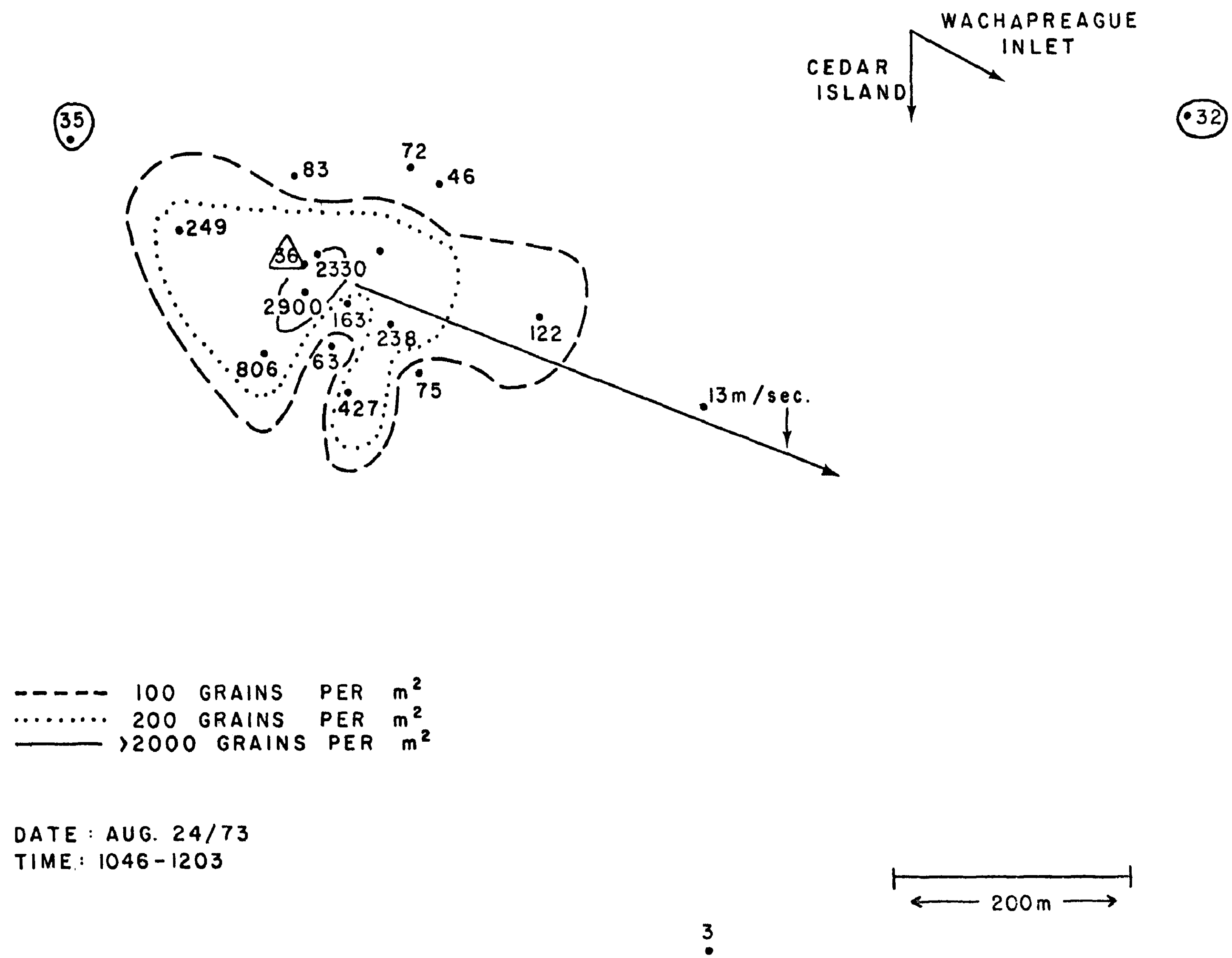
WACHAPREAGUE INLET
CEDAR ISLAND
35
32
83
72
46
249
36
2330
2900
163
238
122
806
63
75
427
13m/sec.
100 GRAINS PER m²
200 GRAINS PER m²
>2000 GRAINS PER m²
DATE: AUG. 24/73
TIME: 1046-1203
200m
3

Figure 36. Dyed sediment concentration contours. Second time period, August 24, 1973 flood, time of drop 10:46 am EST. Arrow indicates velocity of deployed drogue, circled numbers show extremes of sampling grid, 36 represents drop site, numbers below scale are stations on Cedar Island.

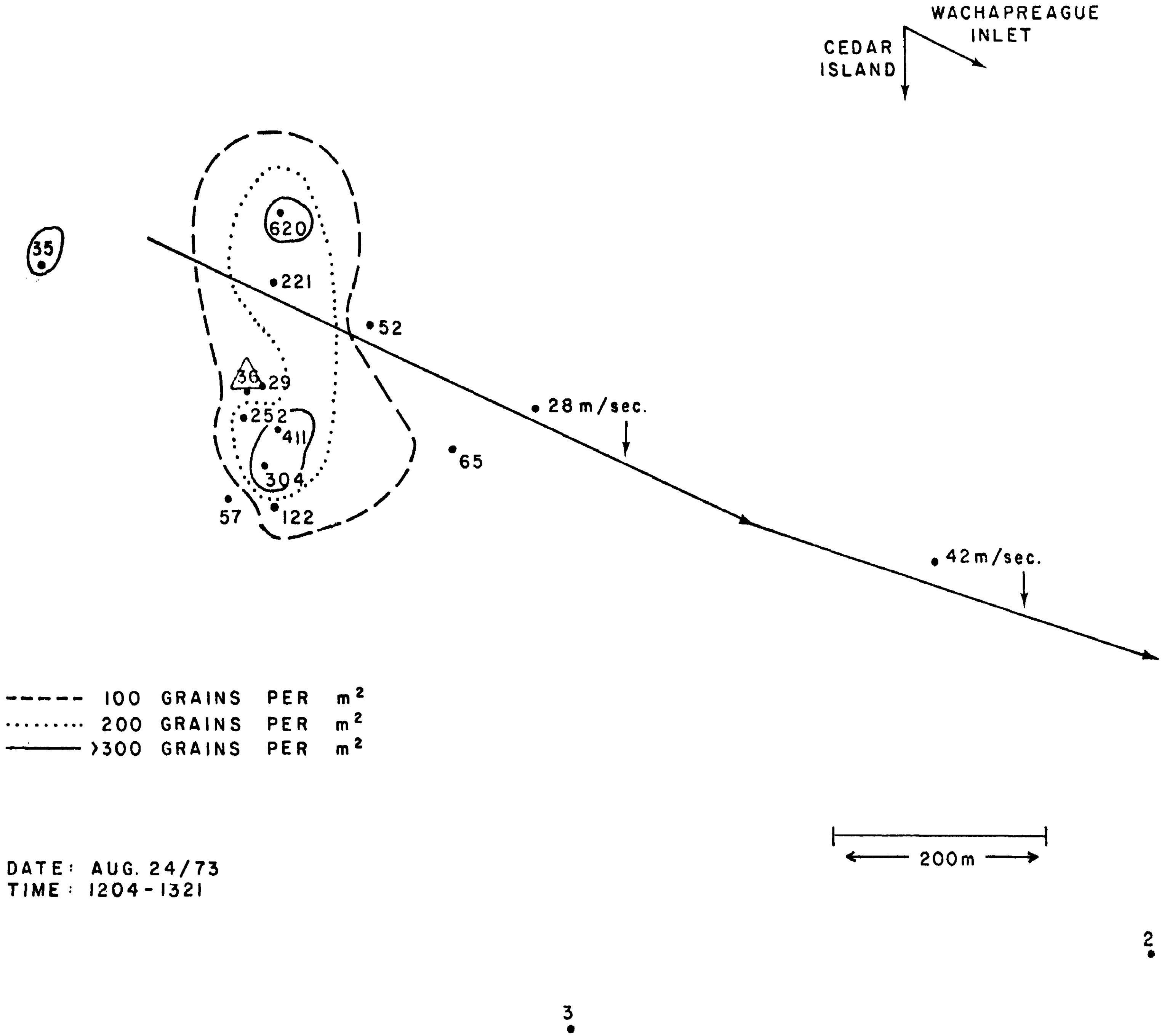
WACHAPREAGUE INLET
CEDAR ISLAND
35
620
221
52
36
29
252
411
304
57
122
65
28 m/sec.
42 m/sec.
100 GRAINS PER m^2
200 GRAINS PER m^2
>300 GRAINS PER m^2
DATE: AUG. 24/73
TIME: 1204-1321
200m
2
3

Figure 37. Dyed sediment concentration contours. Third time period, August 24, 1973 flood, time of drop 10:46 am EST. Arrow indicates velocity of deployed drogue, circled numbers show extremes of sampling grid, 36 represents drop site, numbers below scale are stations on Cedar Island.

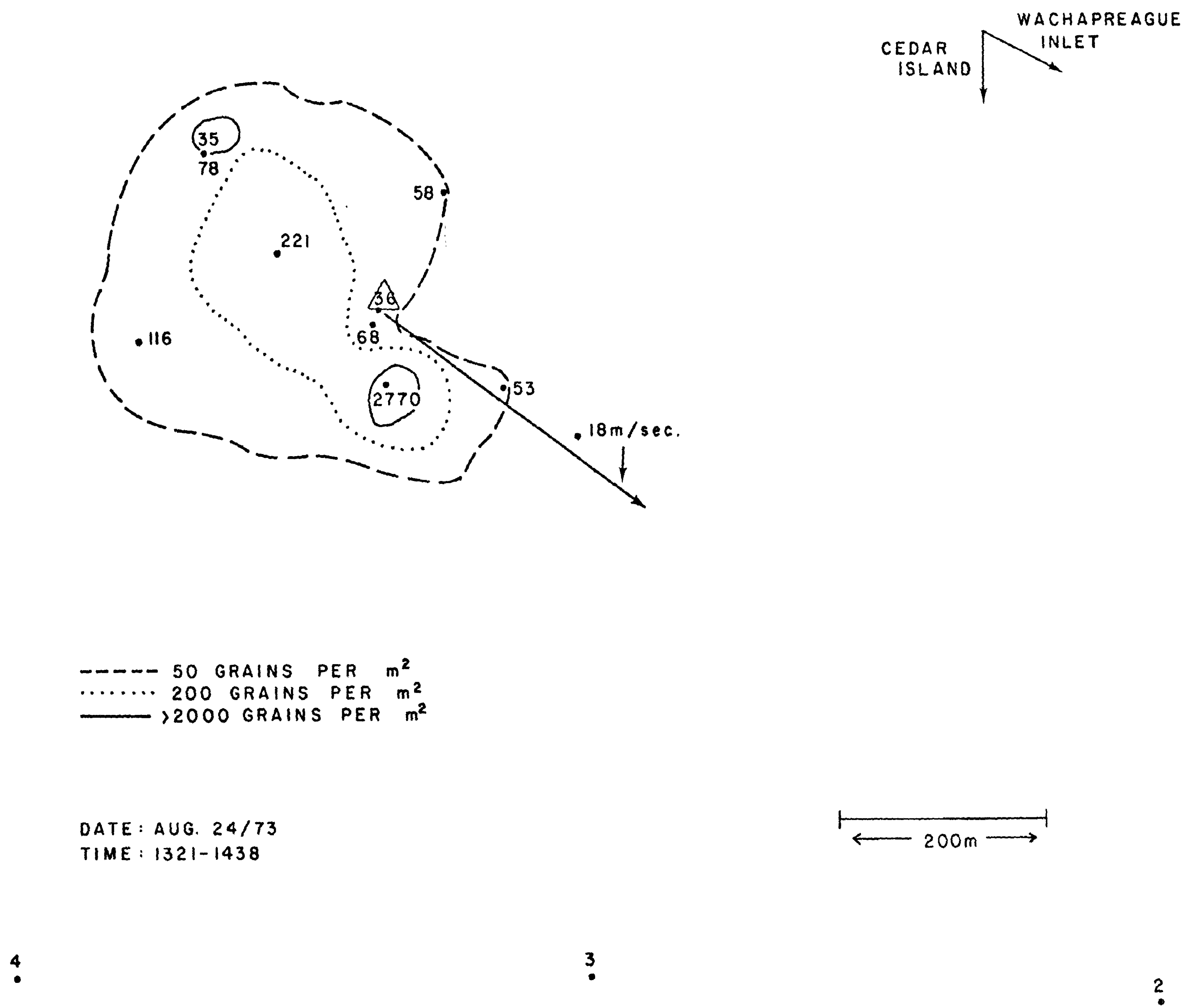

WACHAPREAGUE
INLET
CEDAR
ISLAND
35
78
58
221
36
68
116
53
2770
18m/sec.
50 GRAINS PER m²
200 GRAINS PER m²
>2000 GRAINS PER m²
DATE: AUG. 24/73
TIME: 1321-1438
200m
4
3
2

Figure 38. Dyed sediment concentration contours. First time period, September 7, 1973 flood, time of drop 9:45 am EST. Arrow indicates velocity of deployed drogue, circled numbers show extremes of sampling grid, 36 represents drop site, numbers below scale are stations on Cedar Island.

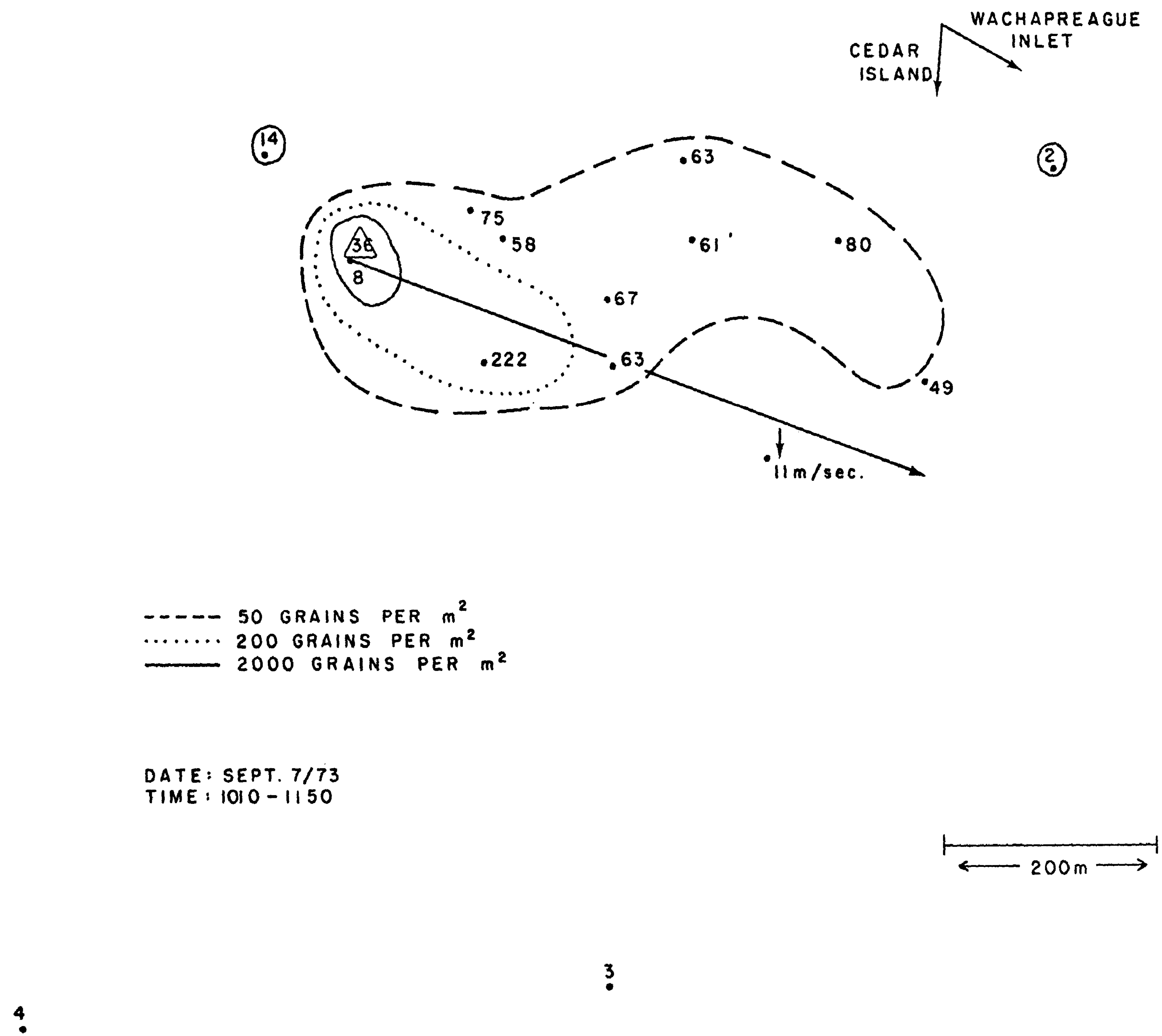
WACHAPREAGUE INLET
CEDAR ISLAND
14
2
36
8
75
58
222
63
67
61
80
63
49
11m/sec.
50 GRAINS PER m²
200 GRAINS PER m²
2000 GRAINS PER m²
DATE: SEPT. 7/73
TIME: 1010 - 1150
200m
4
3
2

Figure 39. Dyed sediment concentration contours. Second time period, September 7, 1973 flood, time of drop 9:45 am EST. Arrow indicates velocity of deployed drogue, circled numbers show extremes of sampling grid, 36 represents drop site, numbers below scale are stations on Cedar Island.

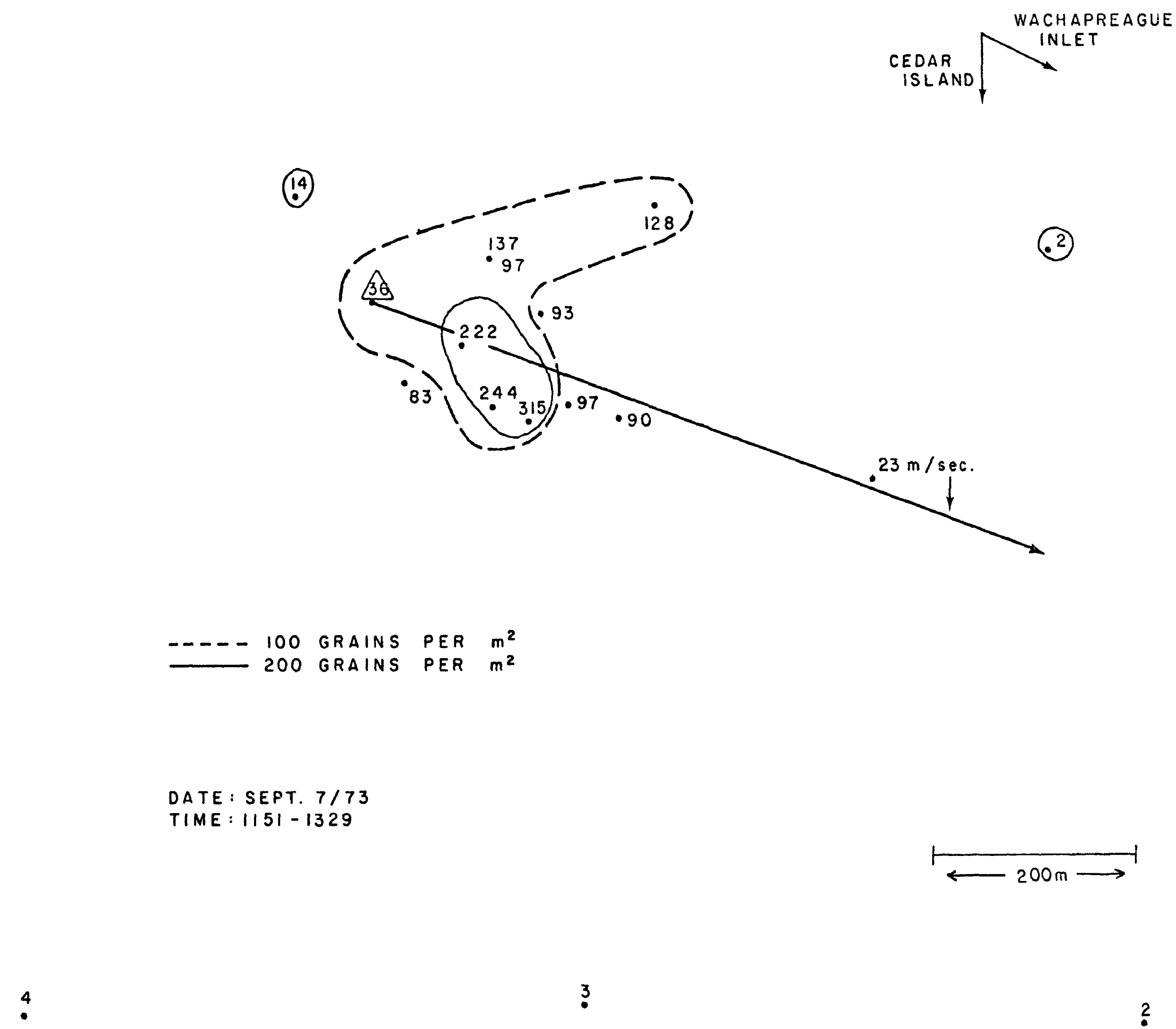

WACHAPREAGUE
INLET
CEDAR
ISLAND
14
128
137
97
36
93
222
83
244
315
97
90
2
23 m/sec.
100 GRAINS PER m2
200 GRAINS PER m2
DATE: SEPT. 7/73
TIME: 1151 - 1329
200m
4
3
2

Figure 40. Dyed sediment concentration contours. Third time period, September 7, 1973 flood, time of drop 9:45 am EST. Arrow indicates velocity of deployed drogue, circled numbers show extremes of sampling grid, 36 represents drop site, numbers below scale are stations on Cedar Island.

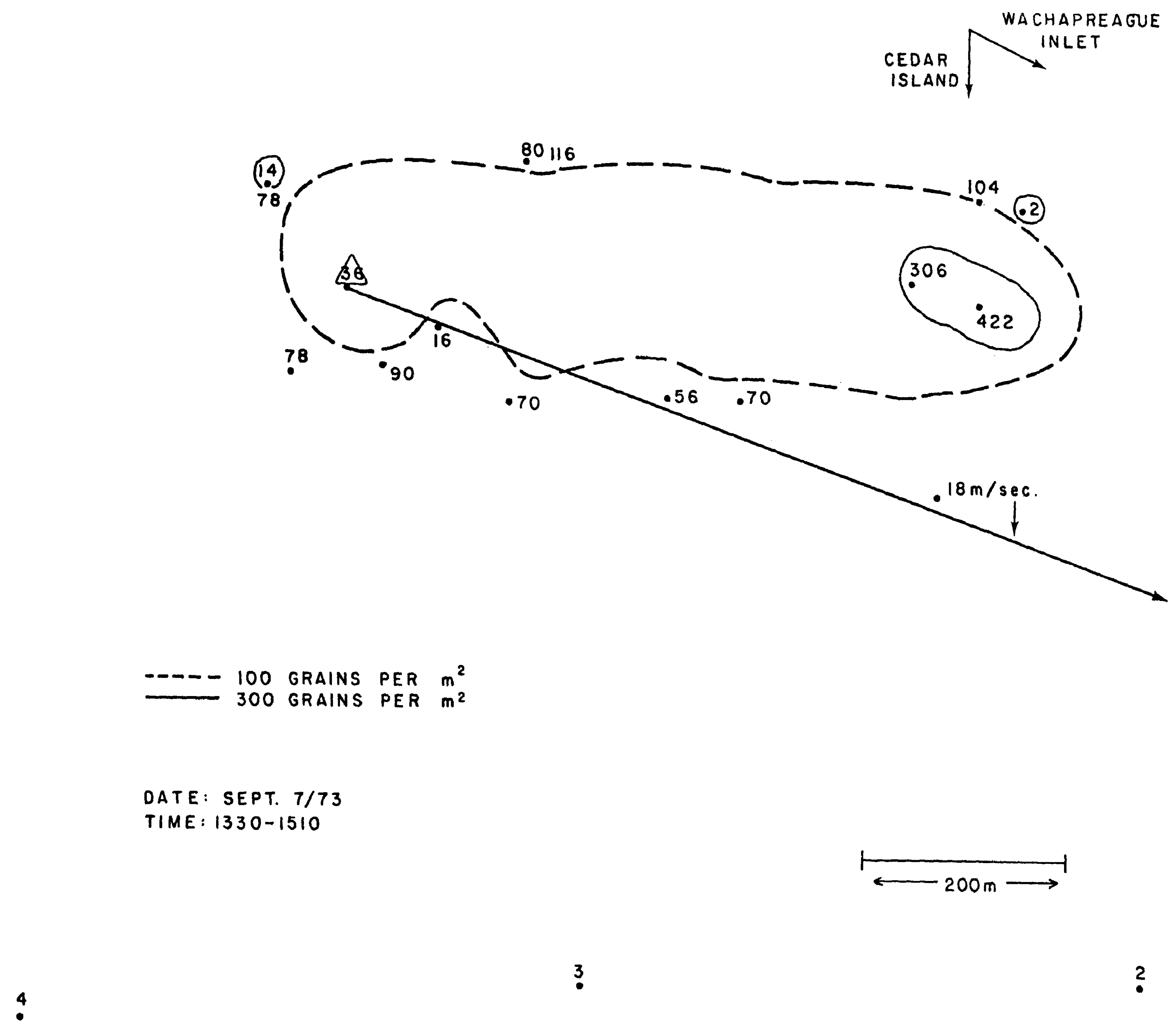
WACHAPREAGUE INLET
CEDAR ISLAND
14
78
80
116
104
2
36
306
422
78
16
90
70
56
70
18m/sec.
100 GRAINS PER m²
300 GRAINS PER m²
DATE: SEPT. 7/73
TIME: 1330-1510
200m
4
3
2

Figure 41. Dyed sediment concentration contours. First time period, August 29, 1973 ebb, time of drop 9:15 am EST. Arrow indicates velocity of deployed drogue, circled numbers show extremes of sampling grid, 36 represents drop site, numbers below scale are stations on Cedar Island.

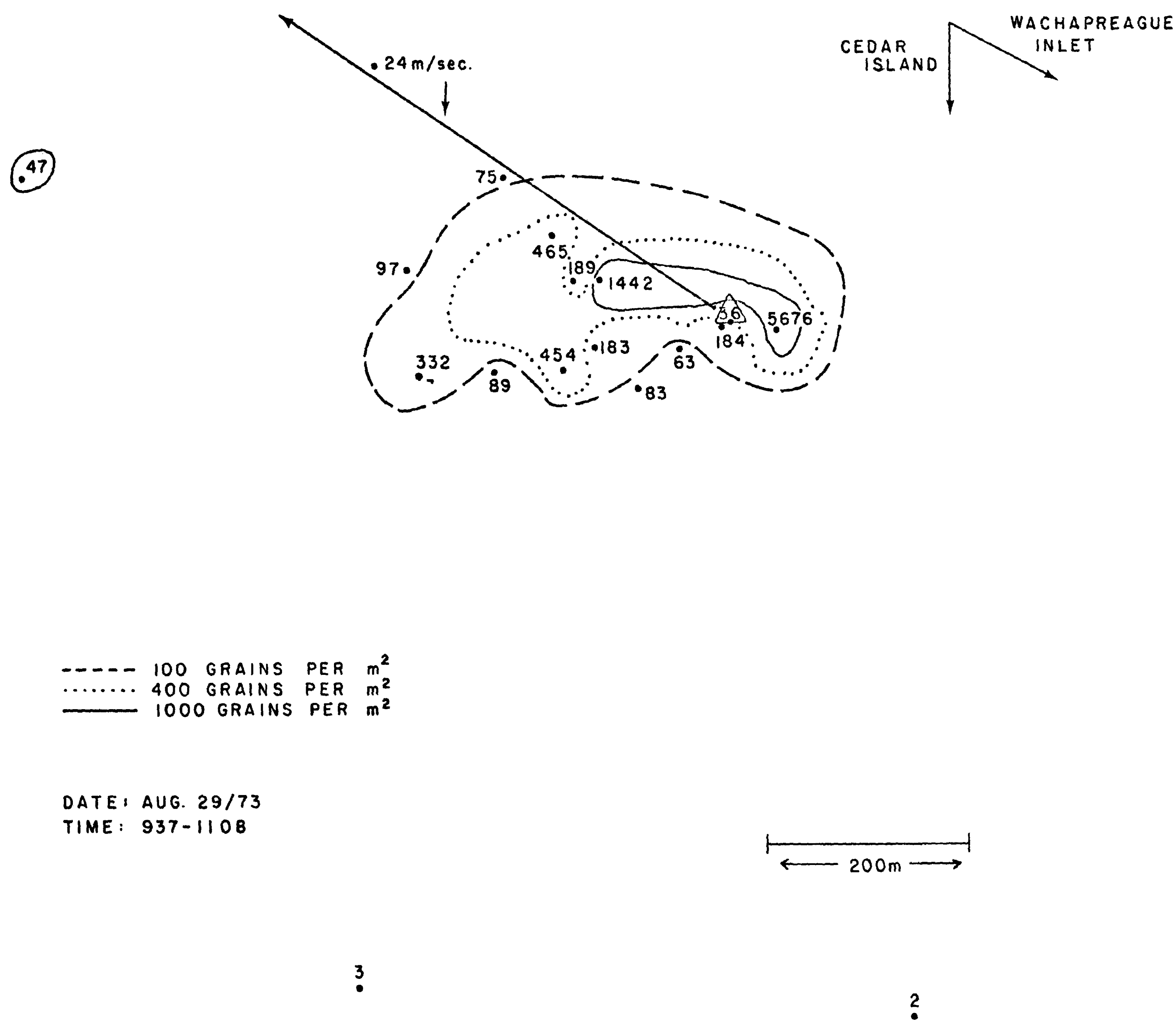

24m/sec.
WACHAPREAGUE INLET
CEDAR ISLAND
47
75
465
97
189
1442
36
5676
184
183
454
63
332
89
83
100 GRAINS PER m²
400 GRAINS PER m²
1000 GRAINS PER m²
DATE: AUG. 29/73
TIME: 937-1108
200m
3
2

Figure 42. Dyed sediment concentration contours. Second time period, August 29, 1973 ebb, time of drop 9:15 am EST. Arrow indicates velocity of deployed drogue, circled numbers show extremes of sampling grid, 36 represents drop site, numbers below scale are stations on Cedar Island.

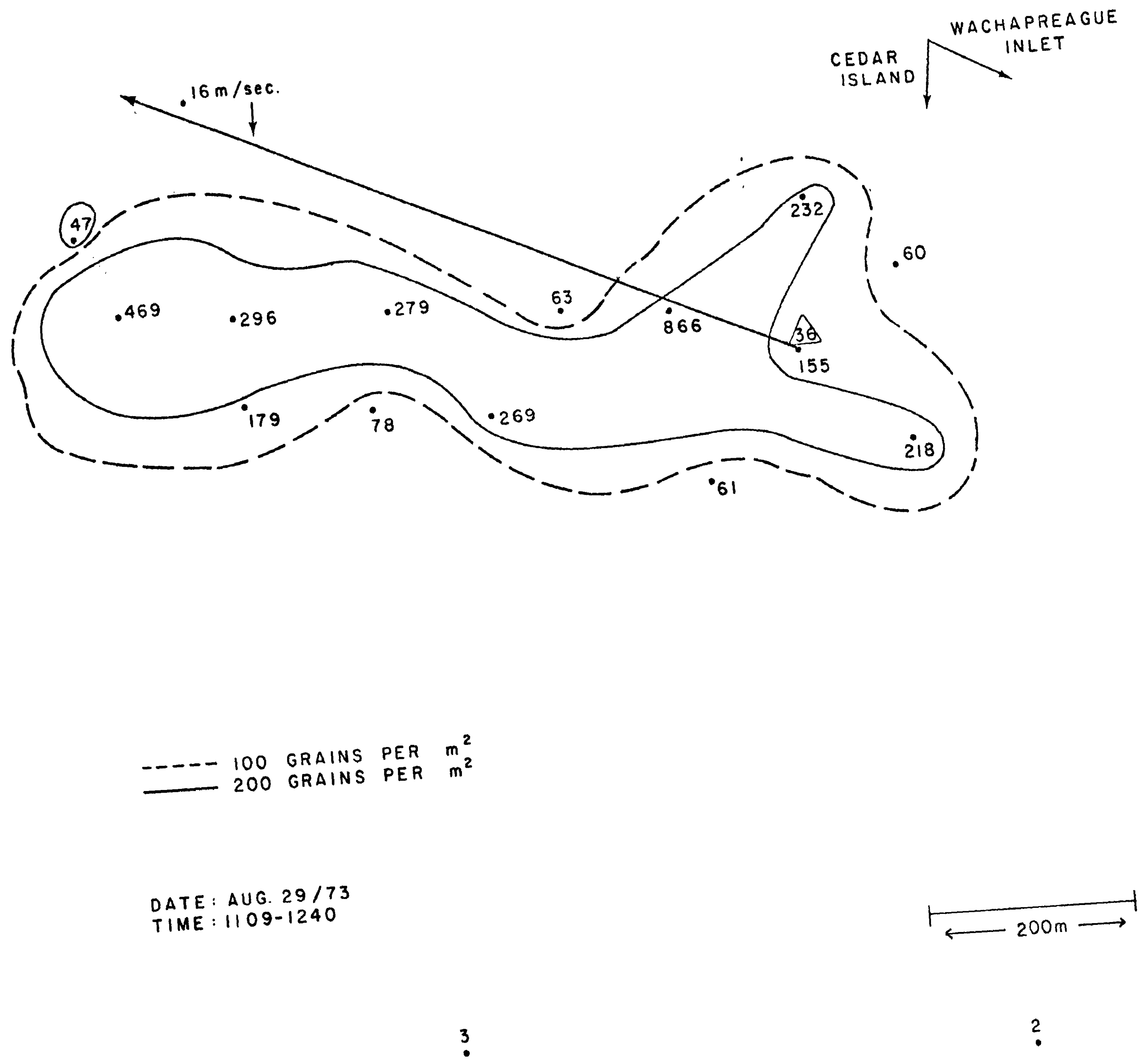

WACHAPREAGUE INLET
CEDAR ISLAND
16 m/sec.
47
469
296
279
63
866
232
60
36
155
179
78
269
218
61
100 GRAINS PER m^2
200 GRAINS PER m^2
DATE: AUG. 29/73
TIME: 1109-1240
200m
3
2

Figure 43. Dyed sediment concentration contours. Third time period, August 29, 1973, ebb, time of drop 9:15 am EST. Arrow indicates velocity of deployed drogue, circled numbers show extremes of sampling grid, 36 represents drop site, numbers below scale are stations on Cedar Island.

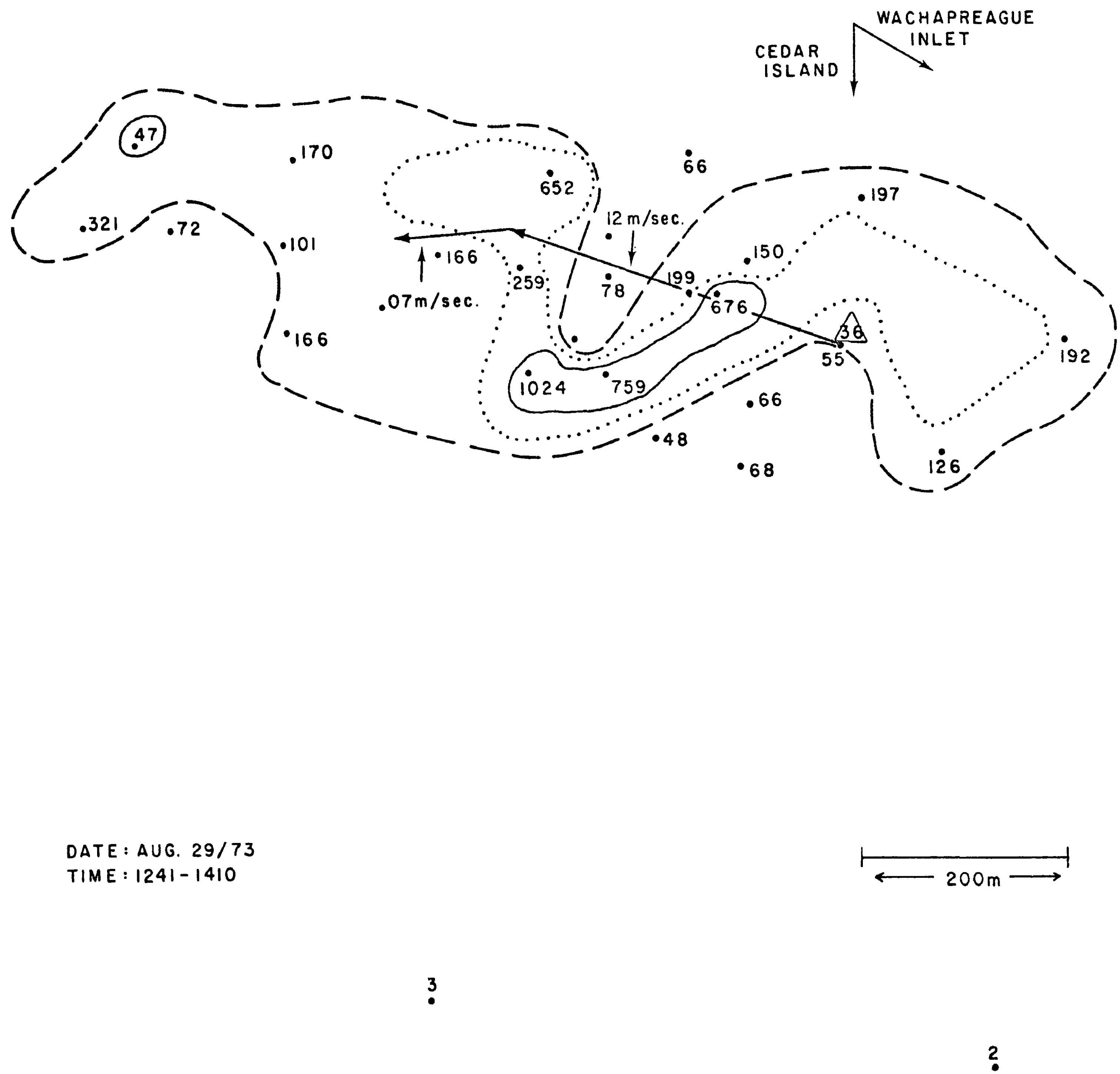
WACHAPREAGUE INLET
CEDAR ISLAND
47
321
72
170
101
166
652
66
12 m/sec.
197
166
.07m/sec.
259
78
199
150
676
36
55
192
1024
759
66
48
68
126
DATE: AUG. 29/73
TIME: 1241-1410
200m
3
2

Figure 44. Dyed sediment concentration contours. First time period, August 30, 1973 ebb, time of drop 9:25 am EST. Arrow indicates velocity of deployed drogue, circled numbers show extremes of sampling grid, 36 represents drop site, numbers below scale are stations on Cedar Island.

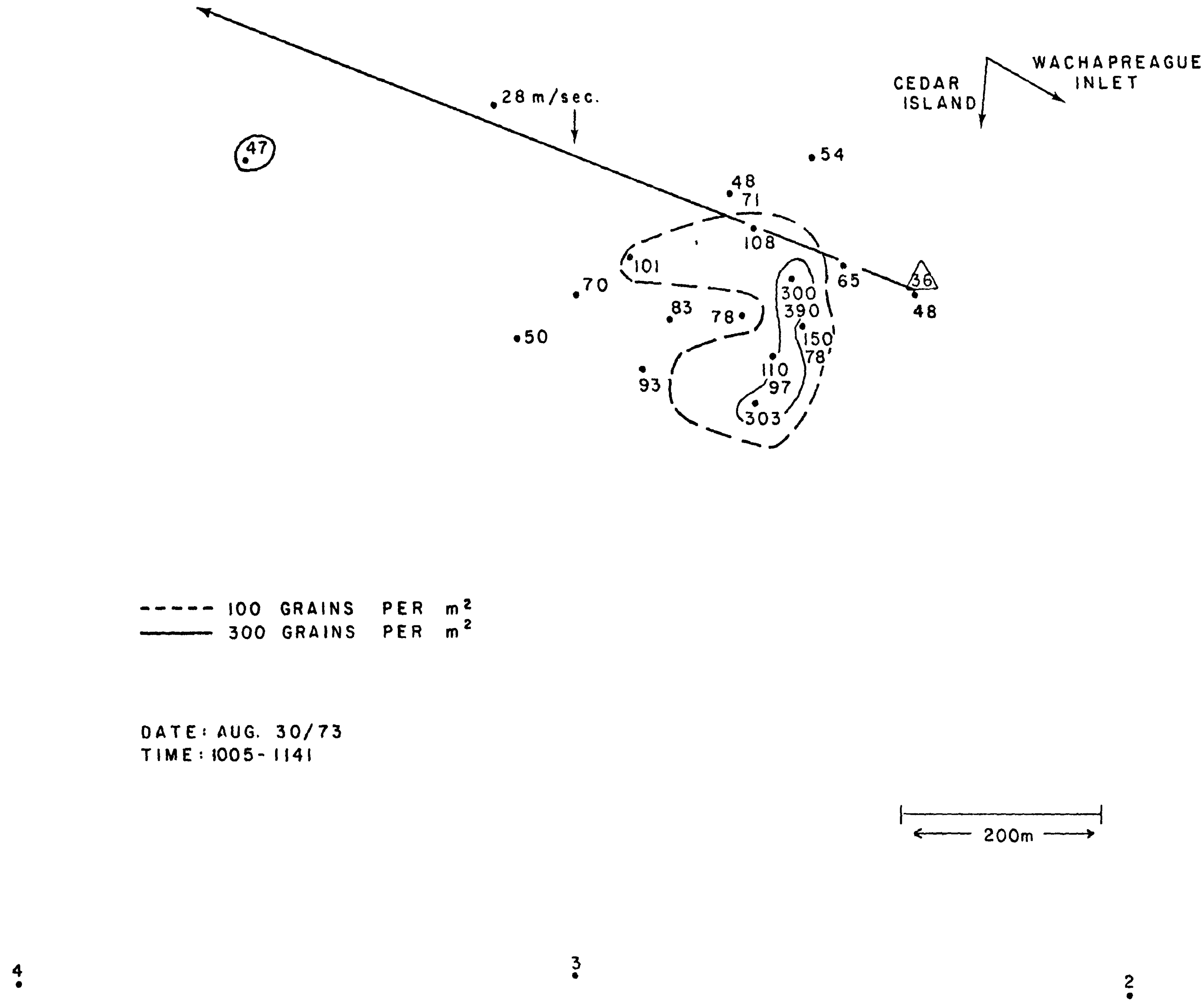
WACHAPREAGUE INLET
CEDAR ISLAND
28 m/sec.
47
54
48
71
108
101
70
65
36
48
300
390
83
78
150
78
50
110
97
93
303
----- 100 GRAINS PER m²
——— 300 GRAINS PER m²
DATE: AUG. 30/73
TIME: 1005-1141
200m
4
3
2

Figure 45. Dyed sediment concentration contours. Second time period August 30, 1973 ebb, time of drop 9:25 am EST. Arrow indicates velocity of deployed drogue, circled numbers show extremes of sampling grid, 36 represents drop site, numbers below scale are stations on Cedar Island.

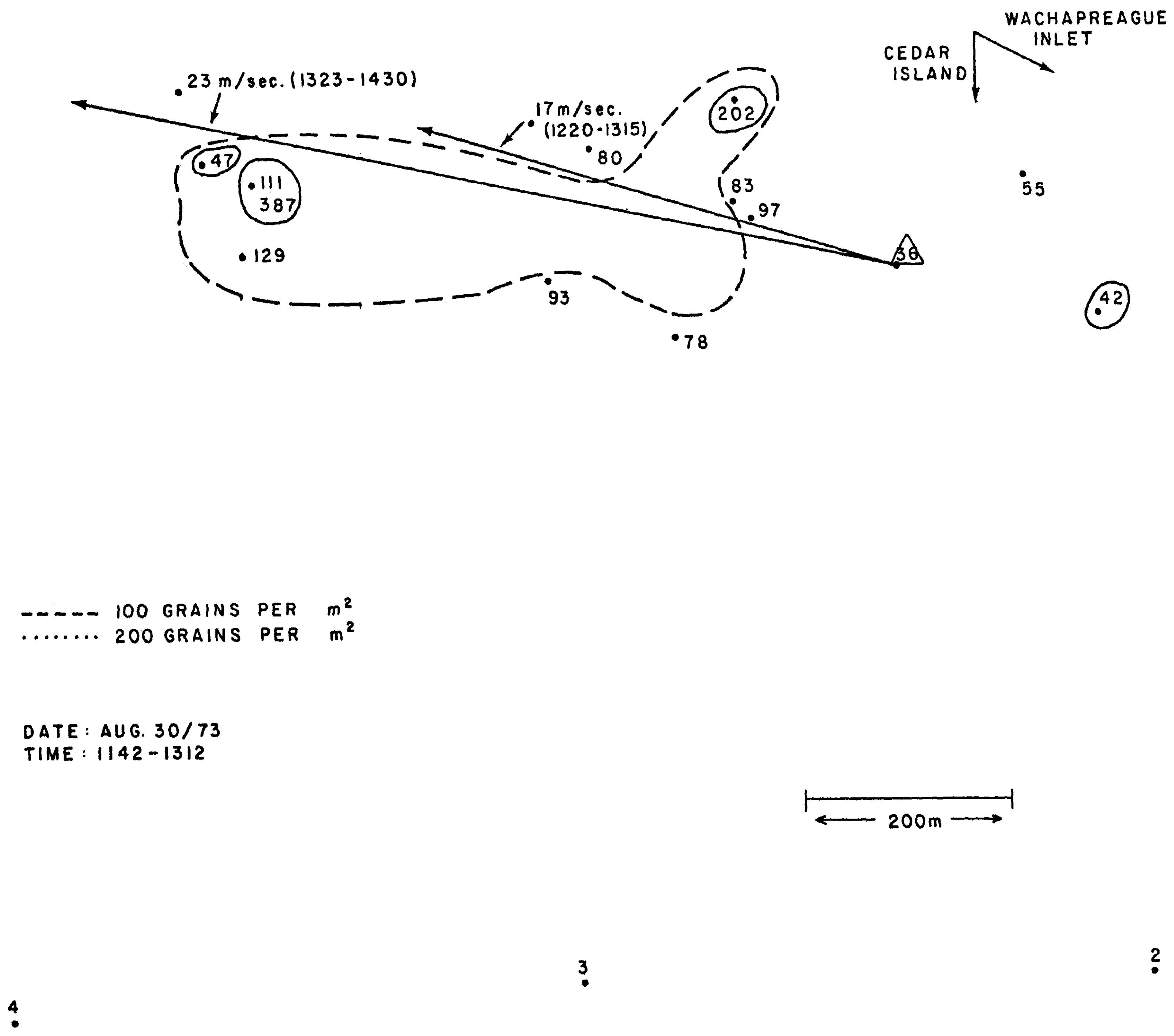
WACHAPREAGUE INLET
CEDAR ISLAND
23 m/sec. (1323-1430)
17m/sec. (1220-1315)
202
80
83
97
47
111
387
129
93
78
36
55
42
100 GRAINS PER m²
200 GRAINS PER m²
DATE: AUG. 30/73
TIME: 1142-1312
200m
4
3
2

Figure 46. Dyed sediment concentration contours. Third time period August 30, 1973, ebb, time of drop 9:25 am EST. Arrow indicates velocity of deployed drogue, circled numbers show extremes of sampling grid, 36 represents drop site, numbers below scale are stations on Cedar Island.

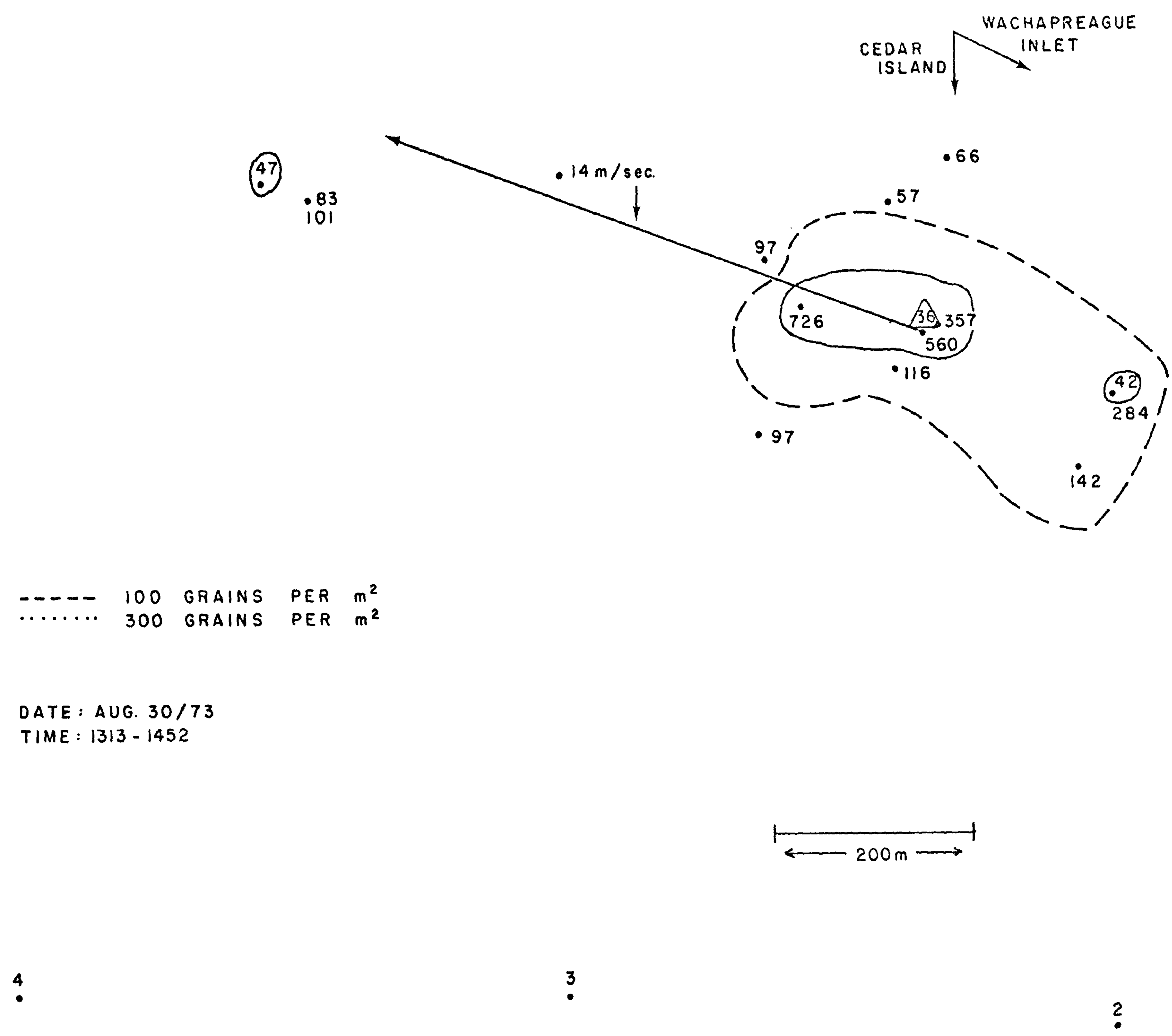

WACHAPREAGUE INLET
CEDAR ISLAND
14 m/sec.
47
83
101
66
57
97
726
36
357
560
116
42
284
97
142
100 GRAINS PER m²
300 GRAINS PER m²
DATE: AUG. 30/73
TIME: 1313 - 1452
200m
4
3
2

Figure 47. Average grains/m^2 vs. distance for three time periods (I-III) during flood. Sampling grid divided into ten equal sectors 120 meters apart.

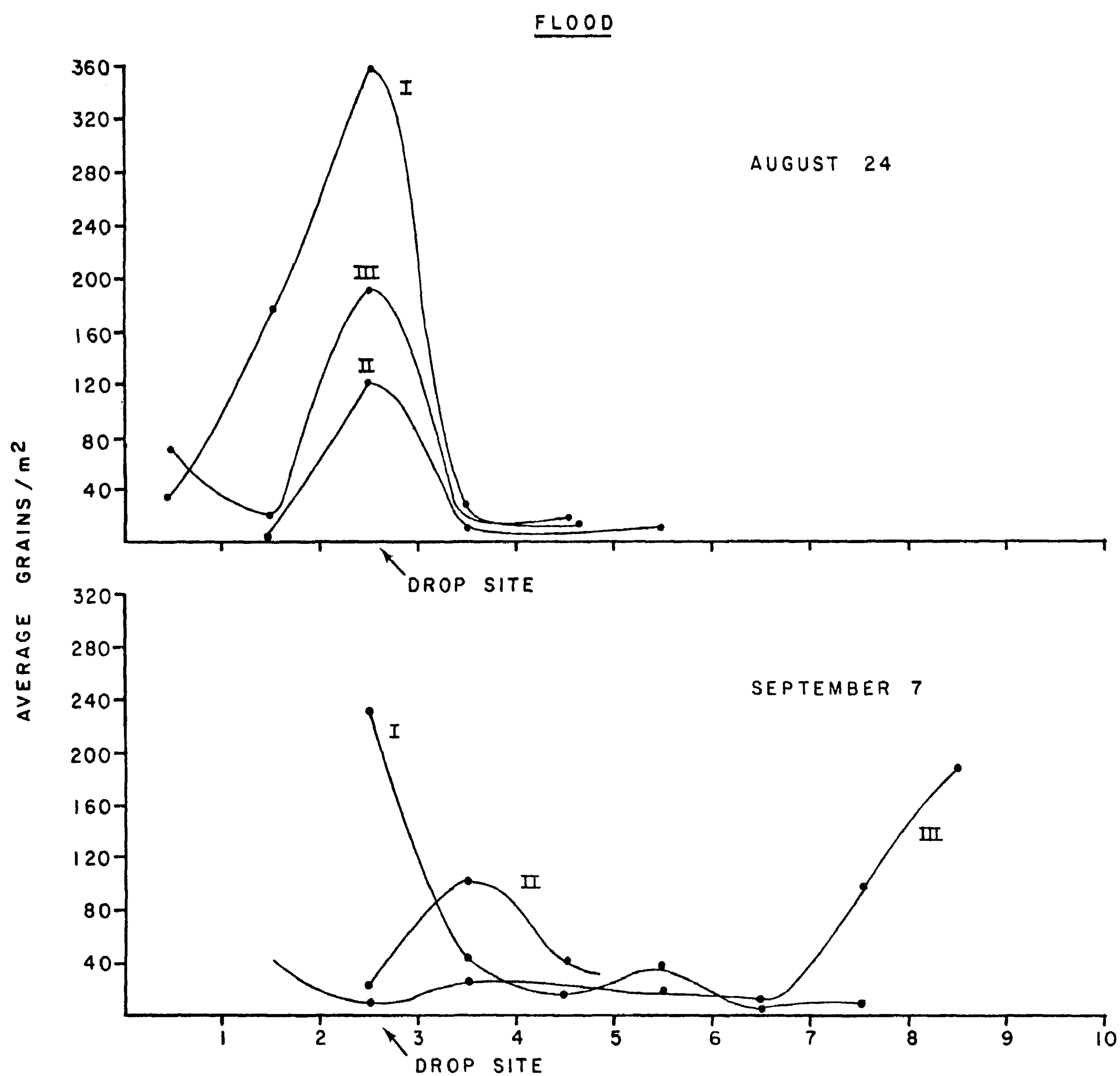
FLOOD
AUGUST 24
SEPTEMBER 7
AVERAGE GRAINS / m2
360
320
280
240
200
160
120
80
40
I
II
III
DROP SITE
1
2
3
4
5
6
7
8
9
10

Figure 48. Average grains/m^2 vs. distance for three time periods (I-III) during ebb. Sampling grid divided into ten equal sectors, 120 meters apart.

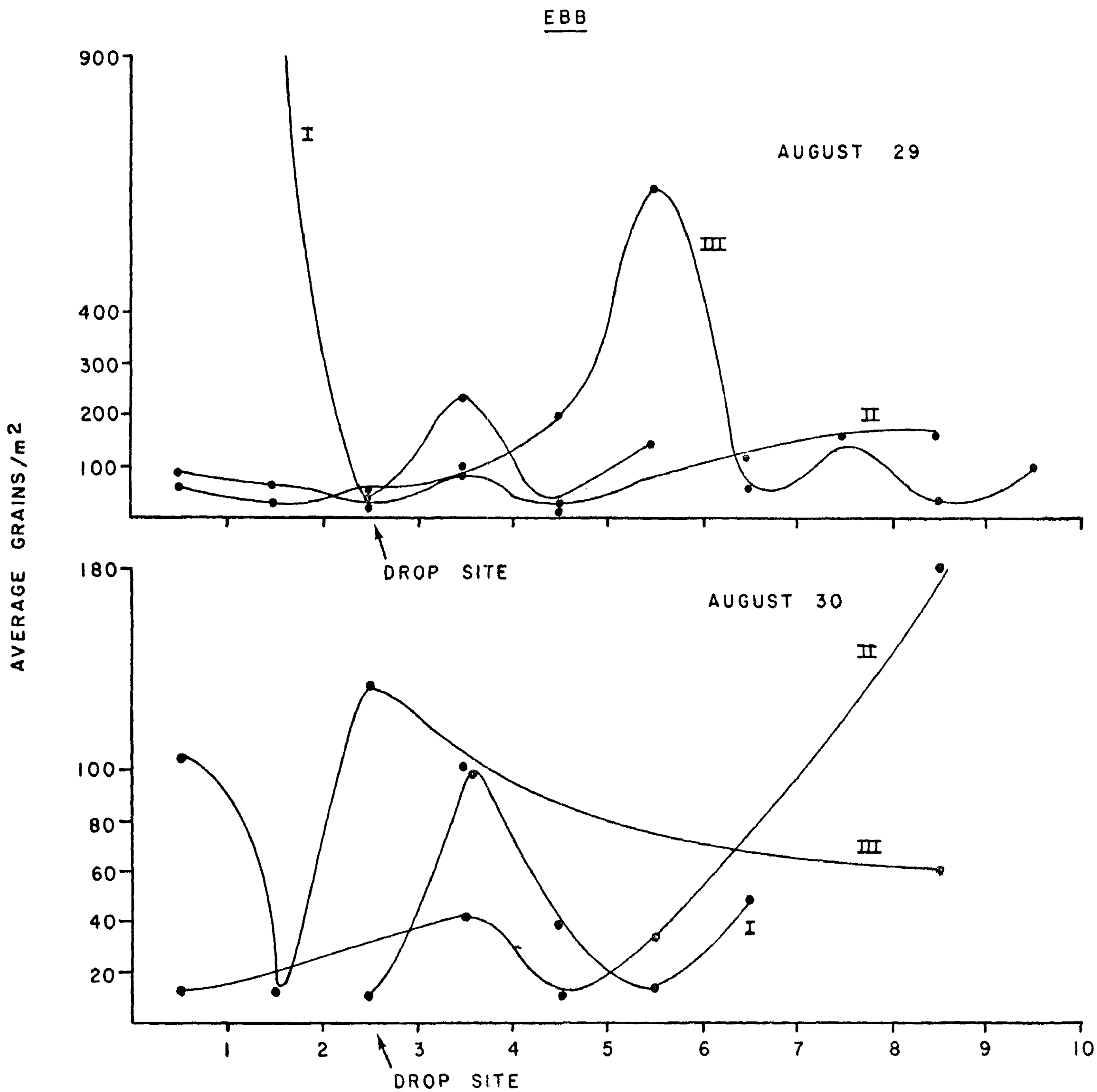
EBB
AVERAGE GRAINS/m2
900
400
300
200
100
I
AUGUST 29
III
II
DROP SITE
180
100
80
60
40
20
AUGUST 30
II
III
I
1
2
3
4
5
6
7
8
9
10
DROP SITE

(1973) analysis of sediment movement under oscillatory waves. Waves of eight second period, fifteen meter wavelength, and .3 meter height occurred during the second flood experiment on September 7th. Calculated maximum bottom orbital velocities for these waves were 9.8 cm/sec.

Tidal range on August 24th was 1.5 meters, .4 meters above the mean tidal range. Maximum velocities in the inlet were 1.1 m/sec. In contrast the September 7th experiment took place under neap tidal conditions. Current meter data for days of similar tidal range and maximum stage show a maximum velocity in the inlet of .75 m/sec. (It was suspected that the current meter in service on Sept. 7th was fouled).

According to Hjulstrom's and Komar's theories for initiation of sediment movement, neither waves nor currents alone at times during the experiment had sufficient energy to commence sediment movement, yet movement was recorded as described below. A combination of these forces and their interaction with the rippled bottom creating turbulence are apparently sufficient to cause sediment motion. Stone and Summer (1972) found that sand transport in the near shore bed rippled region occurred at much lower velocities than predicted by laboratory studies. This lends credence to the argument for initiation of sediment transport at velocities below those predicted by theory.

Movement of the dyed sediment on August 24th is shown in Figure 35-47. The area of peak concentration moved shoreward and, surprisingly, little influence of the unidirectional tidal currents was seen. Cook and Gorsline (1972) found that 95% of sediment transport occurs within 15 cm. of the bottom. With this assumption and a fall velocity of 1 cm/sec. for the given sediment size range, a displacement of some hundreds of meters toward the inlet would be expected depending on how frequently the sediment was swept into suspension by local wave induced turbulence.

One can speculate on the rate of sediment movement on August 25th by assuming that the area of peak concentration represents the average trend. During the time interval a movement of approximately 100 meters shoreward was realized suggesting an average rate of movement of .7 cm/sec.

Examination of the movement of high concentration of sediment on September 7th (Figure 38-40) shows a displacement toward the inlet and parallel to the island. This pattern shows greater dispersion and distribution of the tracer sand toward the inlet than the August 24th experiment. It is interesting to note that the area of peak concentration moved only a short distance (175 meters) from the time of the drop to the end of the second time interval. However, after this time the area of high density (based on two samples) entered the domain of increasing flood tidal influence and moved 500 meters. The sediment transport velocities during the first and second time periods were 1.1 cm/sec. and 18 cm/sec. respectively. This trend further reinforces the existance of a significant sphere of flood tidal influence.

Tracer sediment sampling on August 24th during a time of large waves and spring tides did not show a strong displacement toward the inlet. Weak lateral dispersion parallel to the shore could be seen during the first and third periods of sampling. An onshore, offshore dispersion was recorded during the second sampling period. Failure to observe greater advection toward the inlet could have been due to lack of adequate sampling and rapid dispersion of the dyed sand by the strong wave field. Since the sediment drop occurred in an area where flood tidal influence is weak it is also possible that the bulk of the dyed sediment was displaced landward by waves, and moved transversely to the longitudinal axis of the grid beyond the range of sampling. If this were the case advection toward the inlet by tidal currents would not have been seen.

During low wave and neap tide conditions on September 7th, a definite elongation of the dispersion pattern was observed. These findings are consistant with the intuitive concept that waves stir up the sediment and the unidirectional flood tidal currents transport the sediment toward the inlet.

High energy waves can increase the quantity of sediment in suspension for transport by tidal currents. The Aug. 24th experiment demonstrated the ability of a strong wave field to move and disperse sediment rapidly. A strong wave field and an increase in the rate of sediment advection toward the inlet during flood as the inlet is approached are two factors which will tend to choke and close this inlet.

During the ebb experiment introduction of the tracer sand took place in area number three. As defined by the drogue work, this area is little effected by tidal ranges or stages in the inlet and is beyond the area of direct ebb tidal influence. Tidal current velocities in this area are of the order of .2 m/sec. (measured by the drogues placed in at the drop site during the experiment) and are capable of transporting sediment according to Hjulstrom but insufficient to initiate movement.

Relatively calm sea conditions occurred during both ebb investigations on the 29th and 30th of August. Waves having a period of six seconds, a height of .2 meters and a wavelength of 11 meters occurred on the 29th. Similar conditions existed on August 30th (Table 2). Maximum bottom orbital velocities were 4.9 and 8.5 cm/sec. calculated for August 29th and August 30th respectively. Neither velocity is capable of initiating sediment motion according to Komar's analysis of sediment movement under oscillatory waves, but movement did occur, probably for the reasons described earlier.

The significant scatter of tracer on August 29th is shown in Figures 41-43. There is a trend away from the inlet, parallel to the island and an ill defined area of peak concentration moved approximately 250 meters from the drop site during the experiment at an average rate of 1.4 cm/sec.

On August 30th a movement of a well defined area of high tracer sand concentration did not appear. An aberrant trend was observed (Figure 48) in the movement of a higher concentration of dyed grains toward the inlet during the third time period.

During both ebb experiments there was a general dispersion and advection away from the inlet and parallel to the island. The lack of a well defined coherent center of sediment movement is in agreement with the absence of a significant zone of ebb tidal influence.

VI.

DISCUSSION AND CONCLUSIONS

O'Brien's conception of ebb tidal current behavior (Figure 4) for an inlet without an offset was not found to concur with the findings of this study of the offset Wachapreague Inlet. No evidence was found of ebb entrainment induced eddy currents nor were any nearshore currents flowing toward the inlet discovered. During flood, O'Brien's current behavior was verified and the extent of the currents influence was further defined.

During flood the hydraulic currents in the coastal current zone run parallel to the island and approach the inlet through a 1500 meter zone in which the currents intensify and respond directly to tidal changes in the inlet. North of this zone the currents attenuate rapidly and assume a near constant value which is essentially independent of tidal stage or range. During ebb this significant sphere of influence is lacking; the issuing jet is confined to the main channel by its inertia and only slight leakage into the coastal current zone occurs. This local current behavior may be influenced by regional morphological conditions.

The bathymetry of Wachapreague Inlet and vicinity (Figure 49) shows the position of shoals flanking the

Figure 49. Bathymetry of Wachapreague Inlet and Vicinity

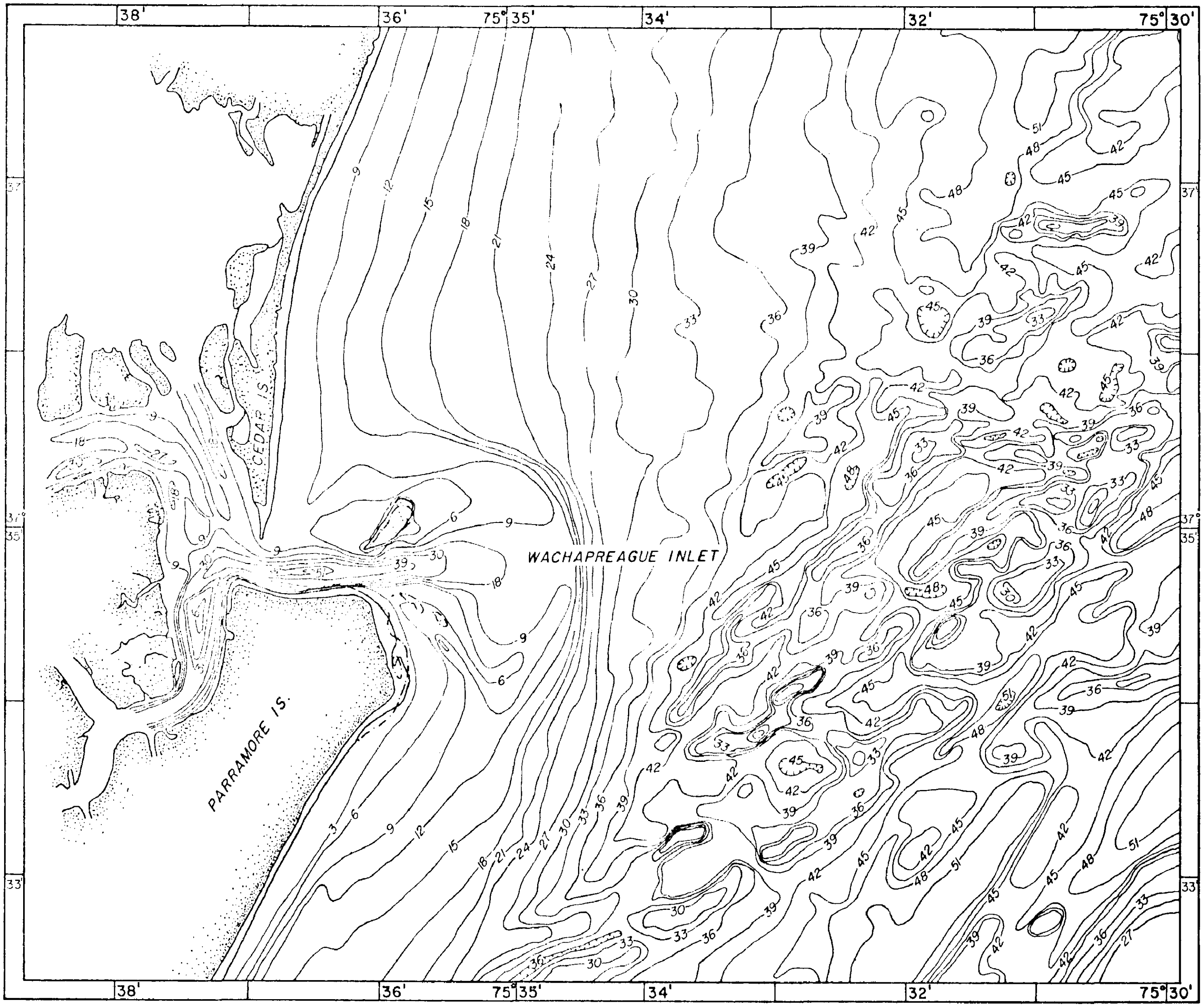
WACHAPREAGUE INLET
CEDAR IS.
PARRAMORE IS.
38'
36'
75° 35'
34'
32'
75° 30'
37°
35'
33'

north side of the channel, and located in front of Cedar Island. The equation of continuity, an analytical expression of the general principle of conservation of mass, and the position of the shoal suggests an argument for the existance of a zone of significant flood tidal influence. Area transects perpendicular to Cedar Island and out to the 24 foot contour were constructed at 600 meter intervals at the mid points of the individual study areas as depicted in Figure 6. These areas were expressed as a ratio of individual area divided by maximum area encountered (located in the middle of area three) and plotted with respect to distance up Cedar Island north of the inlet. Figure 50 shows a sudden decrease in cross sectional area in the same region that the drogue study defined the zone of flood tidal influence. The increase in velocity (expressed as a ratio over tidal velocity in the inlet) in this area as found during the drogue study is shown in Figure 51.

It is of interest, by analogy with a pipe flow case, to construct an idealized shoreline of the Wachapreague inlet area without the inlet and to speculate how this theoretical configuration, illustrated in Figure 52, might be used to model the actual tidal inlet area.

Regional tidal currents flow north during ebb and south during flood (inferred by limited drogue studies

Figure 50. Area ratio (individual area to 24 ft. contour/maximum area) vs. distance up Cedar Island. Distance between sectors averages 630 meters.

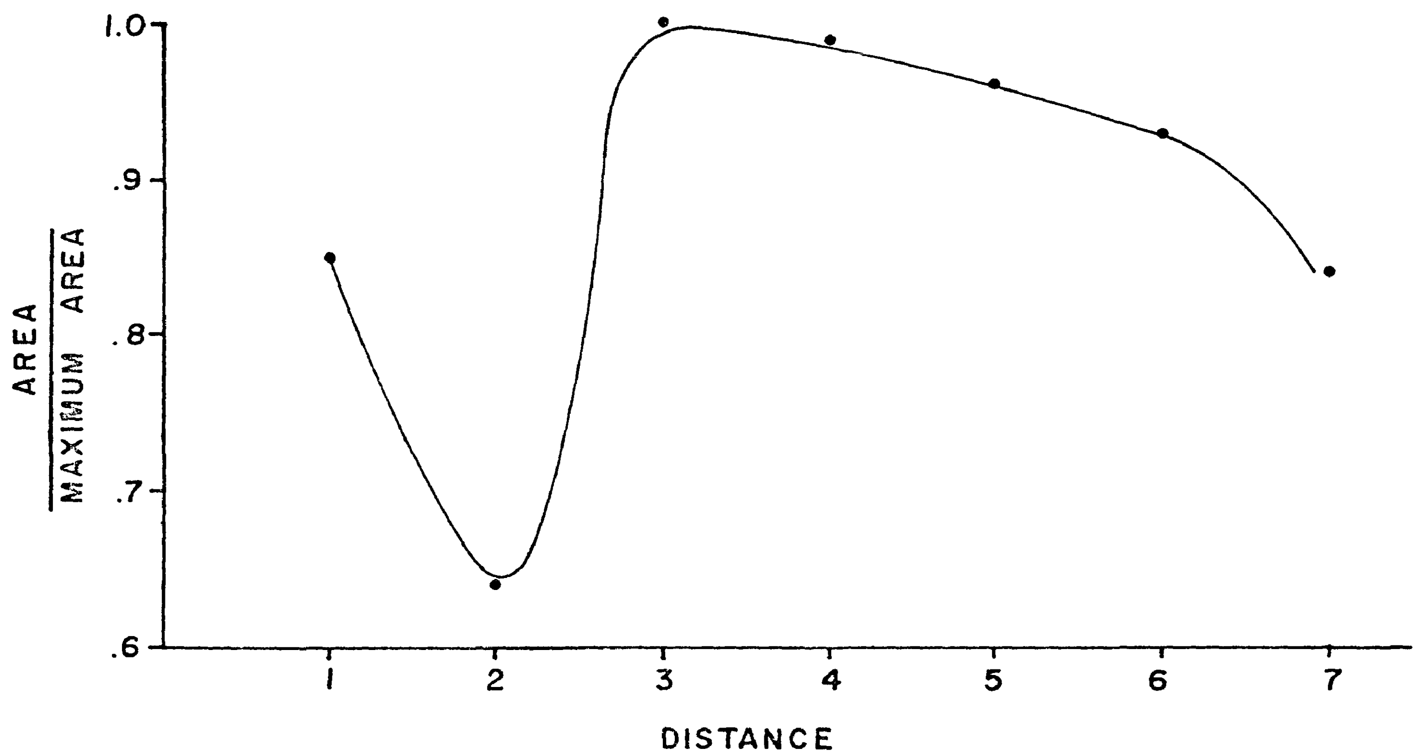
1.0
.9
.8
.7
.6
AREA
MAXIMUM AREA
1
2
3
4
5
6
7
DISTANCE

Figure 51. Velocity ratio (corrected current velocity/ tidal velocity in inlet) vs. distance. Distance between sectors averages 630 meters.

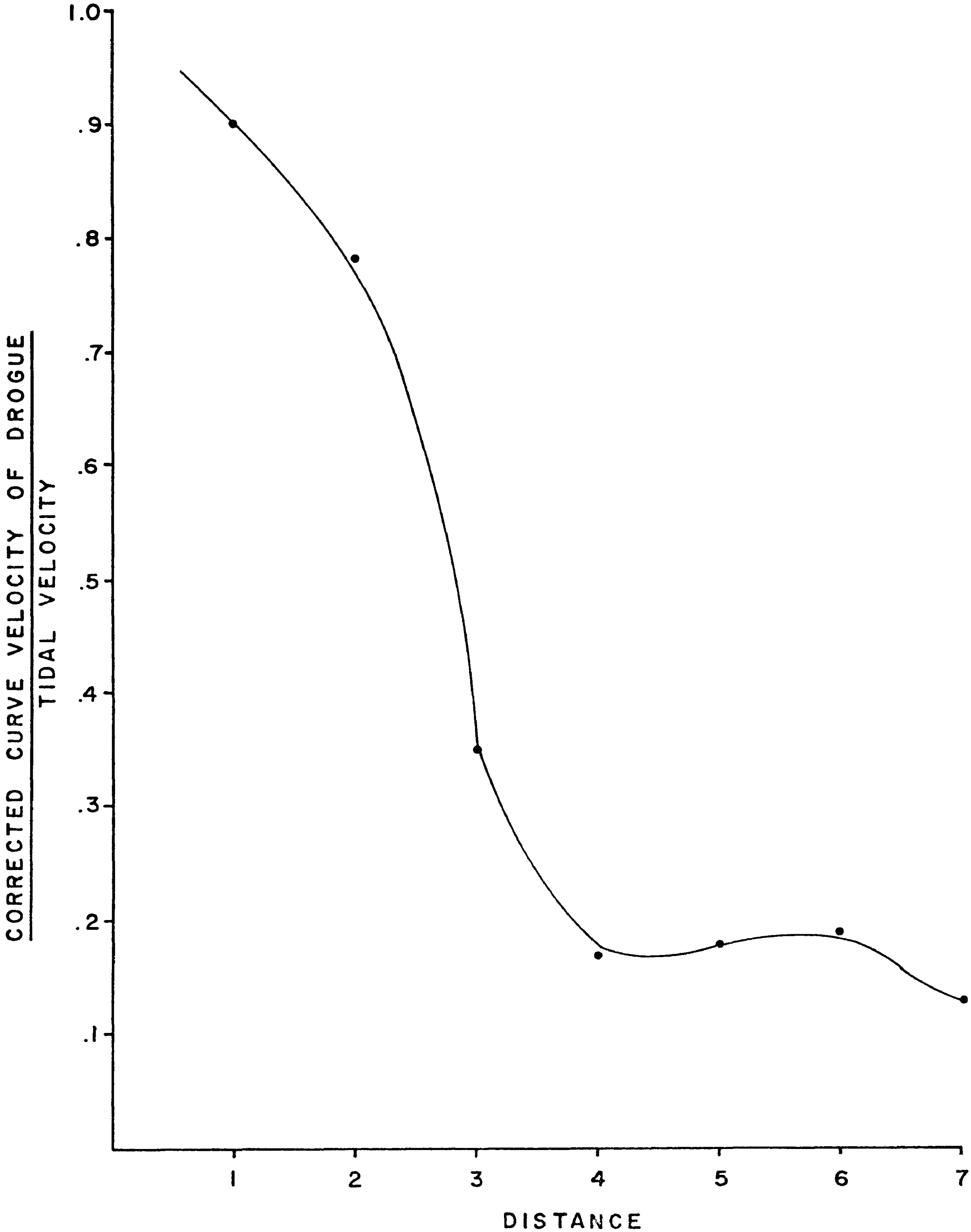

CORRECTED CURVE VELOCITY OF DROGUE
TIDAL VELOCITY
1.0
.9
.8
.7
.6
.5
.4
.3
.2
.1
1
2
3
4
5
6
7
DISTANCE

Figure 52. Idealized conception of Wachapreague Inlet shoreline, with schematic representation of streamlines.

EBB

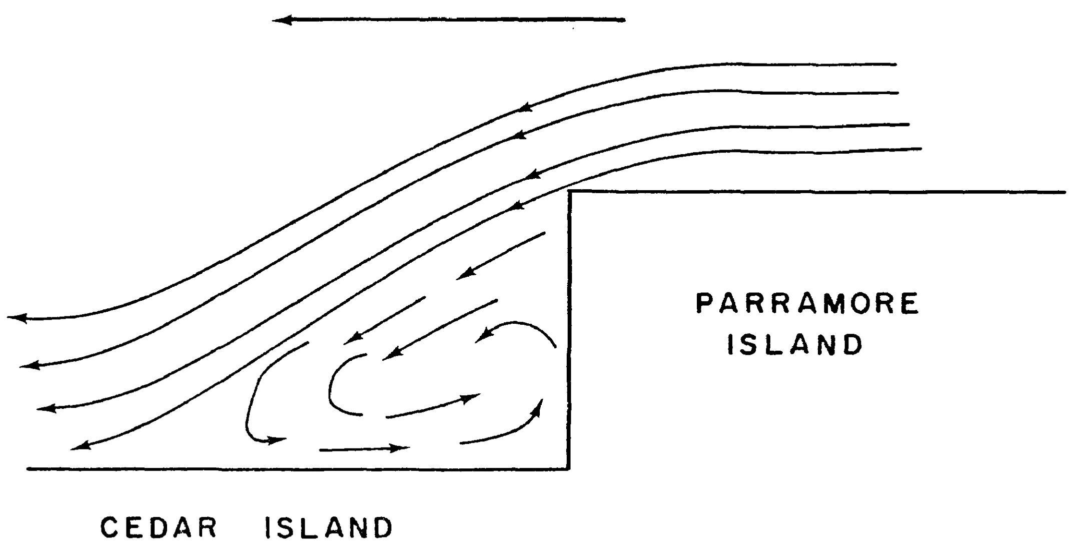
PARRAMORE
ISLAND
CEDAR ISLAND

FLOOD

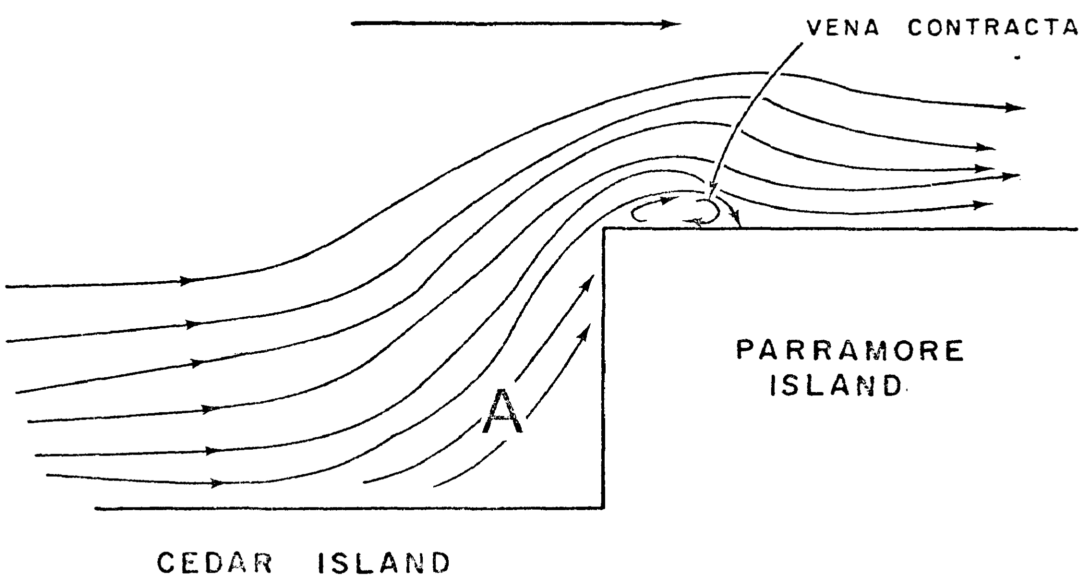
VENA CONTRACTA
PARRAMORE
ISLAND
A
CEDAR ISLAND

conducted off Wallops Island 20 miles north of Wachapreague Inlet (personal communication, Robert J. Byrne, 1974)). Ideally this leads to expanding and contracting flows (Figure 52).

During ebb (expanding flow conditions) there is a dissipation of energy through the creation of turbulence and eddy formation in what would be the coastal current zone study area. Superimposing the leakage from the issuing ebb tidal jet on this idealized shoreline one would expect the coastal current zone to behave sluggishly with the hydraulic currents of the inlet interacting with and imposing a unidirectional component upon the turbulent field created by the abrupt change in the shoreline.

During contracting flow conditions (flood) most of the energy is dissipated at the expansion of the flow downstream of the _vena contracta_ and a somewhat stagnant condition exists in area A as indicated in Figure 52. Opening an inlet at the base of a stagnation zone would cause the streamlines to be directed toward this sink. It is of interest to note that a shoaled area at the tip of Parramore Island exists corresponding to the position of a _vena contracta_.

Theoretical framework for the prediction of sediment transport rates in an interacting wave and current environment is not available. The intention of this study is qualitatively to determine the behavior of the sediment under the influence of the ambient conditions.

During flood tide, significantly greater sediment transport originates in the coastal current zone in response to the inlet's hydraulic currents than during ebb. This would be expected as previous flow gaging experiments in the inlet and the results of the drogue study show a dominance of the flood currents over ebb currents in this area. During flood, sediment is carried toward the inlet; the rate of transport increases as it enters the area of predominate flood tidal influence.

With the exception of the August 24th flood case, tracer sediment showed increasing dispersion away from the drop site in the direction of the drogue measuring the ambient current field. Response of the sediment to the inlet's hydraulic currents in the coastal current zone during ebb are less defined than during flood and the rate of transport slower, corresponding to the less intense ebb tidal currents.

Wave action near Wachapreague Inlet generally operates at right angles to the tidal current field in the coastal current zone. In front of Cedar Island, adjacent to the inlet, the ebb tidal delta and flanking shoals cause waves approaching from the south or southeast to be refracted orienting their approach to the east to northeast. Waves and wind driven currents from the northeast would increase the capability of the flood tidal currents to transport sediment into the inlet. Winds and waves from the same direction would act against the already weak ebb currents and could possibly overcome their effect.

VII.

SUMMARY

The hydraulic currents of the coastal current zone adjacent to Wachapreague Inlet are intrinsically dependent upon the phase and behavior of the tide in the inlet and are a function of the local bathymetry and island orientation. Net sediment transport is south, toward the inlet through a unique zone of significant flood tidal influence. There is no corresponding ebb influenced area. Local wave approach just north of the inlet is confined to the east through northeast because of the orientation of the ebb tidal delta. Therefore, wave activity is most likely to enhance sediment advection toward the inlet and further mask the already weak ebb tidal currents.

VIII.

APPENDIX

Figure 53. Sample vector calculation of drogue correction method. Refer to text pages 16-18.

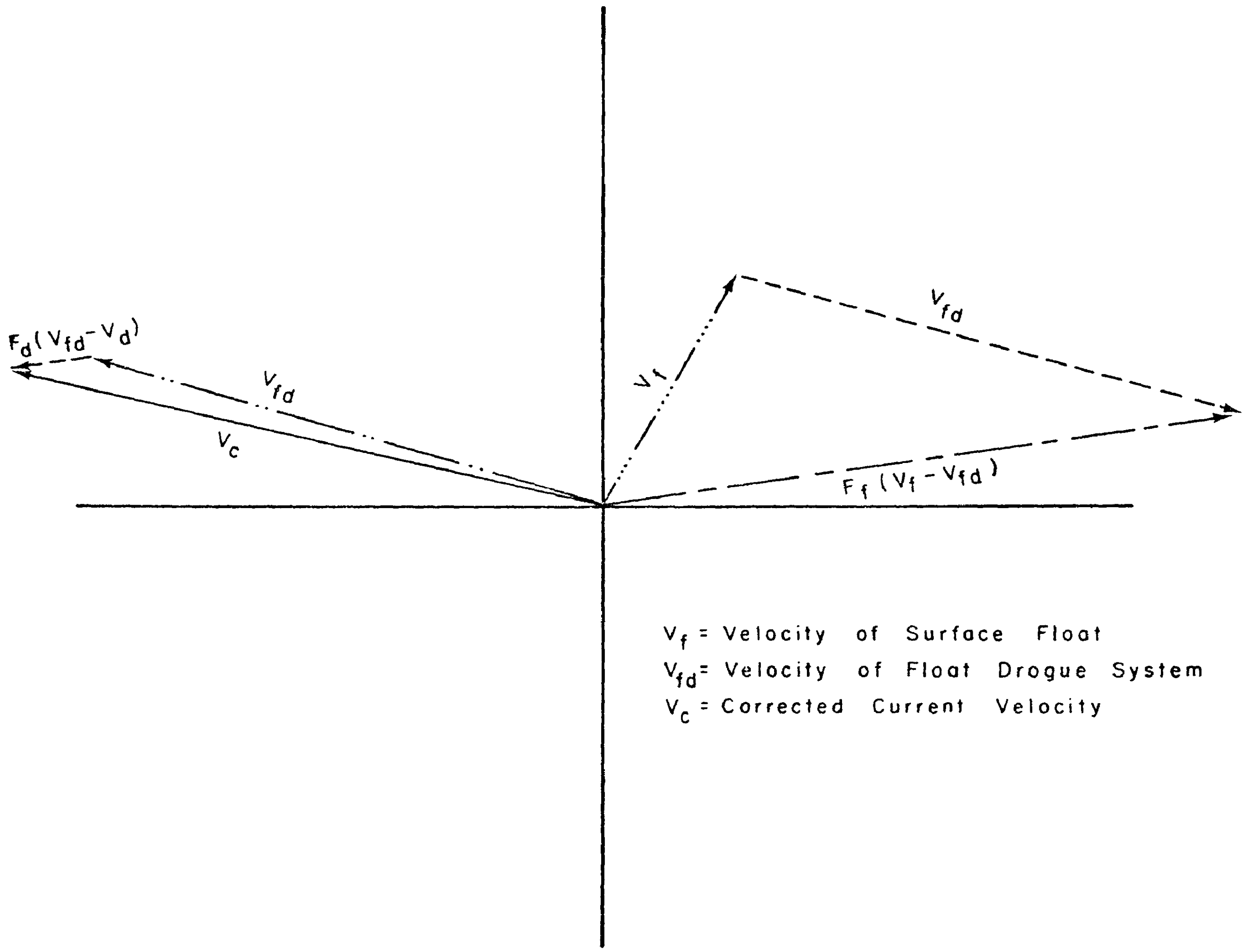

$F_d(V_{fd}-V_d)$
V_{fd}
V_c
V_f
V_{fd}
$F_f(V_f-V_{fd})$
V_f = Velocity of Surface Float
V_{fd} = Velocity of Float Drogue System
V_c = Corrected Current Velocity

TABLE 1

AMBIENT CONDITIONS

DROGUE EXPERIMENTS

Flood

Date	Time of Low Water EST	Time of High Water EST	Tide Range Meters	Wind Velocity m/sec. direction	Wave Height meters direction
May 10	8:00 am	14:40 pm	.9-2	1.7N	1.2E
May 11	9:00 am	16:00 pm	.84-2	4.5-6.5W	.6E
May 22	5:30 am	11:30 am	.96-1.74	2.5SW	.4E
June 5	5:00 am	11:30 am	.63-1.86	2.1-4.5WSW	.1-.2SW
June 7	6:50 am	13:00 pm	.63-1.9	6.5-8.8SSW	.3-.6SW
June 21	5:30 am	11:30 pm	.96-1.0	0.0-2.5SW	.1SW

Ebb

Date	Time of High Water EST	Time of Low Water EST	Tide Range Meters	Wind Velocity m/sec. direction	Wave Height meters direction
May 4	9:00 am	14:40 pm	1.01-.66	2.1N	.6E
May 21	11:00 am	16:30 pm	1.86-1.	6.5-8.8NW	.3NE
June 4	10:40 am	16:20 pm	1.96-.54	4.5-6.5SW	.15SW
June 13	6:20 am	12:20 pm	1.62-.72	4.5-6.5SW	.15SW
June 14	7:20 am	12:30 pm	1.8-.93	2.1-4.5N	.15NE

TABLE 2

AMBIENT CONDITIONS

TRACER EXPERIMENTS

	Aug. 24 Flood	Sept. 7 Flood	Aug. 29 Ebb	Aug. 30 Ebb
WIND				
speed(m/sec.)	3.6	2.2-3.6	1.8	2.2
direction	ENE	ENE	E	N
WAVE				
period(sec.)	7-8	8	5.6	7-8
length(meters)	40	15	11	15
height(meters)	.6-1	.3	.2	.3
bottom velocity maximum(cm/sec.)	81	9.8	4.9	8.5
direction	E	E	E	E
TIME(EST)				
start	10:46 am	9:45 am	9:15 am	9:25 am
finish	14:38 pm	15:10 pm	14:10 pm	14:52 pm
elapsed(min)	232	325	295	327
WATER DEPTH(m)	3.4	3.	2.9	3.1
RIPPLE MARKS				
wave length(cm)	3.8-5.1	2.5-3.8	11	7.5-9.
height (cm)	1.2	1.2-2.	2.5	2.5-3.5
form	linear	linear	lunate linguoid	lunate linguoid
SEDIMENT				
mean ø, cm	3.3, .010	3.3, .010	2.47,.017	2.66,.016
standard die.ø	.562	.549	.438	.472
skewness	.114	.093	.248	.116
kurtosis	.651	.620	.322	.342
TIDAL VELOCITY				
maximum(m/sec.)	1.1	.75*	1.6	1.45
TIDAL RANGE				
meters	1.5	0.9	1.5	1.43
PERCENT RECOVERY				
out of 180 samples taken	24$	18%	31%	23%

* estimated velocity in inlet.

TABLE 3

PROGRAM FOR CORRECTING DROGUE VELOCITIES

```
      DIMENSION TITLE (20)
      DO 38 N=1,500
      READ(5,10) A,B,VFD,VF,TV,IT
   10 FORMAT (F6.2,5X,F7.2,3X,F6.3,4X,F6.3,2X,F5.2,3X,I4)
      IF (A.LE.400.) GO TO 950
      READ(5,11) TITLE
   11 FORMAT(20A4)
      WRITE(6,12) TITLE
   12 FORMAT(20A4)
      GO TO 38
C     CONVERT ANGLES TO RADIANS
  950 CONTINUE
      RADA=A*3.14159/180.0
      RADB=B*3.14159/180.0
      VFDX=VFD*COS(RADA)
      VFDY=VFD*SIN(RADA)
      VFX=VF*COS(RADB)
      VFY=VF*SIN(RADB)
      VFRX=VFX-VFDX
      VFRY=VFY-VFDY
      VFR=SQRT((ABS(VFRX))**2+(ABS(VFRY))**2)
      RTAN=VFRY/VFRX
      C=VFRY/VFR
      D=VFRX/VFR
      IF(C.GT.0.0)GO TO 15
      IF(D.GT.0.0)GO TO 21
      ANGLE=(3.14159 +ATAN(RTAN))
      GO TO 33
   21 ANGLE=(6.28318+ATAN(RTAN))
      GO TO 33
   15 IF (D.GT.0.0)GO TO 27
      ANGLE=(3.14159+ATAN(RTAN))
      GO TO 33
   27 ANGLE=ATAN(RTAN)
      GO TO 33
       ROTATE ANGLE BY 180 DEGREES
   33 ANGLE=ANGLE +3.14159
      VFR=VFR*100
      FF=221.*(VFR)**2
      VD=SQRT(FF/9840.)
      VD=VD*0.01
      VRX=VD*COS(ANGLE)
      VRY=VD*SIN(ANGLE)
      VWX=VRX+VFDX
      VWY=VRY+VFDY
      WV=SQRT((ABS(VWX))**2+(ABS(VWY))**2)
      ANGLE=(ANGLE*180.)/3.14159
      WVDIR=VWY/VWX
      WVDIR=ATAN(WVDIR)
```

```
      VC=WV/TV
      IF(VWX.LT.C.C) GO TO 50
      IF(VWY.GT.C.C)GO TO 52
      WVDIR=6.28318 +WVDIR
      GO TO 61
50    IF(VWY.LT.C.C) GO TO 51
      WVDIR=3.14159+WVDIR
      GO TO 61
51    WVDIR=WVDIR+3.14159
```



```
      GO TO 61
52    WVDIR=WVDIR
      GO TO 61
61    WVDIR=(WVDIR*180.)/3.14159
      GO TO 37
37    WRITE(6,36)IT,A,VFD,B,VF,TV,WV,WVDIR
38    CONTINUE
36    FORMAT(5XI4,4X,F6.2,4X,F5.3,6X,F6.2,4X,F5.3,4X,F6.3,6X
     1F6.3,4X,F7.2)
      STOP
      END
```

RAW AND FINAL DATA
DROGUE EXPERIMENT

TIME EST	DROGUE ANGLE*	DROGUE VELOCITY METERS/SEC.	FLOAT ANGLE	FLOAT VELOCITY METERS/SEC.	VELOCITY IN TIDAL INLET METERS/SEC.	CORRECTED CURRENT VELOCITY METERS/SEC.	CORRECTED CURRENT DIRECTION
MAY 10 DROGUE RUN NO 1 X(0)=-3413 Y(0)= 1090 T(0)=0845							
916	277.60	0.040	237.10	0.070	0.560	0.039	287.76
940	332.50	0.030	225.90	0.100	0.680	0.041	352.82
1020	316.60	0.070	227.20	0.080	0.760	0.081	325.08
1048	332.30	0.080	235.20	0.200	0.770	0.100	349.57
1116	317.90	0.090	219.20	0.120	0.820	0.108	327.40
1133	318.50	0.060	219.20	0.120	0.880	0.074	332.36
1214	326.00	0.070	183.10	0.440	0.830	0.139	342.64
1235	332.90	0.060	183.10	0.440	0.880	0.130	347.65
MAY 10 DROGUE RUN NO 2 X(0)=-2668 Y(0)= 605 T(0)=1348							
1425	338.20	0.200	183.10	0.440	0.280	0.291	343.67
MAY 10 DROGUE RUN NO 3 X(0)=-3323 Y(0)= 1130 T(0)=0850							
912	150.20	0.040	237.10	0.070	0.570	0.047	137.21
945	136.80	0.010	237.10	0.070	0.670	0.017	99.14
1007	229.00	0.010	227.20	0.080	0.760	0.001	11.14
1058	8.10	0.020	235.20	0.200	0.770	0.049	34.93
1121	254.40	0.030	219.20	0.120	0.780	0.049	9.41
1140	323.50	0.030	219.20	0.120	0.880	0.043	347.61
1201	112.10	0.030	183.10	0.440	0.820	0.064	33.90
1245	290.40	0.050	183.10	0.440	0.830	0.100	329.63
1330	220.50	0.020	183.10	0.440	0.690	0.053	344.70
1354	125.00	0.010	183.10	0.440	0.500	0.061	12.36
1416	163.20	0.040	183.10	0.440	0.460	0.028	37.70

MAY 11 DROGUE RUN NO 1 X(0)=-2953 Y(0)= 776 T(0)=0937

1010	9.40	0.080	73.70	0.300	0.500	0.083	340.20
1037	280.60	0.050	10.60	0.610	0.710	0.108	222.77
1105	278.90	0.060	74.50	0.240	0.770	0.103	270.59
1143	272.40	0.060	94.40	0.230	0.830	0.103	273.07

MAY 11 DROGUE RUN NO 2 X(0)=-2660 Y(0)= 696 T(0)=1152

1216	269.20	0.050	95.70	0.170	0.830	0.083	271.19
1250	303.10	0.030	43.90	0.390	0.860	0.073	251.47
1316	346.70	0.030	43.90	0.390	0.780	0.049	260.00

MAY 11 DROGUE RUN NO 3 X(0)=-2808 Y(0)= 1160 T(0)=0943

1007	164.20	0.020	73.70	0.300	0.410	0.057	231.59
1035	282.70	0.020	10.60	0.610	0.640	0.093	204.84
1107	317.60	0.070	74.50	0.240	0.770	0.102	299.26
1136	306.50	0.070	94.40	0.230	0.830	0.111	297.02
1220	278.00	0.060	95.70	0.170	0.850	0.094	277.38
1249	293.90	0.040	95.40	0.170	0.820	0.071	287.33
1313	281.10	0.020	43.90	0.390	0.810	0.073	239.15
1352	329.30	0.060	43.90	0.390	0.700	0.078	282.80
1416	308.60	0.050	21.00	0.380	0.540	0.068	255.17
1506	308.70	0.040	26.20	0.340	0.350	0.061	253.80

MAY 22 DROGUE RUN NO 1 X(0)=-1600 Y(0)= 475 T(0)=0540

607	313.90	0.020	127.50	0.150	0.150	0.045	310.74
628	315.90	0.050	132.50	0.120	0.350	0.075	315.09
655	333.00	0.050	105.30	0.120	0.490	0.071	322.18
719	355.40	0.070	91.00	0.130	0.540	0.085	342.16
745	35[illegible].70	0.070	74.00	0.170	0.530	0.078	340.29
812	6.90	0.080	83.20	0.170	0.550	0.089	350.84
831	353.60	0.070	76.80	0.180	0.570	0.082	334.49
858	354.90	0.070	77.10	0.200	0.550	0.082	333.66
917	3.30	0.080	77.10	0.200	0.500	0.086	349.30
939	359.80	0.090	62.10	0.190	0.460	0.094	344.19
1007	356.10	0.110	49.30	0.220	0.440	0.110	342.21
1027	358.80	0.120	42.50	0.210	0.390	0.117	348.11
1046	352.70	0.140	42.50	0.210	0.330	0.143	343.00

MAY 22 DROGUE RUN NO 2 X(0)=-1635 Y(0)= 727 T(0)=0545

610	161.00	0.030	127.50	0.150	0.150	0.028	221.54
631	63.30	0.080	132.50	0.120	0.340	0.087	52.19
65[illegible]	202.50	0.080	105.30	0.120	0.390	0.075	283.17
[illegible]25	357.00	0.070	91.00	0.130	0.540	0.085	341.79

MAY 22 LRCCUE RUN NO 3 X(0)=-1270 Y(0)= 900 T(0)=0816

900	2.20	0.050	83.20	0.170	0.570	0.059	337.01
920	340.20	0.050	76.80	0.180	0.500	0.066	316.34
941	345.00	0.060	77.10	0.200	0.480	0.076	321.86
1012	355.20	0.070	62.10	0.190	0.440	0.074	334.50
1032	335.20	0.070	49.30	0.220	0.350	0.078	311.27
1052	12.90	0.050	42.50	0.210	0.230	0.034	345.61

JUNE 5 LRCCUE RUN NO 1 X(0)=-1173 Y(0)= 361 T(0)=0515

602	340.70	0.051	118.80	0.200	0.280	0.083	326.81
638	279.20	0.032	111.10	0.180	0.500	0.063	284.23

JUNE 5 LRCCUE RUN NO 2 X(0)=- 680 Y(0)= 505 T(0)=0525

600	272.00	0.038	118.80	0.200	0.270	0.074	294.77
636	267.80	0.030	111.10	0.180	0.500	0.061	289.25
712	295.10	0.030	98.90	0.170	0.570	0.059	287.38

JUNE 5 LRCCUE RUN NO 3 X(0)=- 135 Y(0)= 640 T(0)=0835

907	322.80	0.500	350.10	0.610	0.910	0.495	317.94
924	323.20	0.560	325.10	0.430	0.830	0.580	322.99

JUNE 5 LRCCUE RUN NO 4 X(0)=- 983 Y(0)= 300 T(0)=0643

718	298.30	0.032	96.90	0.170	0.810	0.061	289.57

JUNE 5 LRCCUE RUN NO 5 X(0)= 55 Y(0)= 485 T(0)=0951

1031	333.00	0.390	13.30	0.530	0.570	0.391	325.45

JUNE 5 LRCCUE RUN NO 6 X(0)=- 950 Y(0)= 410 T(0)=0722

753	1.40	0.120	61.90	0.120	0.750	0.130	354.49
831	357.70	0.200	19.60	0.180	0.830	0.205	354.89
914	342.00	0.190	350.10	0.610	0.850	0.129	336.25
930	339.40	0.490	350.10	0.610	0.780	0.474	337.35
942	338.20	0.650	12.90	0.550	0.730	0.681	334.25

JUNE 5 DROGUE RUN NO 7 X(0)=- 570 Y(0)= 403 T(0)=0716							
759	339.50	0.097	61.90	0.150	0.770	0.111	327.90
JUNE 5 DROGUE RUN NO 8 X(0)=-1117 Y(0)= 624 T(0)=0520							
604	0.0	0.043	118.80	0.200	0.280	0.069	337.65
645	344.20	0.076	111.10	0.180	0.500	0.083	329.21
705	353.00	0.065	61.90	0.150	0.560	0.092	339.83
756	343.30	0.120	61.90	0.150	0.700	0.135	333.93
823	341.10	0.230	19.60	0.180	0.820	0.244	337.15
910	350.60	0.210	325.50	0.430	0.840	0.185	359.09
939	299.50	0.700	325.50	0.430	0.780	0.748	296.26
JUNE 5 DROGUE RUN NO 9 X(0)= 114 Y(0)= 270 T(0)=1010							
1037	341.10	0.390	301.50	1.250	0.530	0.327	2.54
JUNE 5 DROGUE RUN NO 10 X(0)= 140 Y(0)= 321 T(0)=0934							
955	109.10	0.130	13.30	0.530	0.670	0.175	134.98
1005	326.00	1.880	301.50	1.250	0.580	1.996	330.40
JUNE 7 DROGUE RUN NO 1 X(0)=-1430 Y(0)= 411 T(0)=1145							
1226	178.20	0.195	160.30	0.300	0.630	0.182	182.55
JUNE 7 DROGUE RUN NO 2 X(0)=- 31 Y(0)= 449 T(0)=0728							
755	347.20	0.320	165.20	0.120	0.420	0.386	344.25
825	332.20	0.310	165.20	0.120	0.470	0.374	332.82
JUNE 7 DROGUE RUN NO 3 X(0)= 5 Y(0)= 490 T(0)=0934							
1007	337.10	0.600	306.60	0.180	0.790	0.667	338.28
1015	271.80	0.910	312.00	0.210	0.820	1.023	270.66
JUNE 7 DROGUE RUN NO 4 X(0)=- 920 Y(0)= 558 T(0)=0735							
803	214.50	0.058	165.20	0.120	0.340	0.057	228.43
837	202.90	0.068	157.30	0.220	0.500	0.060	226.04
917	187.30	0.079	174.00	0.320	0.560	0.046	201.32
936	165.70	0.119	160.30	0.300	0.710	0.098	197.03
1026	152.20	0.130	160.30	0.300	0.800	0.114	204.25
1137	179.50	0.104	160.30	0.300	0.800	0.079	190.35
JUNE 7 DROGUE RUN NO 5 X(0)=-1545 Y(0)= 555 T(0)=0740							
815	175.80	0.110	165.20	0.120	0.400	0.109	177.54
841	174.70	0.088	157.30	0.220	0.540	0.070	182.75
913	167.80	0.130	157.30	0.220	0.580	0.117	170.74
941	174.60	0.195	160.30	0.300	0.710	0.181	178.12
1030	169.40	0.176	160.30	0.300	0.840	0.165	197.04

JUNE 7 DROGUE RUN NO 6 X(0)= 26 Y(0)= 493 T(0)=1126							
1152	0.50	0.420	322.20	0.310	0.780	0.447	4.19
1213	268.40	0.750	323.90	0.700	0.600	0.808	262.25
JUNE 7 DROGUE RUN NO 7 X(0)=- 625 Y(0)= 620 T(0)=1043							
1130	323.10	0.180	312.00	0.210	0.820	0.176	325.07
1214	341.20	0.130	322.20	0.310	0.640	0.164	346.50
JUNE 7 DROGUE RUN NO 8 X(0)=- 64 Y(0)= 495 T(0)=1022							
1050	328.60	0.490	312.00	0.210	0.870	0.533	328.93
1107	324.10	0.490	322.20	0.310	0.830	0.517	324.27
1114	233.70	0.890	322.20	0.310	0.810	1.018	237.11
JUNE 7 DROGUE RUN NO 9 X(0)= 161 Y(0)= 353 T(0)=0830							
849	331.70	0.520	306.60	0.180	0.550	0.574	332.84
926	267.40	0.270	306.60	0.180	0.610	0.290	264.03
JUNE 21 DROGUE RUN NO 1 X(0) 51 Y(0)= 670 T(0)=0815							
857	333.60	0.400	335.00	0.190	0.700	0.431	333.51
913	255.80	1.390	297.90	1.120	0.680	1.478	251.43
JUNE 21 DROGUE RUN NO 2 X(0)=- 85 Y(0)= 570 T(0)=0717							
746	326.50	0.450	301.70	1.310	0.610	0.349	340.14
759	5.10	0.490	335.90	0.350	0.750	0.518	7.93
810	289.40	0.810	270.00	1.410	0.740	0.735	294.88
832	259.30	0.500	270.00	1.410	0.700	0.369	253.20
JUNE 21 DROGUE RUN NO 3 X(0)=- 615 Y(0)= 588 T(0)=0652							
719	350.10	0.170	356.00	0.320	0.540	0.148	348.19
744	338.70	0.230	335.90	0.350	0.600	0.212	339.39
820	342.20	0.420	335.90	0.350	0.720	0.431	342.96
JUNE 21 DROGUE RUN NO 4 X(0) - 55 Y(0)= 546 T(0)=1006							
1036	328.90	0.420	320.70	0.820	0.540	0.362	331.68
1058	341.90	0.410	320.70	0.820	0.400	0.360	349.00
1115	277.80	0.560	320.70	0.820	0.200	0.560	269.21
JUNE 21 DROGUE RUN NO 5 X(0)=- 94 Y(0)= 400 T(0)=0556							
624	340.50	0.390	353.30	0.330	0.230	0.399	345.66
653	311.70	0.420	295.00	0.720	0.390	0.381	316.37
712	232.60	0.380	295.00	0.720	0.540	0.399	218.72
JUNE 21 DROGUE RUN NO 6 X(0)= 628 Y(0)= 180 T(0)=0724							
740	323.80	0.920	301.70	1.310	0.600	0.879	328.62
750	227.10	0.690	301.70	1.310	0.750	0.765	212.78

JUNE 21 LRCCUE RUN NC 7 X(C)=- 633 Y(C)= 416 T(0)=C6C3

630	0.50	C.180	353.30	C.33C	C.250	0.158	2.75
700	341.50	C.220	295.CC	C.72C	C.420	0.195	5.15
724	338.80	0.390	356.CC	C.32C	C.53C	0.403	336.78

JUNE 21 LRCCUE RUN NC 8 X(C) - 392 Y(C)= 526 T(C)=C92C

956	334.30	0.270	335.C0	C.19C	C.68C	0.282	338.63
1030	330.70	0.600	320.70	C.82C	C.5CC	0.569	332.85
1047	234.70	0.560	320.7C	C.82C	C.48C	0.647	223.78

JUNE 21 LRCCUE RUN NC 9 X(C)=- 511 Y(C)= 585 T(0)=C838

924	337.00	C.250	335.CC	C.19C	C.68C	0.259	337.22
952	340.80	C.560	338.4C	C.44C	C.68C	0.578	341.07
1000	288.10	C.740	297.90	1.12C	C.62C	0.686	285.71

JUNE 21 LRCCUE RUN NC 1C X(0) 65 Y(C)= 776 T(0)=C936

958	326.10	0.270	320.70	C.82C	C.68C	0.188	329.62

JUNE 21 LRCCUE RUN NC 11 X(C) 365 Y(C)= 631 T(0)=1014

1028	322.80	1.140	320.7C	C.82C	C.55C	1.188	323.02
1052	263.20	C.560	320.7C	C.82C	C.48C	0.587	253.03

JUNE 21 LRCCUE RUN NC 12 X(C)=- 600 Y(C)= 545 T(0)=C756

817	340.10	0.200	335.90	C.35C	C.74C	0.178	341.34
841	340.80	0.260	335.9C	C.35C	C.71C	C.247	341.84
916	330.40	0.600	270.CC	1.41C	C.7CC	0.614	347.82
926	262.90	0.740	270.CC	1.41C	C.71C	0.642	260.57

MAY 4 LRCCUE RUN NC 1 X(C)= 506 Y(C)= 861 T(0)=C924

944	171.20	0.36C	136.60	C.27C	-C.62C	0.381	174.65
1006	149.20	C.420	132.7C	C.37C	-1.13C	0.499	151.01
1028	104.90	0.250	123.2C	C.45C	-1.37C	0.224	99.49
1100	103.20	0.220	123.2C	C.45C	-1.44C	0.191	96.26

MAY 4 LRCCUE RUN NC 2 X(C)= 570 Y(C)= 472 T(C)=C914

930	149.60	C.18C	136.60	C.27C	-C.58C	0.168	152.71
947	144.60	C.250	136.60	C.27C	-C.8CC	0.247	145.90
1012	143.50	0.240	132.7C	C.37C	-1.2CC	0.222	146.19
1037	156.70	0.300	123.2C	C.45C	-1.42C	C.291	164.05
1113	145.30	0.190	75.2C	C.21C	-1.39C	0.210	153.41
1142	185.20	0.410	75.20	C.21C	-1.340	0.483	188.71

MAY 4 DROGUE RUN NO 3 X(O)=- 876 Y(O)= 960 T(O)=1120							
1155	158.20	0.180	75.20	0.210	-1.300	0.206	166.94
1219	156.70	0.160	113.30	0.400	-1.200	0.146	173.05
1243	123.90	0.220	45.40	0.400	-1.050	0.248	137.60
1315	135.00	0.230	65.20	0.320	-0.760	0.254	148.37
MAY 4 DROGUE RUN NO 4 X(O)=-1244 Y(O)= 445 T(O)=1203							
1231	116.50	0.130	113.30	0.400	-1.180	0.090	118.64
1252	155.90	0.090	45.40	0.400	-0.830	0.137	180.18
MAY 21 DROGUE RUN NO 1 X(O)= 336 Y(O)= 224 T(O)=1015							
1038	2.20	0.270	30.70	0.460	0.140	0.252	354.70
1100	138.40	0.300	68.10	0.350	-0.100	0.331	146.98
1142	110.90	0.080	93.00	0.500	-0.270	0.031	158.97
1213	127.70	0.250	116.30	0.990	-0.680	0.145	139.37
1240	116.60	0.160	116.30	0.990	-1.000	0.036	117.85
MAY 21 DROGUE RUN NO 2 X(O)= 400 Y(O)= 585 T(O)=1250							
1322	187.10	0.230	85.50	0.430	-1.020	0.285	199.92
1343	71.60	0.210	60.30	1.190	-0.840	0.075	99.29
MAY 21 DROGUE RUN NO 3 X(O)= 371 Y(O)= 365 T(O)=0540							
1318	88.00	0.200	85.50	0.430	-1.000	0.166	88.97
MAY 21 DROGUE RUN NO 4 X(O)=- 110 Y(O)= 282 T(O)=1020							
1045	17.90	0.130	30.70	0.460	0.100	0.084	7.38
1115	103.80	0.040	68.10	0.350	-0.070	0.031	187.46
1140	134.30	0.200	93.00	0.500	-0.270	0.181	150.19
1210	192.00	0.140	93.00	0.500	-0.570	0.188	215.20
1232	143.80	0.850	116.30	0.990	-0.910	0.849	148.43

JUNE 4 DROGUE RUN NO 1 X(0)= 636 Y(0)= 60 T(0)=1017							
1044	128.30	0.120	135.60	0.420	0.030	0.076	123.16
1130	161.70	0.410	145.70	0.540	-0.350	0.394	164.94
1216	166.10	0.200	161.30	0.430	-0.800	0.166	167.96
1250	149.50	0.120	154.10	0.370	-0.990	0.083	146.42
1329	158.30	0.130	161.10	0.400	-1.000	0.090	156.43
1405	171.10	0.140	179.80	0.400	-0.960	0.102	166.01
1442	169.70	0.100	178.00	0.380	-0.820	0.059	161.72
1525	170.30	0.090	177.10	0.320	-0.660	0.056	164.50
1550	168.30	0.120	174.30	0.440	-0.610	0.073	163.81
JUNE 4 DROGUE RUN NO 2 X(0)= 451 Y(0)= 636 T(0)=1023							
1046	128.10	0.060	135.60	0.420	0.110	0.011	76.82
1235	170.60	0.240	145.70	0.540	-0.350	0.206	180.41
1215	114.70	0.240	161.30	0.430	-0.890	0.236	103.27
1254	130.20	0.120	154.10	0.370	-0.980	0.090	115.77
1323	143.20	0.100	161.10	0.400	-1.020	0.061	125.56
1409	139.20	0.090	179.80	0.400	-0.960	0.070	105.26
1437	159.20	0.190	178.00	0.380	-0.810	0.166	152.84
1535	170.20	0.190	178.00	0.380	-0.620	0.162	167.47
JUNE 4 DROGUE RUN NO 3 X(0)= 10 Y(0)= 323 T(0)=1029							
1050	165.00	0.150	135.60	0.420	0.010	0.122	179.72
1127	171.50	0.260	145.70	0.540	-0.320	0.229	180.35
1205	170.20	0.210	161.30	0.430	-0.770	0.178	173.41
1242	164.40	0.160	161.30	0.430	-0.980	0.120	166.07
1331	176.70	0.150	161.10	0.400	-1.020	0.116	184.70
1403	162.10	0.100	179.80	0.400	-0.950	0.055	184.60
1445	164.20	0.090	178.00	0.380	-0.820	0.050	148.46
1522	169.00	0.110	177.10	0.320	-0.670	0.079	164.11
1545	166.70	0.120	177.10	0.320	-0.520	0.091	161.25

JUNE 13 DROGUE RUN NO 1 X(0)= 746 Y(0)= 324 T(0)=0625							
659	180.80	0.240	146.60	0.530	-0.240	0.215	192.79
737	173.10	0.360	146.60	0.530	-0.830	0.345	179.00
825	190.10	0.180	166.30	0.340	-1.320	0.158	184.51
JUNE 13 DROGUE RUN NO 2 X(0)=- 74 Y(0)= 434 T(0)=0557							
631	183.20	0.054	146.60	0.530	0.110	0.047	275.22
703	175.20	0.200	146.60	0.530	-0.250	0.165	188.55
745	171.40	0.180	166.30	0.340	-0.820	0.156	173.06
833	171.30	0.130	169.30	0.320	-1.330	0.102	172.24
905	179.10	0.150	169.30	0.320	-1.430	0.125	182.83
1003	175.10	0.089	171.50	0.250	-1.300	0.065	177.17
1037	162.60	0.100	136.00	0.320	-0.870	0.075	179.18
1137	166.10	0.085	133.00	0.270	-0.650	0.068	185.19
JUNE 13 DROGUE RUN NO 3 X(0)=- 933 Y(0)= 588 T(0)=0605							
635	193.00	0.130	146.60	0.530	0.260	0.111	224.27
709	171.20	0.150	146.60	0.530	-0.270	0.106	189.45
747	160.20	0.160	166.30	0.340	-0.830	0.158	184.64
837	171.90	0.150	136.00	0.320	-1.380	0.137	183.78
912	176.60	0.110	171.50	0.250	-1.370	0.089	178.74
953	166.40	0.140	150.20	0.420	-1.230	0.102	176.31
1042	158.80	0.120	150.20	0.420	-0.860	0.076	165.88
1115	156.20	0.120	150.20	0.270	-0.540	0.098	158.68
JUNE 13 DROGUE RUN NO 4 X(0)=- 959 Y(0)= 596 T(0)=0924							
902	173.70	0.210	169.30	0.320	-1.410	0.194	174.79
957	150.50	0.200	171.50	0.250	-1.240	0.193	158.38
1032	151.90	0.170	136.00	0.320	-0.950	0.154	169.73
1120	127.20	0.130	133.00	0.270	-0.600	0.109	125.06

JUNE 14 DROGUE RUN NO 1 X(0)=- 10 Y(0)= 30 T(0)=0722							
759	72.20	0.290	154.20	0.180	-0.330	0.349	68.44
823	149.60	0.220	156.50	0.320	-0.560	0.205	147.99
907	161.10	0.160	170.00	0.190	-0.870	0.156	159.48
945	163.70	0.120	172.80	0.120	-0.960	0.120	162.34
JUNE 14 DROGUE RUN NO 2 X(0)=- 30 Y(0)= 145 T(0)=0913							
943	68.50	0.081	172.80	0.120	-0.950	0.093	77.42
1025	72.60	0.120	172.80	0.120	-0.820	0.142	65.45
1103	197.20	0.039	172.50	0.140	-0.600	0.027	215.98
1138	240.10	0.026	184.30	0.130	-0.440	0.025	280.48
1225	179.00	0.035	184.30	0.130	-0.240	0.021	174.07
1305	314.40	0.075	184.30	0.130	0.100	0.100	322.98
JUNE 14 DROGUE RUN NO 3 X(0)=- 35 Y(0)= 128 T(0)=0804							
831	78.10	0.300	156.50	0.320	-0.600	0.339	70.12
909	165.30	0.200	170.00	0.190	-0.950	0.202	164.64
950	166.20	0.130	172.80	0.120	-0.960	0.132	165.30
1027	172.60	0.087	172.80	0.120	-0.820	0.082	172.56
1059	175.50	0.091	172.50	0.140	-0.600	0.084	176.25
1144	164.10	0.074	184.30	0.130	-0.440	0.066	184.04
JUNE 14 DROGUE RUN NO 4 X(0)=- 35 Y(0)= 188 T(0)=1230							
1256	354.90	0.750	184.30	0.130	0.130	0.882	355.11
1311	182.60	0.280	184.30	0.130	0.220	0.302	182.49

* Drogue angle measured from a line drawn between Cedar Island stations two and four. This line tends 2° east of north and represents 0°--0". Coordinate system originates at station 2 (x = 0, y = 0).

IX.

BIBLIOGRAPHY

Bagnold, R. A. An approach to the sediment transport problem from general physics: Geological Survey Professional Paper 422-I, U.S. Govt. Printing Office, Washington, D.C., 1966.

Boothroyd, J. C. Hydraulic conditions controlling the formation of estuarine bedforms: Univ. of Mass. Geol. Dept. Contribution No. 1, pp. 417-427, 1969.

Brown, E. I. Inlets on sandy coasts: Proc., A.S.C.E. v. 54, pp. 505-553, 1928.

Brunn, P. and Gerristen, Stability of coastal inlets: North Holland Publishing, Amsterdam, Holland, 123 p. 1960.

Brunn, P. Tidal inlets and littoral drift: North Holland Publishing, Amsterdam, Holland, 193 p. 1966.

Byrne, R. J., Bullock, P. and Tyler, D. G. Response Characteristics of a tidal inlet: A case study: 2nd International Estuarine Research Conf. Myrtle Beach, South Carolina, 1973.

Cook, D. O. and Gorsline, D. S. Field observations of sand transport by shoaling waves: Marine Geol. V. 13, pp. 31-55, 1972.

DeAlteris, J. T. The recent history of Wachapreague Inlet, Virginia: Unpublished Masters thesis, School of Marine Science, College of William and Mary, Williamsburg, Va., 1973.

DuBoys, P. in Henderson, F. M. Open channel flow: the Macmilland Company, New York, Collier-Macmillian Limited, London, pp. 446-448, 1968.

Einstein, H. A. Formulas for the transportation of bed load: Trans. Am. Soc. Civil Engs. v. 107, p. 561, 1942.

Hayes, M. O., Goldsmith, V. and Hobbs, C. H. III. Offset coastal inlets: A.S.C.E. Proc. of Twelfth Coastal Engineering Conf. pp. 1187-1200, 1970.

Hjulstrom, F. Studies of the morphological activity of rivers as illustrated by the River Fyris: Bull. Geol. Inst. Univ. Upsala, v. 25, pp. 221-528, 1935.

Ingle, J. C. Jr. The movement of beach sand: Elsevier Publishing Co. Amsterdam, London, New York, 221 p., 1966.

Inman, D. L. and Bowen, A. J. Flume experiments on sand transport by waves and current: Eight Conf. on Coastal Engin-ering, pp. 137-150, 1963.

Inman, D. L. and Tunstall E. B. Phase dependent roughness control of sand movement: A.S.C.E. Thirteenth Coastal Engineering Conf. pp. 1155-1171, 1972.

King, C. A. M. Beaches and coasts: St. Martin's Press, New York, 570 p., 1972.

Komar, P. D. and Miller, M. C. The threshold of sediment movement under oscillatory water waves: Journal of Sedimentary Petrology, v. 43, No. 4, pp. 1101-1110, 1973.

Monahan, E. C., Kaye, G. T. and Michelena, E. D. Drogue measurements of the circulation in Grand Traverse Bay, Lake Michigan: Dept. of Atmospheric and Oceanic Science, College of Engineering, Univ. of Mich. Tech. Report No. 35, 1973.

O'Brien, M. P. Equilibrium flow areas of tidal inlets on sandy coasts: A.S.C.E. Tenth Conf. on Coastal Engineering, pp. 676-686, 1966.

Oertel, G. F. Patterns of sediment transport at nearshore zones influenced by wave and tidal currents: a study utilizing fluorescent tracers: Georgia Marine Science Center, Skidaway Island, Georgia, Tech. Report No. 72-7, 1972.

Price, W. A. Patterns of flow and channeling in tidal inlets: Journal of Sedimentary Petrology, v. 33, No. 2, pp. 279-290, 1963.

Shepard, F. P. Submarine geology: Harper and Row, Publishers, New York, Evanston, and London, pp. 49-82, 1963.

Shields, A. Application of similarity principles and turbulence research to bed-load movement: translated by W. P. Ott and J. C. van Uchelen, S.C.S. Calif. Inst. of Technology, Pasadena, Calif., 1936.

Stone, R. O. and Summers, H. J. Study of subaqueous and subaerial sand ripples: Los Angeles, Univ. Southern Calif. Dept. Geol. Science, Rept. 72-1, 1972.

Terhune, L. D. B. Free-floating current followers: Fisheries Research Board of Canada, Tech. Report No. 85, 1968.

Tizard, T. H. et.al. Challenger Reports: Narrative v. 1, No. 79, 1885.

Yasso, W. E. Fluorescent coatings on coarse sediments, and integrated systems: Office Nav. Res. Georg. Br. Tech. Rept. 1, 48 p., 1962.

Yasso, W. E. Formulation and use of fluorescent tracer coatings in sediment transport studies: Sedimentology, v. 6, pp. 287-301, 1966.

X.

ADDITIONAL REFERENCES

Briggs, L. I. and Middleton, G. V. Hydromechanical principles of sediment structure formation: Soc. of Economic Paleontologists and Mineralogists, Tulsa, Oklahoma, Spec. Pub. No. 21, pp. 5-16, 1965.

Folk, R. L. Petrology of sedimentary rocks: Hemphill's Austin, Texas, 1968.

Harlett, J. C. and Kulm, D. C. Suspended sediment transport on the northern Oregon continental shelf: G.S.A. Bull. V. 84, pp. 3815-3826, 1973.

Henderson, F. M. Open channel flow: the Macmilland Company, New York, Collier-Macmillian Limited, London, 522 p. 1968.

Owczarek, J. A. Introduction to fluid mechanics: International Textbook Co. Scranton, Pennsylvania, 516 p. 1968.

Raudkivi, A. J. Loose Boundary Hydraulics: Pergamon Press, Oxford, London, New York, 331 p. 1967.

Rouse, H. Fluid mechanics for hydraulic engineers: Engineering Societies Monographs, McGraw-Hill, New York, reprinted by Dover Publication, Inc. 422 p. 1961.

Teleki, P. G. Fluorescent sand tracers: Journal of Sedimentary Petrology, v. 36, No. 2 pp. 468-485, 1966.

Teleki, P. G. Wave boundary layers and their relation to sediment transport: Shelf Sediment Transport, Dowden Hutchinson and Ross, Inc. Stroubsburg, Pa. 1972.

Weggel, J. R. An introduction to oceanic water motions and their relation to sediment transport: Shelf Sediment Transport, Dowden Hutchinson and Ross, Inc. Stroubsburg, Pa. 1972.

XI.

VITA

Jerome Peter Sovich

The author was born in Cleveland, Ohio on April 10, 1945. He received a Bachelor of Science degree in Mechanical Engineering from Ohio University in December of 1967. The author worked for Freeport Mineral Company as a power plant engineer at a frasch process sulphur mine in Louisiana. In February of 1971 the author moved to St. Thomas in the U. S. Virgin Islands where he attended classes at the college, served as a lab assistant, and taught high school. The author entered the College of William and Mary's Marine Science Division in February of 1972 and is a candidate for the Masters of Arts degree.